2002

Geo-Electrical Studies in the High Barino,. Bangladesh for Evaluating Aquifer Geometry of the Area

Reza, A.H.M. Selim

University of Rajshahi

GEO-ELECTRICAL STUDIES IN THE HIGH BARIND, BANGLADESH FOR EVALUATING AQUIFER GEOMETRY OF THE AREA

A Thesis Submitted to the Department of Geology and Mining, University of Rajshahi for the Degree of Master of Philosophy in Geology and Mining

Submitted by

A.H.M.Selim Reza

Assistant Professor
Department of Geology and Mining
University of Rajshahi
Rajshahi 6205
Bangladesh

Research Supervisors

Professor Mushfique Ahmed

Director
Institute of Environmental Science
University of Rajshahi
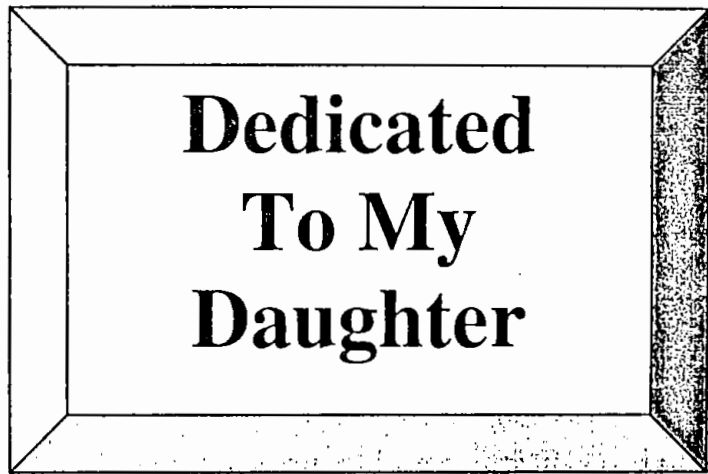Rajshahi 6205, Bangladesh

Professor Quamrul Hasan Mazumder

Department of Geology and Mining
University of Rajshahi
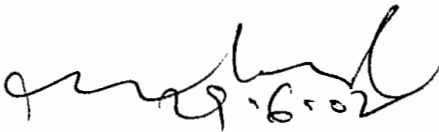Rajshahi 6205, Bangladesh

**DEPARTMENT OF GEOLOGY AND MINING
UNIVERSITY OF RAJSHAHI
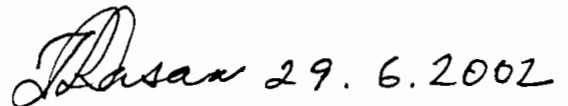RAJSHAHI 6205, BANGLADESH
JUNE 2002**

Dedicated
To My
Daughter

CERTIFICATE

This is to certify that the work presented in the dissertation entitled *"Geo-electrical studies in the High Barind, Bangladesh for Evaluating Aquifer Geometry of the Area"* is based on the work carried out under our supervision in the Department of Geology and Mining, University of Rajshahi and is suitable for submission for the fulfillment of the Degree of Master of Philosophy in Geology and Mining.

Professor Mushfique Ahmed
Director
Institute of Environmental Science
University of Rajshahi
Rajshahi 6205, Bangladesh

29. 6. 2002
Professor Quamrul Hasan Mazumder
Department of Geology and Mining
University of Rajshahi
Rajshahi 6205, Bangladesh

DECLARATION

I hereby declare that the work embodied in this thesis has not been submitted elsewhere in whole or in substance in candidature for any other Degree or Diploma.

Selim 29.6.2002
A.H.M. Selim Reza
Assistant Professor
Department of Geology and Mining
University of Rajshahi
Rajshahi 6205, Bangladesh

ABSTRACT

The Barind Tract is one of the major physiographic units of Bangladesh. During the dry period the discharge from shallow and hand tube wells become minimum and some times it becomes completely nil. Out of total 13 Upazillas, comprising the Barind Tract, Sapahar and Porsha Upazillas, situated in the High Barind are adversely affected by water shortage. The Barind region is now in an acute state of deforestation as a result the scarcity of surface water sources and low rainfall. Considering the above hydrogeological problem, geophysical investigation has been carried out in this area and an attempt has been made to study the feasibility of groundwater sources and characteristics of groundwater aquifer; particularly its depth and thickness.

The lithological characteristics encountered in different drill holes enabled to divide the subsurface zone into three lithostratigrahic units up to 70 m depth from the ground surface. These are: top sandy and silty clay aquitard unit, fine to coarse sand aquifer unit and silty shale unit at the bottom. The top two layers units were underlain by silty clay unit in places. From the study of 21 deep tube well borelogs, it is evident that the main aquifer does not occur within the upper 300 m, and the composite aquifer, the only exploitable one in the area is present within the depth of 100 m.

Stratigraphic panel diagram of the study area is also in good agreement with the geological cross-sections drawn for the study area.

Clay-sand interface map also indicates a diverging zone in the study area. While the thickness map of top sandy and silty clay layer indicates an E-W elongated thick zone located in the northeastern portion of Sapahar Upazilla.

It is observed from the maximum and minimum elevation of groundwater table map that the central part of the study area represents a prominent N-S elongated diverging zone. The groundwater flows radially towards east, west, north and south from the central part of the study area.

The maximum and minimum elevation of groundwater table of the study area varies from 20 to 34 m and 15 to 32 m respectively. Higher value of maximum elevation of groundwater table is observed in the central part of Porsha and lower value of maximum elevation of groundwater table is observed in the northwestern part of Sapahar and southeastern portion of Porsha Upazilla. Higher value of minimum elevation of groundwater table is observed in the central part of Porsha and lower value of minimum elevation of groundwater table is observed in the northwestern part of Sapahar and southeastern portion of Porsha Upazilla. The groundwater table fluctuation varies between 2 and 8 m. The maximum and minimum fluctuations are observed in northwestern part of Sapahar and in the central part of Porsha respectively. The study of hydrograph indicates a direct positive relationship between rainfall and ground water level, and rainfall and river water level fluctuation. Transmissivity values are as derived from pumping test data analysis, varies from 1411 to 1566 m^2/day, which is indicative of a higher degree of transmissivity and suitability for the groundwater resource utilization in irrigation and water supply. Storage coefficient value varies from 9.27×10^{-4} to 8.05×10^{-2}. Hydraulic conductivity value of aquifer zone in the study area ranges from 22 to 74 m/day. The estimated transmissivity, storage coefficient and hydraulic conductivity indicate that the area is suitable for groundwater exploitation.

The study area has the estimated specific yield values varying from 10 to 28%, which increase as the thickness of top sandy and silty clay decreases and vice versa.

Electrical resistivity survey has been carried out in the High Barind, especially in Sapahar and Porsha Upazillas as a reconnaissance investigation for the subsurface lithology.

Vertical electrical sounding (VES) was undertaken with Schlumberger configuration in different areas of the Upazillas considering the current electrode separation up to 170 m. The computerized Direct Method was employed to evaluate the geo-electric layer such as thickness and resistivity of discrete layers.

Geo-electric survey employing vertical electric sounding (VES) technique was carried out in 12 locations. The data have been interpreted as a multi-layer step function resistivity model by means of an iterative process of interpretation. A equivalent model with minimum number of layers has been constructed for each of the VES locations. Results of the geo-electric sounding have been compared with the geological section wherever available. The transverse and longitudinal resistivities at different depth levels along with the coefficient of anisotropy have been calculated.

Results of the resistivity survey reveal the subsurface configuration consisting of three to four layers. On the basis of hydrogeological behaviors, interpreted geo-electrical layers are grouped into two forms: aquitard and aquifer. The first layer of top sandy and silty clay and in some cases, second and third layers, if critically analyzed from hydrogeological point of view can be considered as aquitard and the rest of the layers which are mainly composed of sandy formations are considered as the only aquifer present in the study area. The top sandy and silty clay aquitard shows a general increasing trend in depth towards the northeastern part of the study area and the composite aquifer shows higher thickness in the southeastern and southwestern parts of the study area.

Increasing trends of coefficient of anisotropy towards the central and southwestern parts of the study area indicate that the main aquifer zone is located at relatively lower depths than other parts.

The annual groundwater recharge and discharge of aquifer of the study area is estimated by Thiessen polygon method and varies from 106.41 to 244 Mm^3 and 93.77 to 291.7 Mm^3 respectively. The overall groundwater balance study in the study area indicates that there used to exist a balance between annual recharge and withdrawal up to 1993 but after period of 1993 discharge exceeds the recharge continuing till date. A cumulative annual deficit is found to exist because of progressive annual discharge in Sapahar Upazilla.

ACKNOWLEDGEMENTS

Contents

List of Figures

List of Tables

Chapter-1
Introduction

CHAPTER 1
INTRODUCTION

1.1 General Introduction

Water is essential for the existence of life. Our planet is unique in the sense that about 72% of the earth surface is covered with water, of which 97.2% in the oceans, 2.15% in frozen state and only 0.65% is fresh water. Fresh water occurs on the surface as well as in the atmosphere as vapor. The water occurring beneath the ground surface is termed as groundwater, which is the largest available source of fresh water suitable for human consumption.

Now a days, groundwater is considered as one of the most important resources of a country. Bangladesh, a mainly agricultural country, water plays a vital role in its economic development. Particularly for agricultural development, where surface water potential is seasonal and limited during irrigation season, groundwater is to be developed as an alternate source. But groundwater is also limited and there exists many constraints for its development. For this reason it is essential to determine the nature of subsurface condition and the quantity and the quality of groundwater that can be withdrawn safely for different uses. The present work deals with such a problem of groundwater investigation and management. The study area is located in the High Barind of Greater Rajshahi District, northwest of Bangladesh.

The Barind Tract is one of the major physiographic units of Bangladesh constituting about 13 Upazillas of Greater Rajshahi District. At present many parts of the area suffer from problems of water scarcity. Before 1960 there were no tube wells in many of the villages of the area, particularly in the northwestern part of the Barind Tract, even dug wells were not there. Water demand was met at that time from the surface reservoirs like Ponds, Beels, etc.

During 1967-68, under a program of technical assistance from the Federal Republic of Germany, geophysical and hydrogeological investigations were carried out (Deppermann and Thiele, 1969) in order to develop a plan for groundwater extraction. Results of the investigation suggested that excluding the eastern and southwestern part of the area, the irrigation projects of larger extent would yield no success.

During the early eighties, an ambitious area development program named BIADP (Barind Integrated Area Development Project) initiated a project for sinking and development of few thousands of deep tube wells (DTWs) to provide irrigation facilities to the local farmlands during the dry months. Most of these deep tube wells of the project are sunk within 30 to 51 m and in few places it is about 60 m while the Hand Tube Wells (HTWs) supplied by the Public Health Engineering Department are sunk also within 30 to 48 meter, that is, in the same hydraulic gradient. Now it is evident that during dry season, whenever the deep tube wells are in operation, the discharge of the hand tube wells (HTWs) and shallow tube wells (STWs) become nil.

The water table in the area is deep compared to the other parts of the country and gradually declining further. Once upon a time the area is used to get horizontal percolation from the riverbeds during the dry season. Now most of these become dry during the dry periods and river stages go down compared to the groundwater level and results in loss of water from groundwater storage as base flow at higher rate.

Decline in the groundwater level and decrease in the lean period flow of the rivers are bringing in some major ecological changes in the region. Some parts, particularly the High Barind area, are showing evidences of desertification. Although BIADP is aimed to overcome this adversities, has generated an intellectual debate among the environmental scientists of the country and most of them are against large-scale abstraction of groundwater from the region before the

scientific assessment of the region. According to them, such a large-scale abstraction from an area with minimum rainfall, persistent draught and very low surface water potentiality could bring in severe changes in the ecological balance of the area. The effect may include deforestation, permanent decline in the water table, reduced base flow to the streams and even ultimate land subsidence.

1.2 Objectives

Considering the above intricate problems the present work is designed with the following objectives:

a) To carry out extensive geo-electric resistivity survey.

b) To map isopachs of different geo-electric layers to match them with lithologs.

c) To match established geo-electric layers with lithologs.

d) To delineate different aquifers by defining their geometry (thickness and extent).

e) To determine hydraulic characteristics of the aquifers, such as: transmissivity, hydraulic conductivity, storage coefficient and specific yield.

f) To estimate the recharge and discharge of groundwater using groundwater table fluctuation and specific yield data by Thiessen Polygon methods

1.3 Methods of Aquifer Study

Groundwater properly designates all interstitial water below the water table but only the superficial portion of groundwater principally within 300 m of the ground water surface has been studied and exploited by those interested in water supply. A variety of techniques can provide information concerning its occurrence and under certain conditions even its quality from surface or above surface locations. They include: Geologic Method, Hydrologic Method, Remote Sensing, Geophysical Method etc.

1.3.1 Geologic Method

Geologic studies enable large areas to be rapidly and economically appraised on a preliminary basis to their potential for groundwater development. A geologic investigation begins with the collections, analysis and hydrogeological interpretation of existing topographic maps, aerial photographs, geologic maps and logs and others pertinent records. The geologist utilizes petrography, stratigraphy, structural geology, geomorphology and to a lesser extent other geologic specializations in the search for subsurface water.

1.3.2 Hydrologic Method

Hydrologic method of prospecting for groundwater includes studies of total water available for recharge, ease of recharge, and the location and quantity of groundwater discharged at the surface. The total quantity of water available for recharge includes both natural precipitation and surface water in large perennial streams. In general the opportunity for finding the subsurface water is related more or less directly to the recharge available. However impermeable surfaces such as shale, clay and quartzite prevent adequate groundwater recharge.

1.3.3 Remote Sensing

Photographs of the earth taken from satellite at various electromagnetic wavelengths can provide useful information regarding groundwater conditions (Bowden and Pruitt eds., 1975). Observable patterns, colors and relief make it possible to differentiate between rock and soil types and indicate their permeability and aerial distribution and hence areas of groundwater recharge and discharge (Ray, 1960; Avery, 1977).

1.3.4 Geophysical Methods

Geophysical methods, developed during the last sixty years have proved useful for locating and analyzing groundwater. The geophysical work is, in general, much

more expensive than geologic and hydrologic reconnaissance so that the decision weather or not to use geophysics is most often a questions of economics. If the exploration project is economically important enough and if the geologic framework of the area is favorable geophysics should by all means, be utilized. The most useful applications of all geophysical techniques, however, are in the interpretation of geologic structure and stratigraphy thus eliminating the need of an extensive and expensive drilling program.

Geophysically the location of groundwater may be determined in three ways i) direct, ii) structural and iii) stratigraphy. Different geophysical methods are employed for groundwater exploration. The four major methods are seismic, magnetic, gravity and electrical resistivity. Among these four methods the electrical resistivity method is most widely used in groundwater investigation.

Chapter-2
Geography
and
Geology

CHAPTER-2
GEOGRAPHY AND GEOLOGY

2.1 Geography

The study area lies within the High Barind. This is the uplifted part of the Barind Tract. The area is covered with reddish brown mottled clay with abundant calcareous and ferruginous nodules, which was deposited by the Ganges - Brahmaputra fluvial system. The river Atrai flows towards south between the uplifted and subsided Barind while the Punarbhaba flows along the western periphery of western uplifted Barind.

The study area is located in the Barind region and is a part of the Naogaon district (Fig.-2.1). It lies between 24°54′N and 25°13′N latitudes and 88°23′E and 88°39′E longitudes. It comprises a total area of 497.3 sq.km.

Morgan and McIntyre (1959) studied the physiography of Bangladesh. Rashid (1977) have divided the Bengal Basin into twenty-four sub-regions with fifty-four units on the basis of physical features and drainage pattern. The study area falls under the physiographic unit 3.

The Barind Tract: The Barind Tract appears as a terrace landscape as well as closely dissected terrace comprising essentially of compact old alluvium or the Modhupur clay, but in fact represents a series of faulted blocks. In the western part the Tract is hilly and dissected by narrow, usually streamlets valleys (bydes), there it is upwarped and slopes downward both to the west and the east. In the eastern side, the Tract is nearly level, undissected, slightly tilted to the southeast and passes under the adjoining floodplain sediments. The study area covers the central Barind region.

The Barind Tract has been subdivided into five physiographic sub-units mainly according to relief and seasonal flooding. These are: level, intermittently flooded
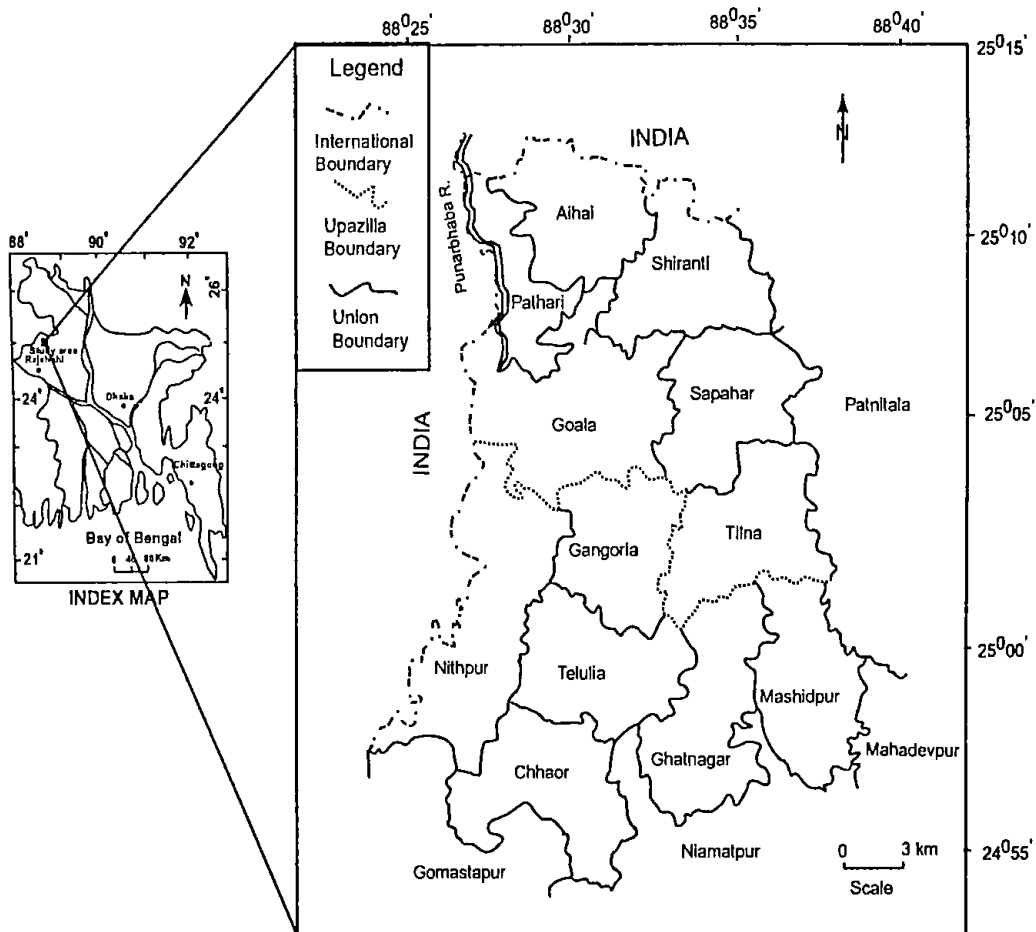
Fig.-2.1: Location map of the study area

terrace: level deeply flooded terrace; broadly dissected terrace; closely dissected terrace and level, covered terrace. The dissected undulated high Barind which occupies about the three fourth of the total study area and the level Barind.

Gray brown silty loam soils of the level, intermittently flooded terraces are found in the western side of Barind. Major soils are mixed yellowish brown and gray to light gray loams to clay loams, rarely clays, grading into a gray usually strongly mottled yellowish brown and red clay below about one meter. The characteristic feature of this unit is abundance of impure calcareous matter in the form of irregular concretions locally known as Kankar. These are formed due to the separation of calcareous and ferruginous materials of the alluvium deposits into nodules.

The Ganges Floodplain:

This physiographic unit covers the southwestern part of the study area. This is generally an area of gentle, low relief and is readily identified by calcareous and non-calcareous nature of the sediments. Yellowish brown to dark brown, dark gray to gray, light brown to brown soils are dominant.

Broad and nearly level ridges and basins characterize the older meander floodplain. The surface floodplain materials are non-calcareous and to some extent oxidized, especially those are lying above normal flood level or only seasonal shallowly flooded (upper part of the ridges) reflecting their greater age than present day and young Ganges alluvium.

The elevation of the area from the mean sea level ranges from a maximum of 40 m in the northeast to a minimum of 22 m in the west. The elevation contour map of the representing the surface configuration of the study area is shown in fig.-2.2.

An intricate network of rather narrow tightly entrenched stream drains the Barind Tract, usually streamlets valleys. The Atrai, the Little Jamuna and the Shib collect
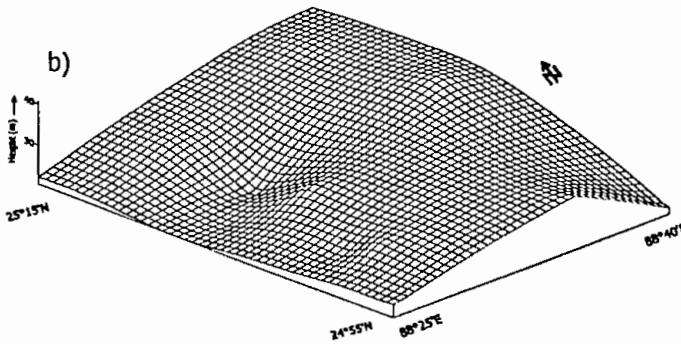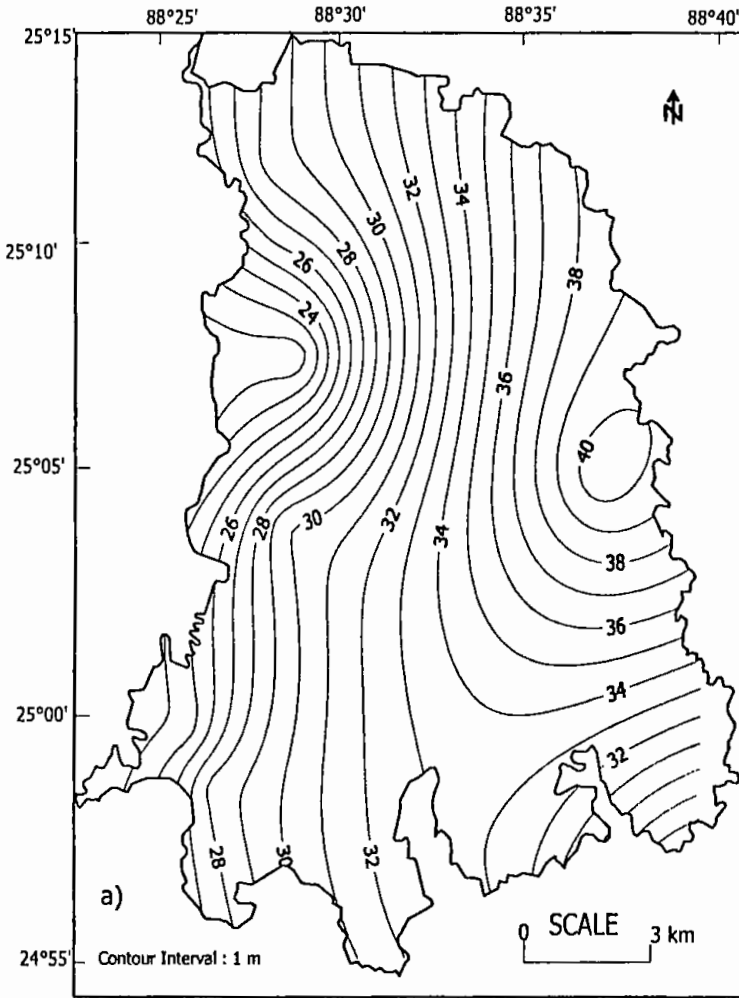
Fig.- 2.2: Contour Map showing the Surface
Configuration of the Area.
a) Contour Map; b) Trend

most of their drainage water in the east while the Mahananda and the Punarbhaba collect their drainage water from the west. All these rivers have long history of migration and formation of flood plains.

Beside the main streams there exists a network of minor tributaries and distributaries along with numerous canals. Most of these become dry in the dry months. There is some standing surface water body like ponds. Another type of surface water body of the area is the low-lying swampy land locally known as Beels. Some of them are quiet big and perennial (SPARRSO, 1989). Ponds present in this area serve as standing surface water body.

2.1.1 River System

Excepting the Ganges or the Padma, the Mahananda, the Punarbhaba and the Atrai of the study area are of little hydrographic importance, as most of the rivers are not active flowing streams except during the rainy season. During the rainy season these rivers act as excellent drainage channels draining off a huge volume of water and have a considerable current. Most of these rivers are narrow and flow along well-defined channels.

The Punarbhaba: The study area is situated in the western part of Punarbhaba river.The river Punarbhaba is a major tributary to the Ganges. The upper course of the Punarbhaba is just a few kilometers west of the Atrai. It is interlocked by the Dhepa, which also rises in a beel. The Dhepa is also known as the Punarbhaba. From just south of Dinajpur town the river flows between the western and the west central Barind, and drains the west of the west-central part. It joins the Mahananda just south of Rohanpur union of Gomastapur Upazilla.

The Atrai: The Atrai is another important river adjacent to the eastern side of the study area, which flows through Naogaon district. Dinajpur-Karatoya is the principal source of the river. Karatoya itself is designated as Atrai when it reaches khansama Upazilla in Dinajpur. The Atrai runs due south and enters Naogaon

district at point 13 km north of the Mohadevpur Upazilla and while passing through the Barind Tract it receives many small rivulets.

2.1.2 Climate

The study area enjoys a tropical monsoon climate with three distinct seasons: winter (November to February) which is cool and almost dry; pre-monsoon (March to May) which is hot and characterized by periodic thunderous shower; and monsoon or rainy season (June to October) which is warm, humid and 80% or more of the annual precipitation occurs during this time. One of the major factors affecting the groundwater and agriculture pattern of the area is unequal seasonal distribution of rainfall. About 80% of the total rainfall occurs during monsoon (June to October). The rest 20% falls during the other seasons. The average annual rainfall of the study area for the period of 1987-2000 is given in table 2.1. The average annual rainfall of the study area is about 1443 mm, which is relatively lower than the countrywide average (2550 mm).

The mean annual maximum and minimum temperatures of the study area are 39.5°C and 5.8°C respectively. The highest temperature occurs during the pre-monsoon period, at times exceeding 40°C. The lowest temperatures occur during the winter when mean monthly minimum temperatures varies from 5.8°C to 8.8°C during the months of January and February, with a mean monthly maximum temperature below 30°C. During the monsoon season, mean monthly maximum and minimum temperatures vary from 34.6°C to 36.3°C and 19°C to 24.6°C respectively. The mean monthly minimum and maximum temperature of the study area for the year 2000 are given in table 2.2.

The maximum rate of evaporation occurs during the months of January, March, May and September when monthly evaporation varied from 101.0 to 183.5 mm. During the monsoon it varies from 51.0 to 183.5 mm. The minimum rate of evaporation occurs during the months of July, August, and November continuing

Table 2.1: Annual rainfall in the study area (1987-2000)

Year	Rainfall in mm	
	Sapahar	Porsha
1987	1897.0	2162.3
1988	1734.7	1708.0
1989	1421.7	1154.6
1990	1145.0	1551.0
1991	1965.0	1998.8
1992	1296.0	1200.6
1993	1320.0	1420.1
1994	1053.0	1120.1
1995	1977.0	2144.7
1996	783.0	1387.9
1997	1031.0	1055.2
1998	1603.0	1750.4
1999	1525.0	1990.4
2000	1485.9	1915.3

till the end of February when monthly evaporation varied from 51.0 to 84.5 mm. The monthly evaporation of the study area for the year 2000 is given in table 2.3.

Table 2.2: Mean monthly max. and min. temperature of the study area for 2000

Month	Minimum (°C)	Maximum (°C)
January	5.8	28.1
February	8.8	28.8
March	13.0	35.8
April	19.3	39.5
May	20.5	38.4
June	24.6	36.3
July	25.3	35.1
August	24.5	35.3
September	23.3	34.6
October	19.0	34.8
November	16.2	32.0
December	10.2	27.3

2.1.3 Vegetation

Old riverbeds, ponds and marches, and streams, with sluggish current have copious vegetations of vallisnenia and other plants. Lands subjected to inundation have usually coverings of Tamarisk and reedy grass. There are no forests. Usually the higher grounds are covered with bamboos and grass such as *Imperata*

arundinacea and *Andopogon ociculutus*. The banyan, pipal and semul may be seen.

Table 2.3: Monthly evaporation of the study area for year 2000

Month	Evaporation (mm)
January	104.0
February	76.5
March	101.0
April	90.5
May	110.0
June	97.5
July	51.0
August	61.0
September	183.5
October	72.5
November	84.5
December	73.5

In the study area palms are grown widely and Khejur or datepalm trees are grown generally in the southern parts. Besides these, numerous species of the babul (*Acacia arabia*) or gum trees are found through out the study area.

2.1.4 Population

According to 1991 population census, the total population of the study area is 201000 shown in table 2.4. The density of population has since considerably increased.

About 38.2% of the total dwelling households depend on tube wells, 61.2% on ponds and shallow wells and 0.5% on river as sources of drinking water.

Table 2.4: Population of the study area

Name of Upazilla	Population
Sapahar	1,03,000
Porsha	98,000

2.1.5 Soil Classification

The soils of the study area are classified into two groups:

a) **Red Clay of the Barind:** Major soils are mixed yellowish brown and grayish loam to clay loams, strongly to moderately acid in reaction. The soil is mainly clayey, reddish to yellow in color and contains an excess of iron and lime and is deficient in silicon minerals. Ferruginous concretions are found frequently. Soil pH varies from 6.0 to 6.5. The soil is generally deficient in nitrogen, phosphates and potassium. When dry, this soil becomes as hard as brick and when wet, becomes slippery rather than soft.

b) **Floodplain Soils:** This soil shows a pattern of friable silty loam or silty clay loam. They are generally dark gray in color and clayey in texture. The soil is comparatively rich in calcium, magnesium and potassium. The pH value of this soil varies from 7.0 to 8.0. Soils are very fertile and suitable for all sorts of cultivation.

2.1.6 Soil Associations

Soil associations are mapping units containing two or more soils occurring side by side in a distinctive pattern, which repeats itself over part or the whole of particular landscape. Each soil series association is unique. The relationship is usually topographical with soils of different types occurring at different levels. Though individual soil distribution therefore forms a very complicated pattern, the regular relationship of some soil made it possible for them to be grouped together in soil associations. The concept of soil associations is simply the groups of related soils occurring regularly together in a distinctive pattern, which is usually determined by relief and drainage. For the purpose of the present study, after details field study a soil association map based on the map prepared by the Department of Soil Survey, Rajshahi (1984) has been prepared (Fig.-2.3). The soil
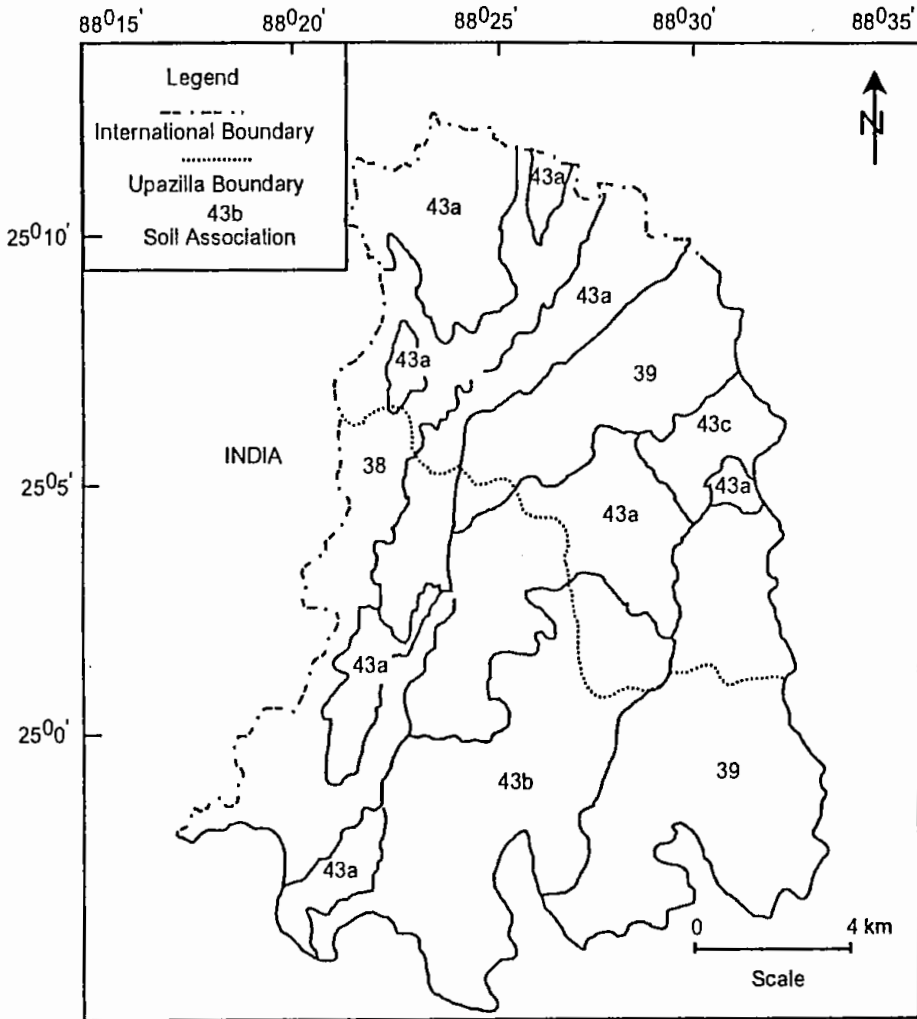
Modified after Department of Soil Survey, Rajshahi, 1984

Fig.-2.3: Soil association map

associations of the study area in different physiographic units are given in table 2.5.

Table 2.5: Soil associations in different physiographic units of the study area

Mapping No.	Physiographic Unit	Name
38	Old flood plain Basins	Jaonia-Bil Association
39	Barind Tract	Amnura-Nijhuri Association
43a	Broadly dissected Terrace	Amnura-Nachole Association, broadly dissected phase
43b	Closely dissected terrace	Amnura-Nachole Association, closely dissected phase
43c	Closely dissected terrace	Amnura-Nachole association, steeply dissected phase

2.2 Geology

In order to ascertain the hydrogeological condition of an area it is very essential to know about geological background. Because the occurrence, movement and storage of ground water are governed by the lithology, structure, thickness and the depth of occurrence of different geologic formations along with tectonic activities prevailing in that area.

Bangladesh is situated in the eastern part of the Bengal Basin, a partly geo-synclinal sedimentation area that is still in course of settlement. The Basin is bounded to the west by the Rajmahal Hills, to the north by the Shillong Plateau of Assam and to the east by the Tripura Hills.

The study area represents a complex geology. Geologically the area occupies a portion of the Indian platform or northwestern stable shelf of the Bengal geo-syncline depository that began in the late Cretaceous and filled with a thick sequence of Tertiary marine-continental deposits. The surface geology consists

entirely of sedimentary formations, mainly riverine in origin. These deposits are greatly affected by regional tectonic activity, both during and after deposition. The surficial deposits of the area are classified into the older alluvial deposits.

The geology of the Barind Tract is of Quaternary age. It is essentially composed of fluvial sediments mainly deposited by the Ganges-Brahmaputra system. The nature and distribution of the surface sediments within the area have been well described by Morgan and McIntyre (1958). The area is chiefly composed of red to yellow lateritic clays in the upper part, which merge into gray clays and argillaceous silts with depth. From the hydrological point of view the surface sediments are the oldest exposed sedimentary sequence of the Pleistocene age. The clays of the unit are yellowish-gray in color and the persistent weathering of the iron rich sediments has produced the characteristic red color and hence locally known as red clay. The clay thickness varies from 4 meter in the southwest to over 36 m in the northeast.

Significant thickness of coarser sand materials are observed below these clays and at places, large boulders have been encountered. Silty clays are also encountered at various depths in other trial boring and geo-electrical soundings. They form a base to the sands throughout the region and their thickness has been proven to be over 900 m.

2.2.1 Stratigraphy

The stratigraphy of the shelf area has been interpreted on the basis of drilling data. Rocks in the Stable Shelf region (Bogra Slope) range in age from Permian to Recent. The generalized stratigraphic succession of the Shelf (Bogra slope) region encountered in boreholes is given in table 2.6.

**Table 2.6: Stratigraphic succession of Shelf Zone (Bogra Slope) of the Bengal Basin
(After Zaher and Rahman, 1980)**

Age	Group/Formation	Lithology
Recent to Sub-recent	Alluvium	Sand, silt and clay.
----------------------------*Unconformity*--		
Pleistocene	Modhupur Clay	Clay, sandy clay, yellow brown, sticky.
----------------------------*Unconformity*--		
Mid-Pliocene to Late Pliocene	Dupi Tila Formation	Sandstone with subordinate pebble bed, grit and shale.
----------------------------*Unconformity*--		
Early Miocene	Jamalganj Formation (Surma Group) (undiff.)	Fine to medium grained sandstone sandy and silty stone, shale.
----------------------------*Unconformity*--		
Oligocene	Bogra Formation	Siltstone, carbonaceous shale and fine-grained sandstone.
----------------------------*Unconformity*--		
Late Eocene	Kopili Formation	Sandstone, locally gluconitic and highly fossiliferous, shale with calcareous bands.
----------------------------*Unconformity*--		
Mid to Late Eocene	Sylhet Limestone Formation	Nummulitic limestone with sandstone interbedded.
Mid Eocene	Tura Sandstone Formation	Grey and white sandstone, greenish grey shale and coal.
Late Cretaceous	Trapwash (Shibganj Formation)	Coarse yellow-brown sandstone, volcanic materials and white clay.
----------------------------*Unconformity*--		
Late Jurassic to Mid Cretaceous	Rajmahal Trap	Amogdoloidal basalts, serpentinized shale and agglomerate.
Late Permian	Pahar pur Formation	Feldspathic sandstone, shale and coal beds.
	Kuchma Formation	Sandstone and grit with subordinate shale, interbedded with coal beds.
----------------------------*Unconformity*--		
Precambrian	Basement Complex	Gneiss, Schist, Granodiorite, Quartz diorite.

2.2.2 Structural Setting and Tectonics of the Study Area

The tectonic elements of Bangladesh have been classified as the Indian Platform, the Bengal Foredeep, the Arakan Yoma Mega Anticlinorium and the Sub-Himalayan Foredeep (Bakhtine, 1966; Guha, 1978; Reimann, 1993). The Indian Platform has been further subdivided in the Dinajpur Slope (the Northern Slope of

the Rangpur Saddle), the Rangpur Saddle and the Bogra Slope (the Southern Slope of the Rangpur Saddle) (Guha, 1978).

A revised classification of the Indian Platform has been proposed (Khan and Rahman, 1992) in which the Indian Platform has been subdivided into four tectonic elements (Fig.2.4) viz. the Northern Slope of the Platform, the Stable Platform, the Nawabganj-Gaibandha Intra-cratonic High and the Southern part of the Platform. Structurally, the study area covers a major portion of the Nawabgang-Gaibandha Intra-cratonic High and partly of the Stable Platform.

The Barind Tract is devoid of any major visible surface structure whereas it is delineated and underlain by a number of major subsurface faults. The area is tectonically active and evidences of recent tectonic activities are found in different places (Morgan and McIntyre, 1959; Khandoker, 1987 and 1989).

The Barind Tract is bounded in the west by the Maldah-Kishanganj Fault in the south by the Padma Fault, in the east by the Dhubri-Jamuna Fault and the Karatoya Fault. The western extension of the Dauki Fault, a major structural unit of the region, cuts across the area. All the Faults are subsurface and some of them are basement faults.

Study of the available structural and tectonic information of the study area and adjoining areas suggest that upliftment of the Barind Tract occurs as a horst block along pre-existing well-defined lines of crustal weakness with compensatory subsidence of the bordering regions. This upliftment was a part of the isostatic adjustments, which took place in the plains of the northern India after removal of ice sheets at the close of the Pleistocene. Faults associated with the origin of the Barind Tract seems still active which indicates the isostatic equilibrium of the Bengal Basin is not yet complete.

The study area is bounded by the major basement faults to the west and to the north. The study area, a southwestern tilted fault block, is flanked on the west by
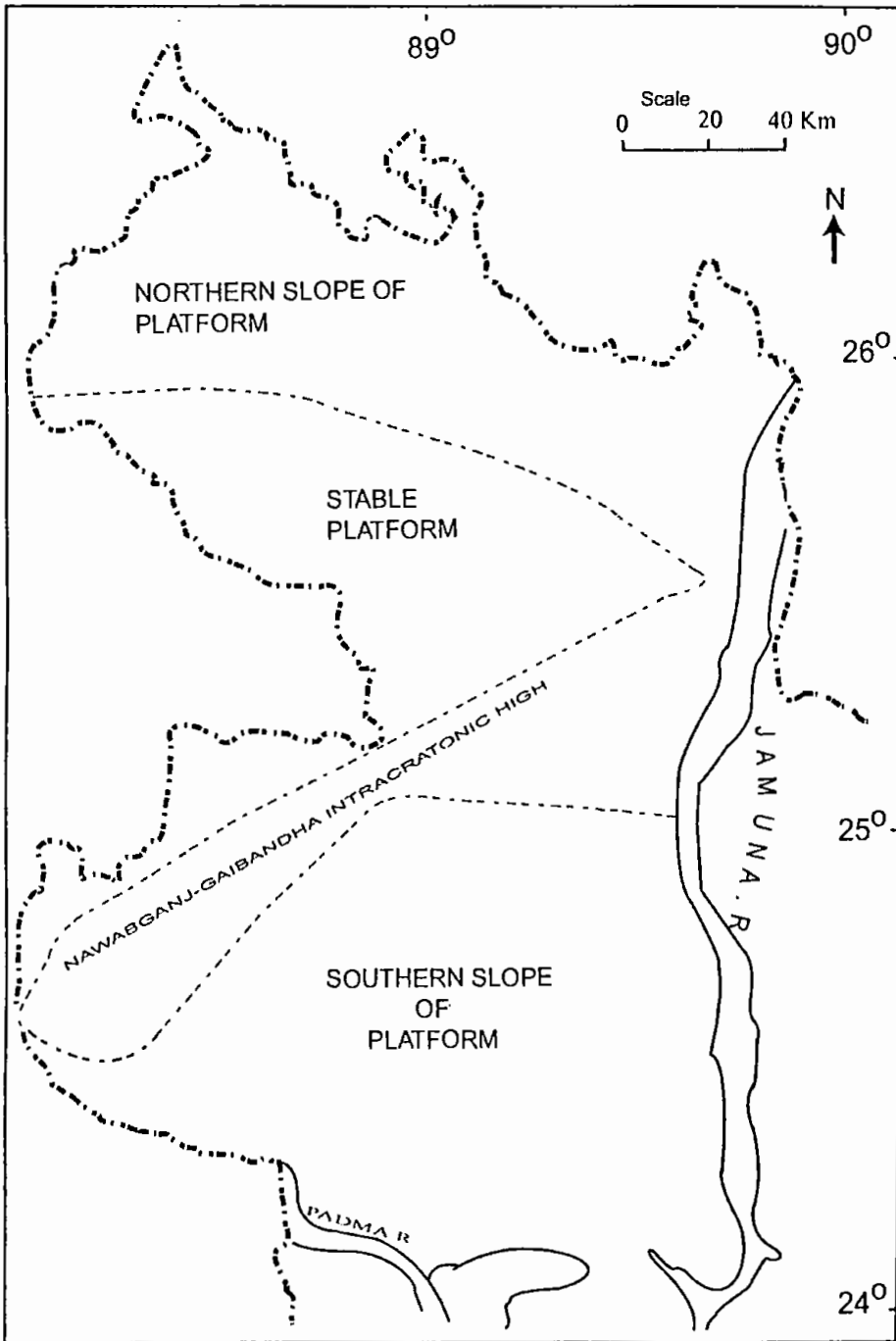
Modified after Khan, 1991 and Khan and Rahman,1992

Fig.-2.4: Tectonic map of the north-western part of Bangladesh

the Mahananda flood plain while its eastern margin is delineated by the Karatoya river.

In the south, the east-west trending basement fault no. 68 (Fig.2.5) indicates that the block, north of fault plane is up-thrown and that of south is downthrown.

On the other hand fault no. 60 (Fig.2.5) oriented in the NNE-SSW direction, has a down-throw to the east and up-throw to the west.

The western upthrown block of the fault no. 60 has been affected by enechelon type of faulting and this enechelon fault trend has separated the Barind high land from the Ganges flood plain.

Structurally the Barind is sub-divided into three units, which are:

- Western Barind - The area between the Mahananda and Punarbhaba rivers.

- Eastern Barind - The area between the Atrai and Karatoya rivers.

- Central or High Barind - The area between the Atrai and Punarbhaba-Mahananda rivers.

The study area is situated in the Central or High Barind area.
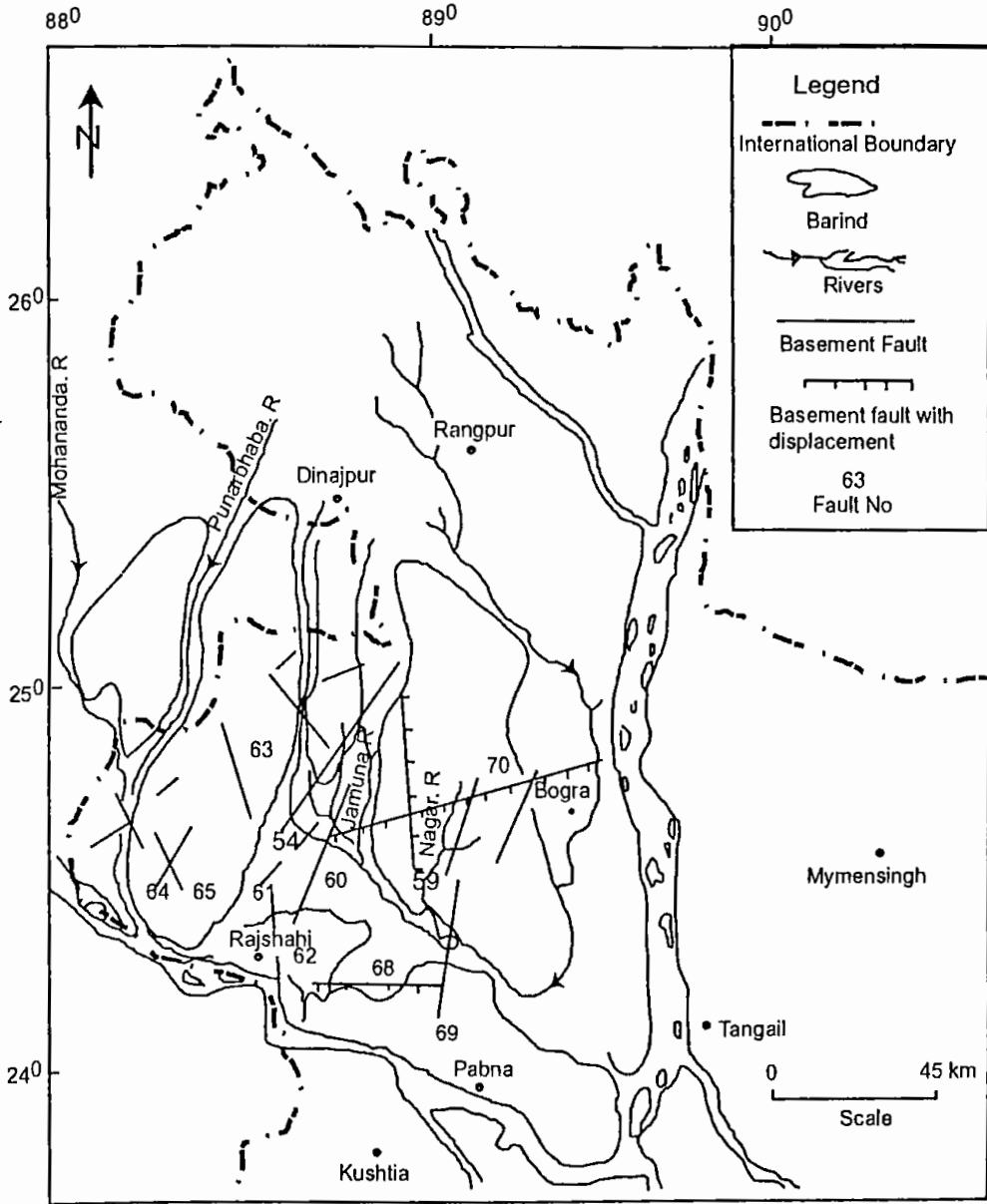
Modified after Hunling Geology and Geophysics ltd,1981

Fig.-2.5: Structural map of Barind Tract

Chapter-3
Hydrogeology

CHAPTER-3
HYDROGEOLOGY

To evaluate aquifer condition of an area it is necessary to determine the aquifer geometry of that area by using available bore log information.

3.1 Hydrogeological Cross Sections

Two hydrogeological cross sections have been constructed along NW-SE and NS directions of the study area (Fig.-3.1) which have been correlated between the wells up to the depth ranging from 37 to 75 m. Mean Sea Level (MSL) is considered as zero level while constructing well columns. Variations of lithological sequences are observed from the cross sections (Fig.-3.2, 3.3). According to the lithological constituents and on the basis of aquifer types the subsurface layers are divided into four zones.

Zone I: The zone extends vertically up to an average depth of 4 to 36 m below the ground surface and is composed mainly of clay with occasional fine sand and silt. Because of its lithological character, low permeability and productivity, this layer forms the aquitard, which is extended through out the whole of the study area. Most of the dug wells are situated in this zone.

Zone II: The thickness of this zone varies from 15 to 51 m and is mainly composed of fine, medium and coarse sand with gravel. From the lithological point of view, this zone forms the regional aquifer in the study area having moderate to highly permeable. Shallow tube well and deep tube well screens are installed in this zone.

Zone III: In some part of the study area there is another silty shale sequence below zone 11 ranging in thickness of about 2 to >17 m.
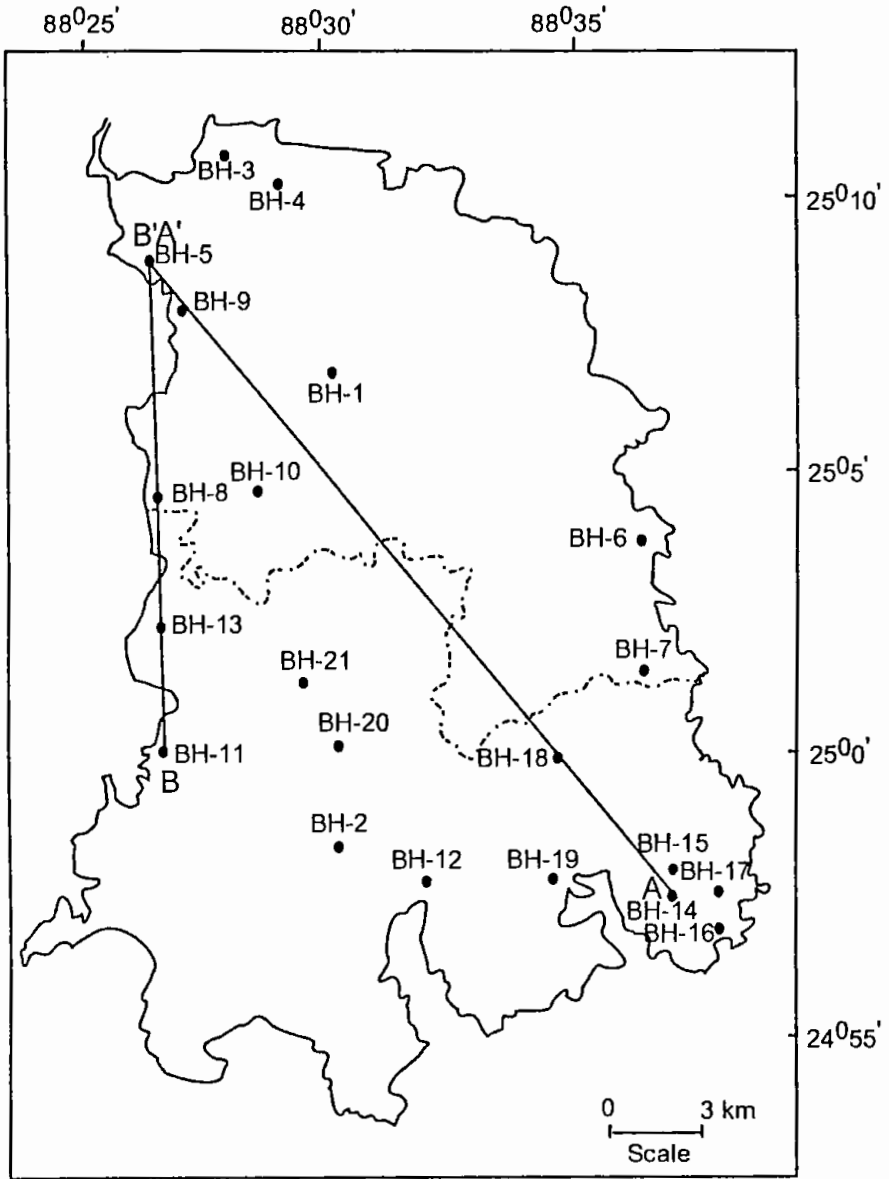
Fig.-3.1: Location map of subsurface regional cross section of the study area
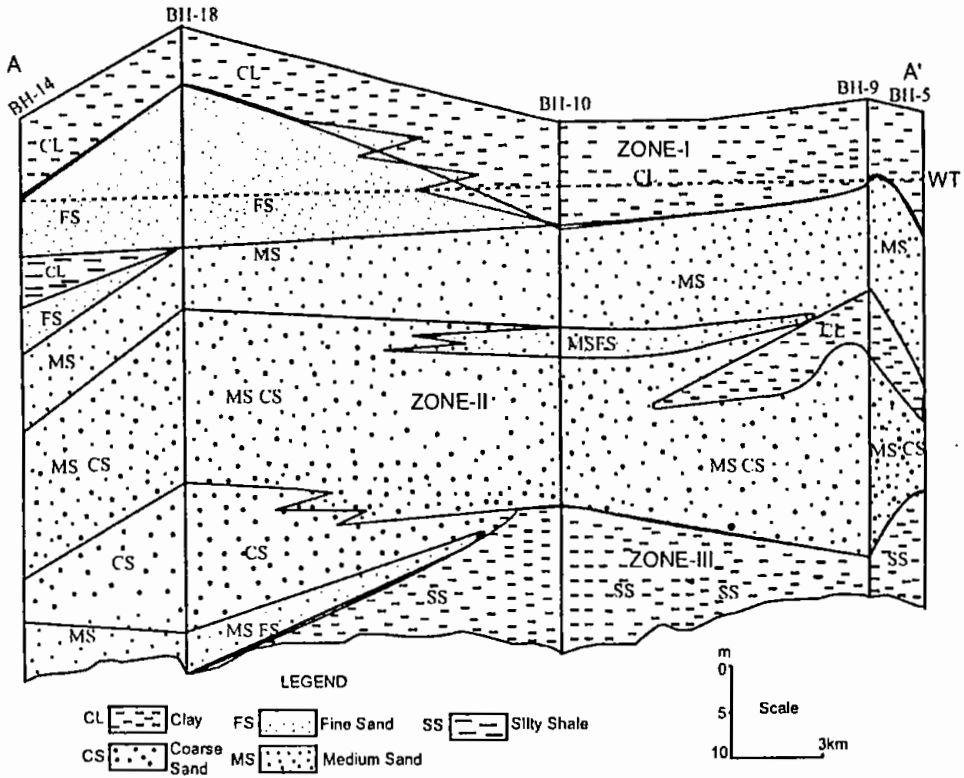
Fig.-3.2: Hydrogeological cross section map of the study area along AA'
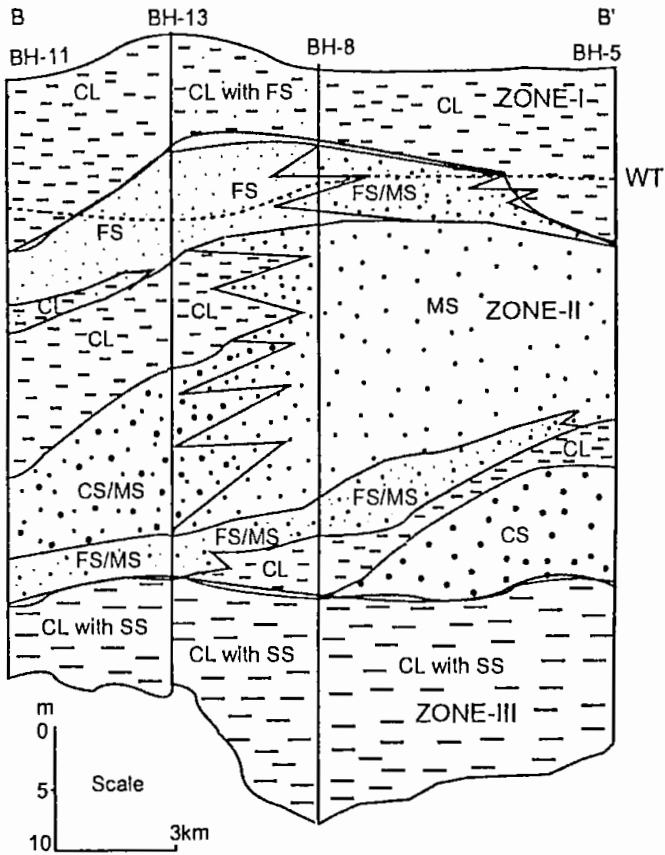
Fig.-3.3: Subsurface regional cross section along BB'

3.2 Stratigraphic Panel Diagram

Stratigraphic panel diagram has been constructed using six borehole lithologies to obtain a clear subsurface picture of the study area (Fig.-3.4). Lithological findings of panel diagram are described below:

The top sandy and silty clay aquitard of the study area varies in thickness from 4 to 36 m. This thickness gradually decreases towards the south. The thickness of the sandy aquifer varies from 15 to 51 m, which is mainly composed of fine, medium to coarse sand and in some places interbedded with find sandy layer. Lower silty shale layer exists in the central portion of the study area represents the lower boundary of the aquifer. Maximum thickness of this layer is found in the northeastern part of Sapahar Upazilla.

3.3 Top Sandy and Silty Clay Isopach

The top sandy and silty clay layer occurs from the ground surface to depth ranging from 4 to 36 m in the study area the thickness of the top sandy and silty clay of the study area is shown in fig.-3.5. The maximum thickness of clay layer (36 m) is observed in the northeastern portion of Sapahar Upazilla. The thickness gradually decreases towards the south. The minimum thickness (4 m) is observed at the northwestern portion of Porsha Upazilla.

The presence of sandy and silty clay at the surface reduces the quantity of groundwater available by gravity drainage and significantly reduces the groundwater potentiality of the study area. Presence of substantial lenses of silts and sands in top clay layer allows the piezometric surface to fall below the base of the clay, which helps to yield small amount of water to shallow wells.
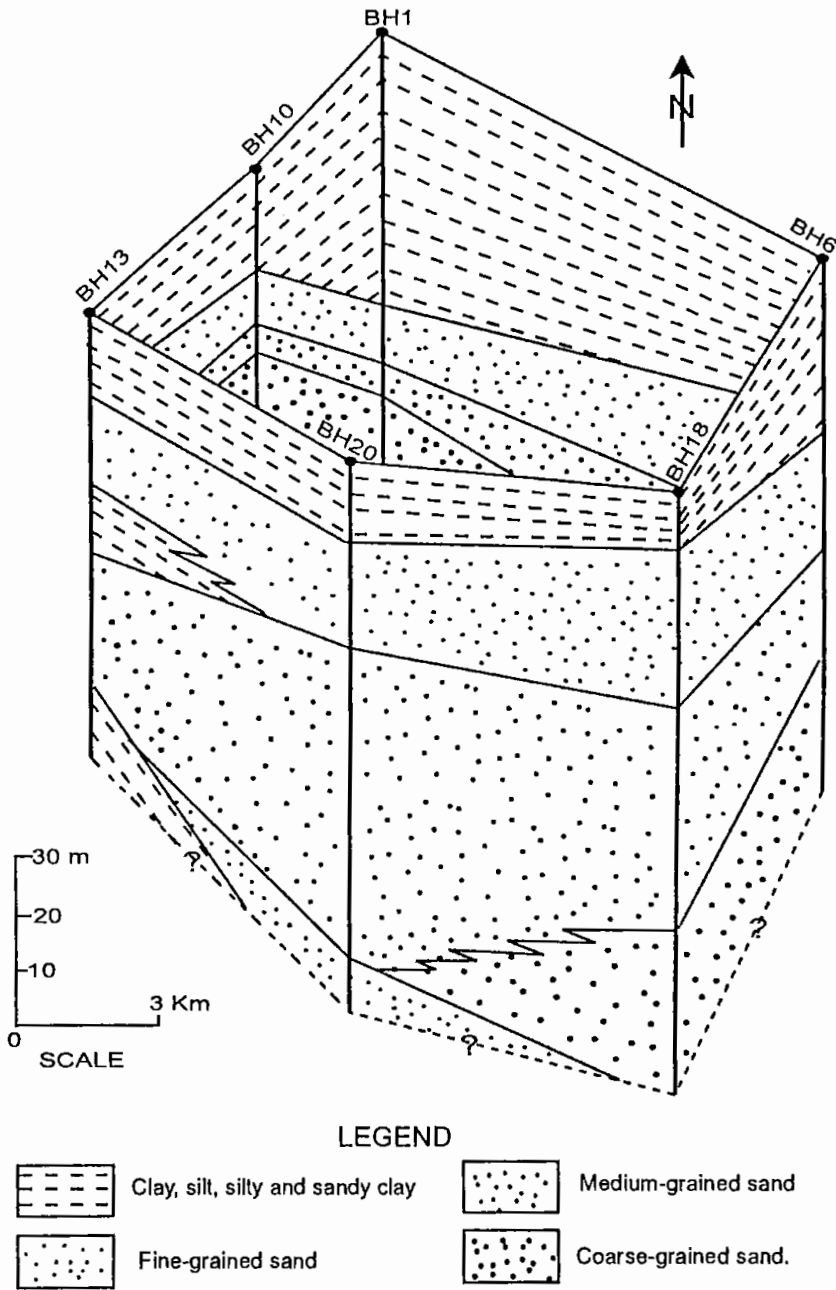
Fig.-3.4: Stratigraphic panel diagram of the study area
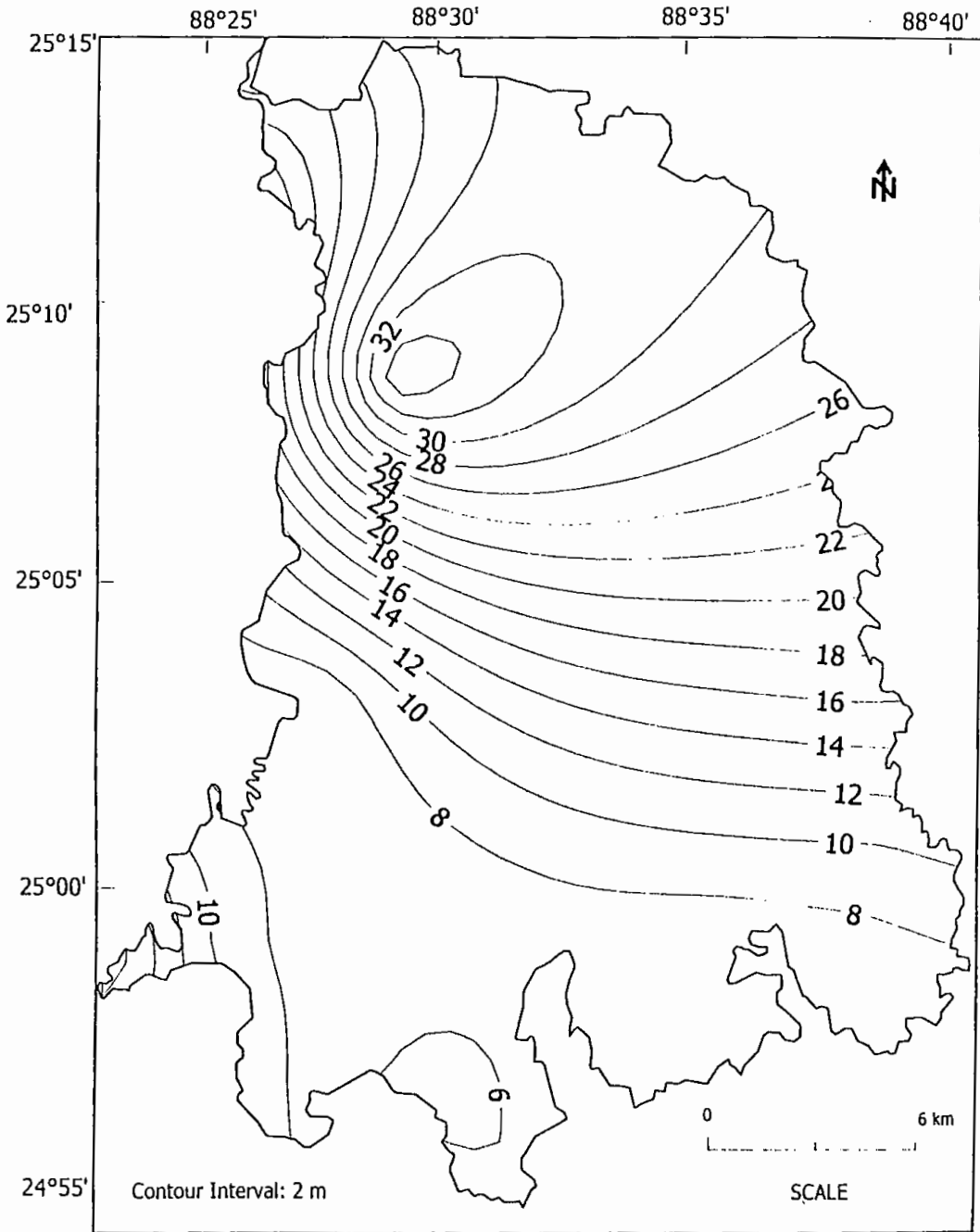
Fig.-3.5: Map Showing the Thickness of Top Clay of the Study Area

3.4 Clay-Sand Interface

The subsurface configuration of the interface between the top sandy and silty clay aquitard layer and the bottom sandy aquifer unit has been determined and shown in fig.-3.6. While preparing the clay-sand interface maps (Khan, et.al.,1986) the elevation of the interface above and below the mean sea level has been considered at each well. It is observed that a thick sandy and silty clay unit characterizes northeastern region where the clay-sand interface is situated at much greater depths. The clay rich depressed zone acts as an effective barrier and regulator to the flow of groundwater in this region.

The central part of Porsha Upazilla where the clay-sand interface map is characterized by several close contours indicating the sand layer (the aquifer) has its positions at much higher elevations than that of the adjacent clay rich zone. This subsurface configuration and their charge character should develop a hydrostatic pressure, which in turn controls the groundwater movements. The zones delineated as divergence and convergence are the resultant effects of the aforesaid conditions. The coincidence of minimum groundwater fluctuation with the zone of divergence also testifies to the existing subsurface hydraulic conditions.

3.5 Sandy Aquifer Isopach

Thickness of fine, medium to coarse sand layer ranges from 15 to 51 m (Fig.-3.7). Maximum thickness (51 m) occurs in the south- eastern portion of study area and minimum thickness (15 m) occurs in the northern portion of the study area.

The borehole information of the study area indicates the presence of fine to coarse sandy layers almost everywhere just below the top sandy and silty clay formations at different depth. The position of water level recorded in different observatories of the study area confirms that the fluctuation of water in the region lies within the sandy aquifer. After rainy season it stands totally within the top sandy and silty
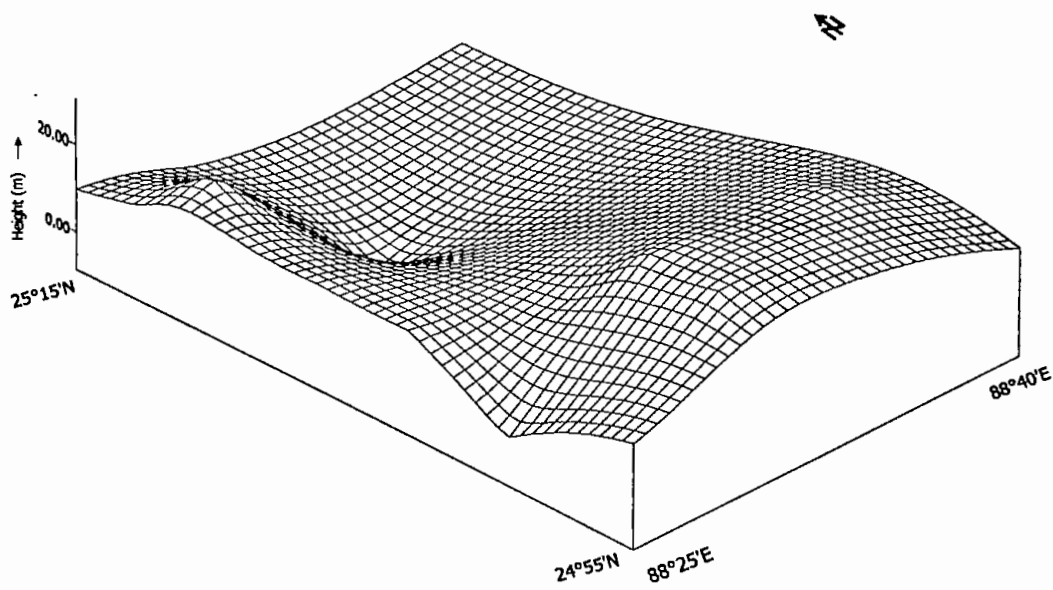
Fig.-3.6: Map Showing the Trend of Clay-Sand Interface
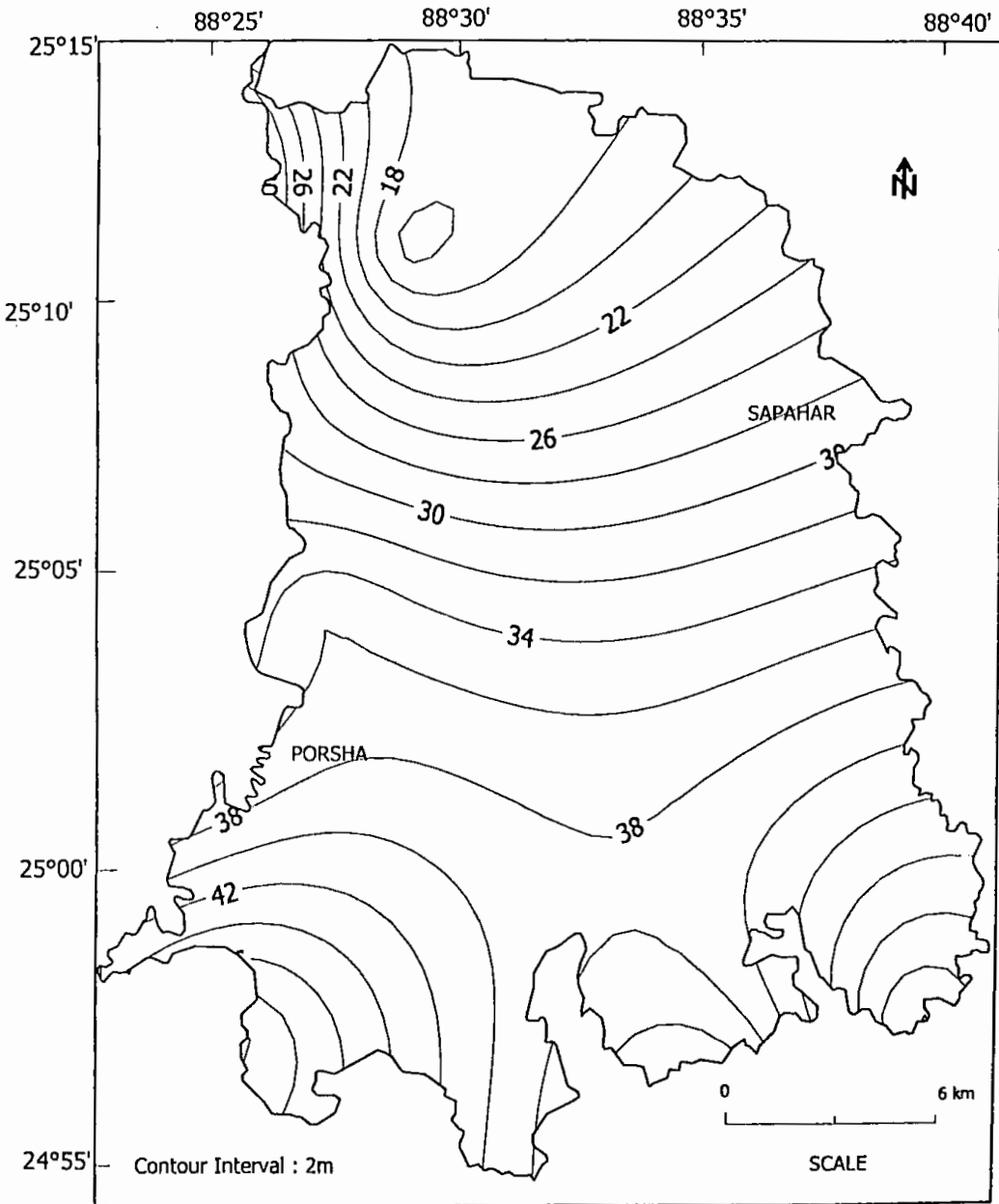
Fig.-3.7: Isopach Map of Composite Aquifer

clay layer and in extreme dry season in many places it falls into the sandy aquifer. In the study area the sandy aquifer serves as a source of groundwater.

3.6 Silty Shale Sequence

The thickness of the silty shale sequence ranges from 2 to >17 m in places. The lower boundary of the unconfined aquifer is a layer of much less permeable material than the aquifer itself. Such impermeable layers may consist of clay or other fine textured granular material or bedrock. As far as the first aquifer is concerned, the passage of the water to and into it and its other characteristics are determined essentially by geographical conditions. As the depth of horizon increases the geographical influence becomes progressively slighter. In the area the only specified water bearing formation is unconfined in nature found within the depth of 37 to 75 m from the earth surface. So the geographical pattern of the intersecting beds of different compositions plays a major role in the occurrence, distribution and movement of underground water. This impermeable zone is underlying the composite sandy formation.

3.7 Analysis of Groundwater Table

Contour maps of the maximum and minimum elevation of groundwater table for the years 1991 and 2000 have been prepared and are shown in fig.-3.8 to 3.11. The maximum and minimum elevation of groundwater table represent water table elevation of rainy (June-Oct) and dry (March-May) respectively. In rainy season elevation of the groundwater table from MSL varies from 20 to 34 m, where highest value (34 m) is observed in the central part of Porsha Upazilla. Lowest value of maximum groundwater table elevation (20 m) is observed in the southeastern and southwestern Porsha Upazilla and northwestern portion of Sapahar Upazilla. The maximum elevation of water table contour maps in rainy season (Fig.-3.8 to 3.9) shows prominent radially diverging pattern in the central portion of Porsha Upazilla.
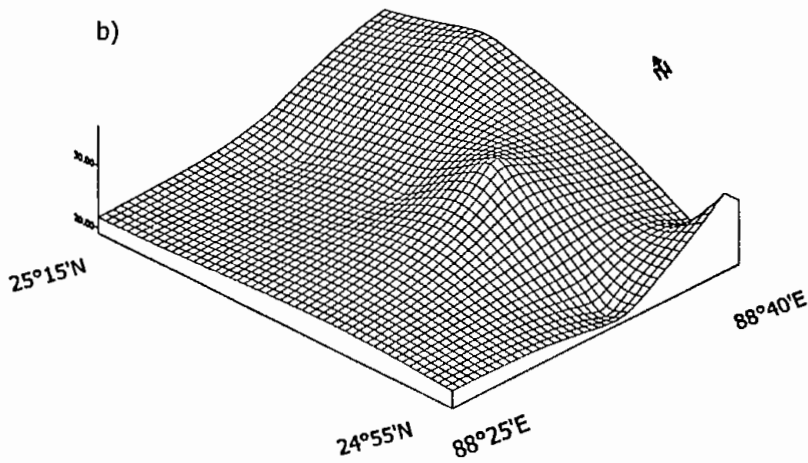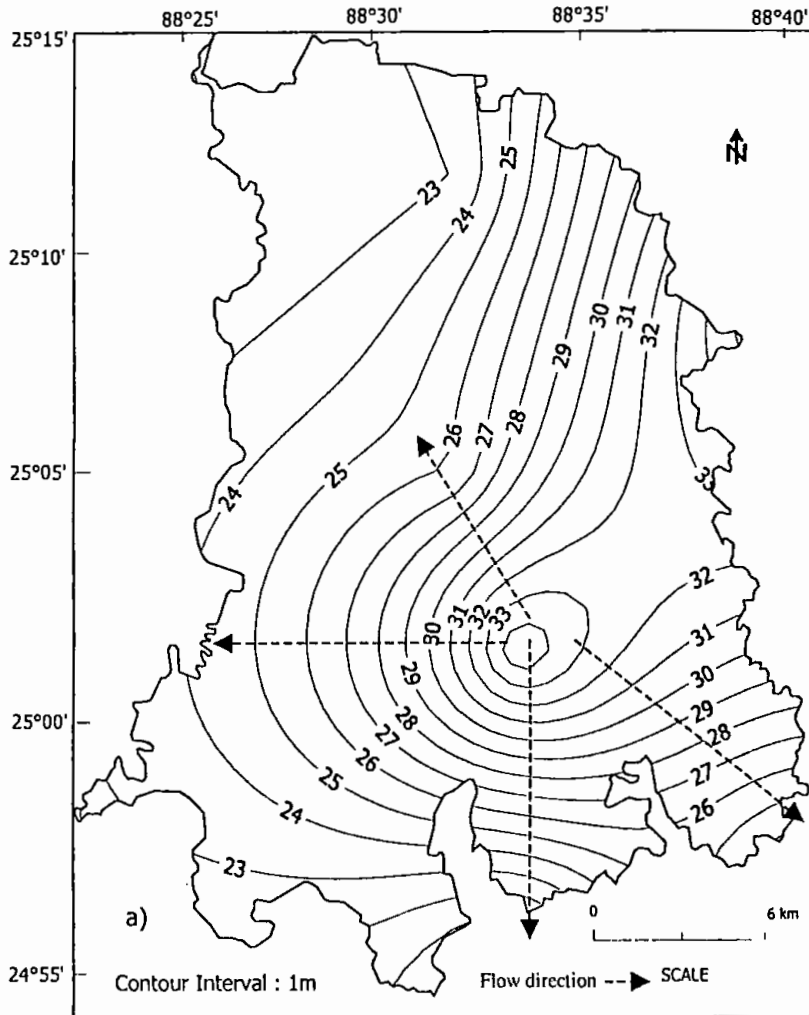
Fig.-3.8:   Maximum Groundwater Table Elevation Map for the Year 1991
a) Contour Map; b) Trend
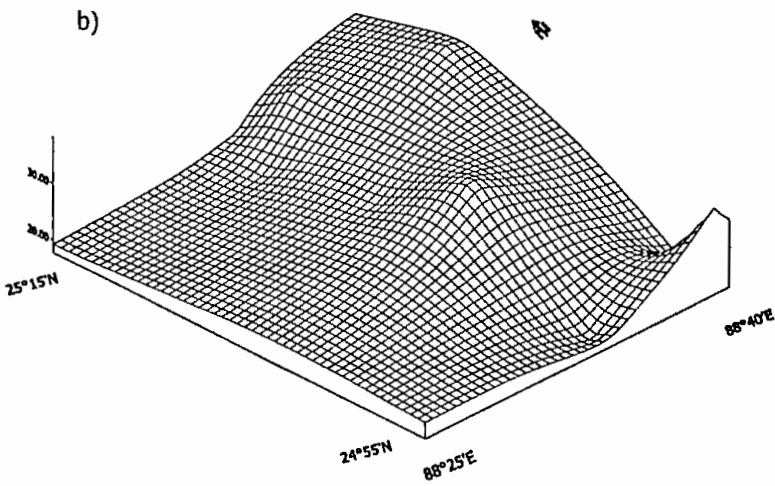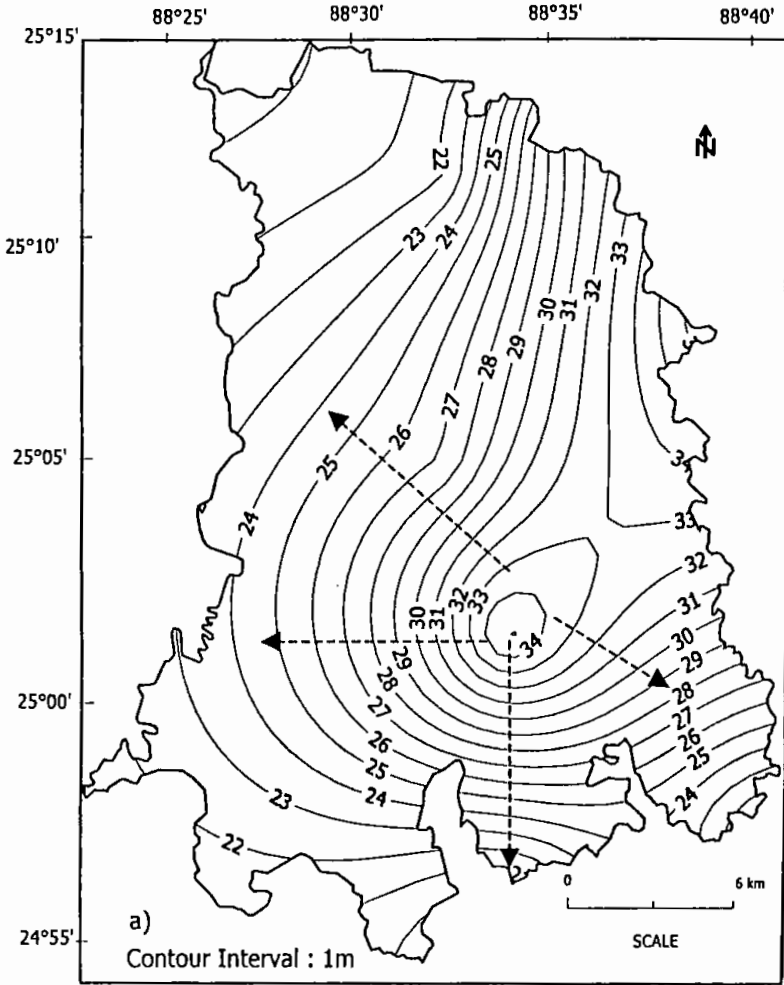
Fig.-3.9: Maximum Groundwater Table Elevation Map for the Year 2000
a) Contour Map; b) Trend
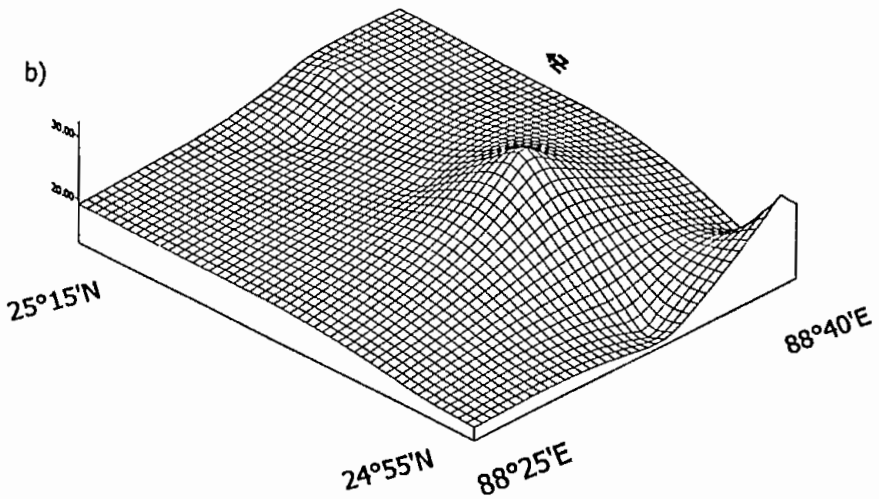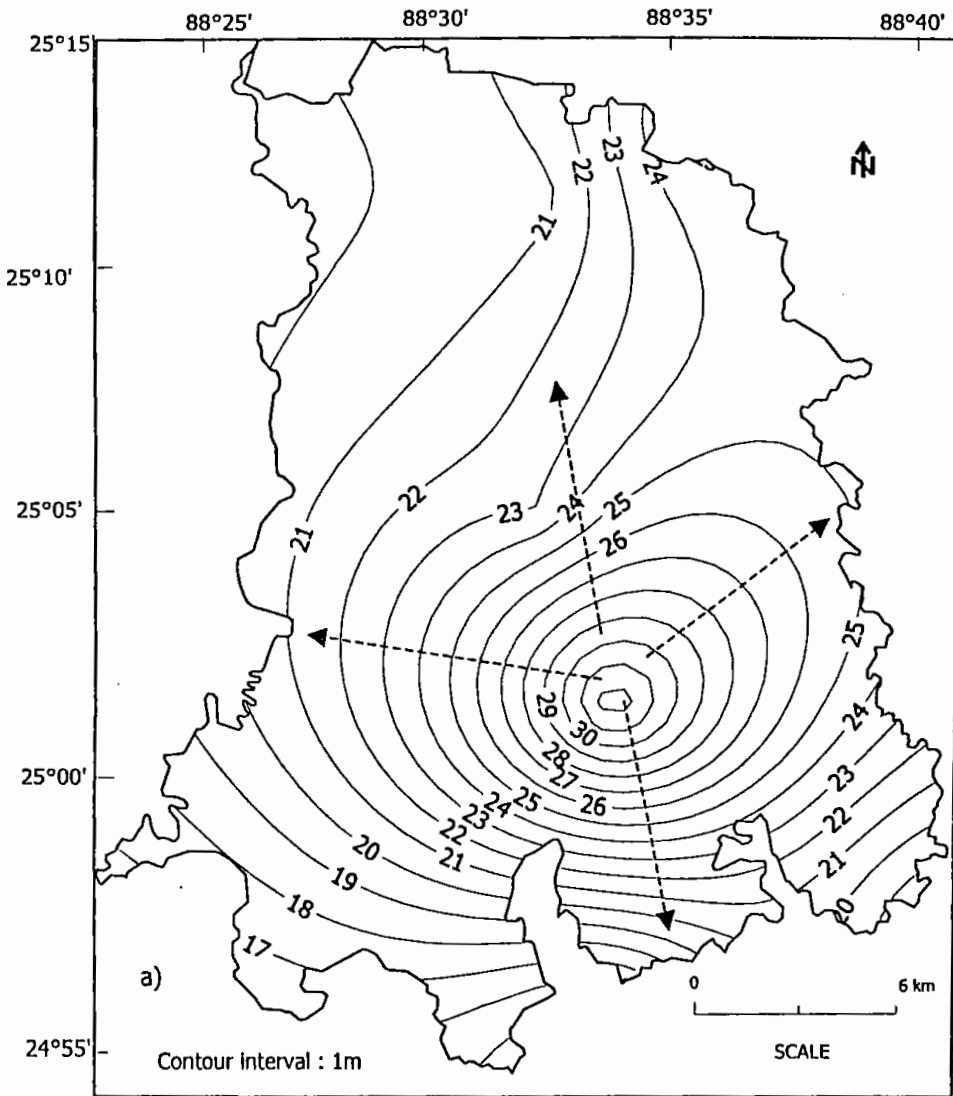
Fig.-3.10: Minimum Groundwater Table Elevation Map for the Year 1991
a) Contour Map; b) Trend
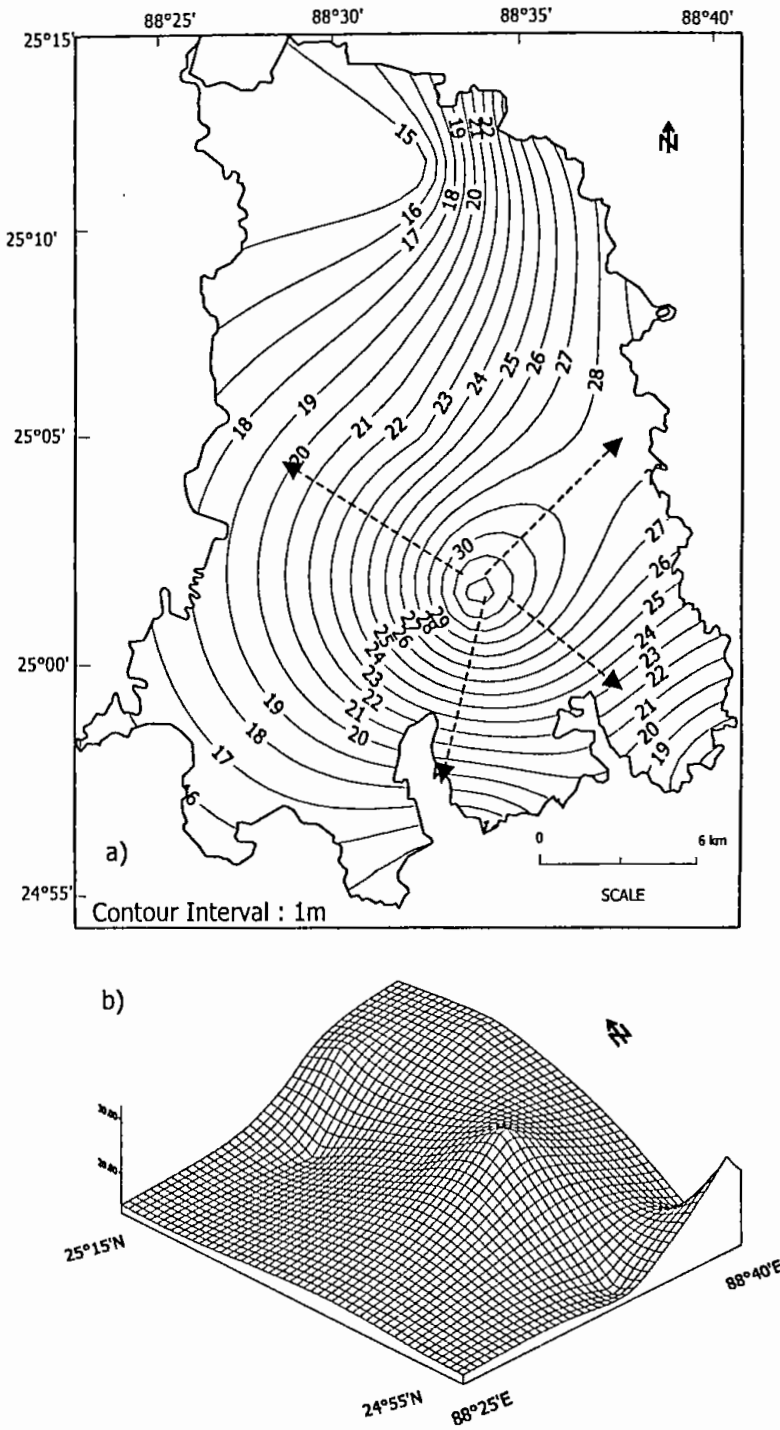
Fig-.3.11: Minimum Groundwater Table Elevation Map for the Year 2000
a) Contour Map; b) Trend

In dry season highest value of groundwater table elevation (32 m) is observed in the central part of Porsha Upazilla and the lowest value (15 m) is observed in the southeastern and southwestern part of Porsha Upazilla and northwestern part of Sapahar Upazilla.

In the Barind area the depth to groundwater table from ground surface is higher than the surrounding areas both in dry and wet season. The maximum depth to the groundwater table from land surface occurred during dry season in the months of May/June of the year 2000 and it varies form 4.32 to 10.75 m. It is also evident from the contour map (Fig. 3.10 to 3.11) of static water level in dry season. In general the depth is greater in the Barind region than the flood plains. The minimum depth to the water table varies from 1.7 to 6.96 m as observed in September/October, 2000.

3.8 Groundwater Table Fluctuation

Change in storage, resulting from difference between supply and withdrawal of water cause level to vary with the span of time. So the groundwater level fluctuation of an area is the difference between the highest and lowest elevation of water table. The groundwater table fluctuation and its trend in the study area for the years of 1999 and 2000 are shown in fig-.3.12 to 3.13.

The groundwater table fluctuation for the years 1991 and 2000 of the study area varies from 2 to 8 m. The maximum value of fluctuation (8 m) is observed in the northern part of the Sapahar Upazilla. The minimum value of fluctuation (2 m) is observed in the central part of Porsha. The annual fluctuation of groundwater table is directly related to recharge and discharge conditions. Most of the groundwater abstractions take place in the dry months starting from January and continues up to May (also June in some dry years). During this period the recharge is almost nil, the rate of evaporation and evapotranspiration is high and most of the river flows receive groundwater from aquifer as base flow. As a result
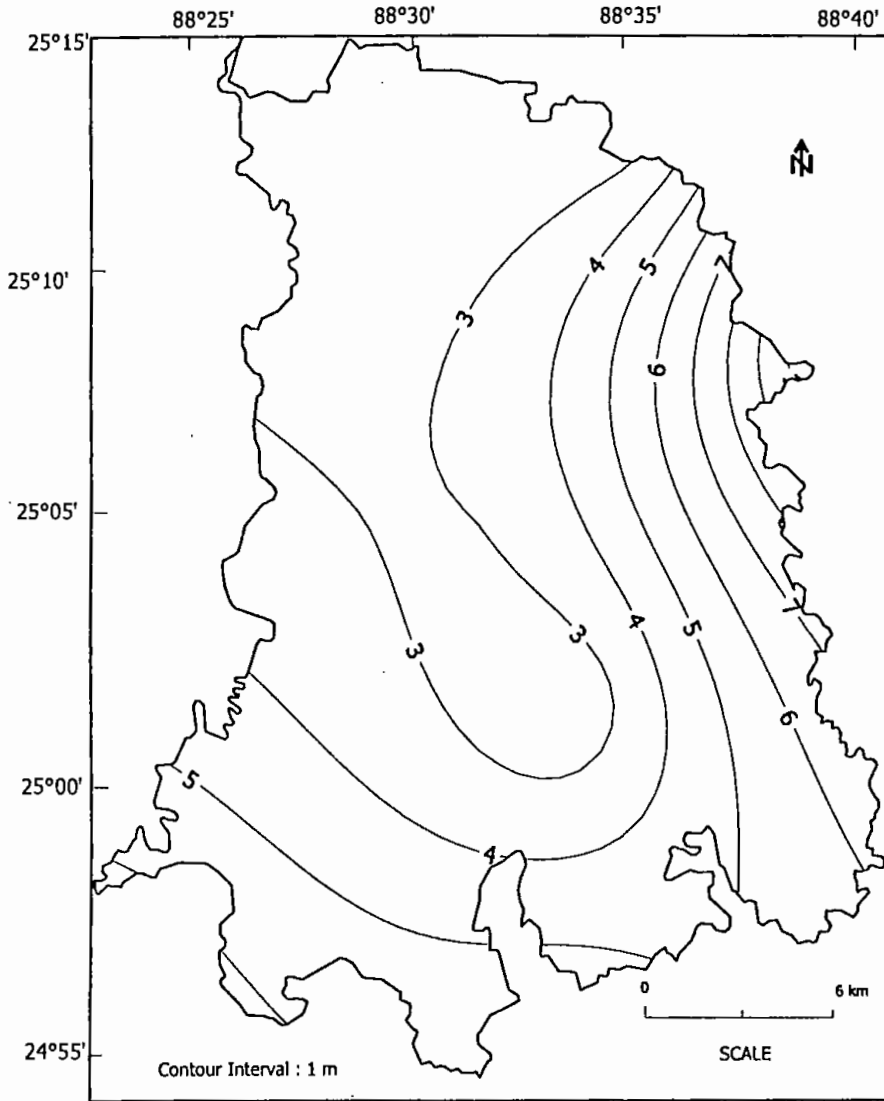
Fig.-3.12:Groundwater Table Fluctuation Map for the Year 1991
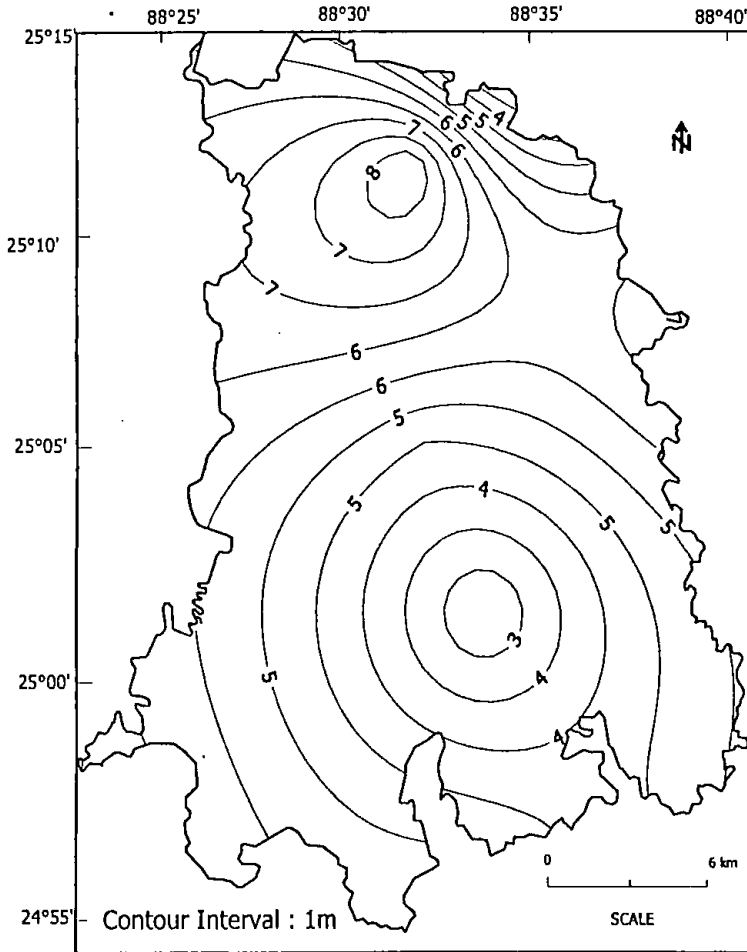
Fig.-3.13: Groundwater Table Fluctuation Map for the Year 2000

of all these natural and artificial withdrawal, the water table declines sharply and reaches to maximum depth in May or June. Rain starts in the pre-monsoon period and at the same time the recharge to the under ground storage begins. The major artificial abstraction of groundwater is also stopped by this time and high relative humidity in the atmosphere reduces the rate of evaporation and evapotranspiration. All these cause a gradual increase in the groundwater reservoir, which is reflected by the change in the water table. The water table starts moving upward and reaches to minimum depth from the land surface in September/October at the end of rainy season. The minimum fluctuation is observed in the flood plains whereas the maximum is found in the high Barind area.

3.9 Groundwater Flow Pattern

The groundwater table contour indicates the energy head, flow lines or streamlines and the lines perpendicular to groundwater table contours furnish the direction and movement of groundwater. Using the groundwater table contour maps not only areas can be selected which suggest the best possible sources of groundwater supply but also areas of favorable permeability can be ascertained (Todd, 1980).

The maximum and minimum groundwater table elevation contour maps were prepared based on data to study the groundwater movement and flow of the study area and are represented in fig.-3.8 to 3.11.

The general trend of groundwater flow is towards the north, west, south and eastern part of the study area from the central part. It is observed from both the maximum and minimum elevation of groundwater table contour map that the central part of the study area represents prominent NS elongated diverging zone. The groundwater flows radially towards east, west north and south from the central part of the study area. So the rivers gain water from the groundwater

reservoir. The water flowing below the ground surface is controlled by its gradient.

Several faults are present in the study area. These faults act as barrier for the groundwater movement from the central part towards the Atrai flood plain region. Central part of the study area has been uplifted and Atrai flood plain region has been subsided. Water cannot move through the sand aquifer because the contact of the subsided part of the top sandy and silty aquitard of clay with the uplifted part of sand unit.

3.10 Surface Water Groundwater Relationship

The mechanism whereby surface water becomes groundwater and vice versa, are important in groundwater hydrology because they determine water balances and hydrologic safe yields of aquifer and groundwater basins. Surface water becomes groundwater through infiltration of rain and irrigation water and seepage from streams and channels.

Following approaches are considered in relating the surface water and groundwater of the study area and are mentioned below:

3.10.1 Hydrograph Correlation

The groundwater hydrograph is related to both the river hydrograph and to the recharge/discharge cycle caused by rainfall recharge and upward capillary losses.

The influence of the fluctuating river levels on the groundwater levels at the observation point is a function of the groundwater systems geometry, its hydrological characteristics and the distance of the observation point from the river.

A well hydrograph is prepared with two of the observation wells information (Well No. RJ-04 and Well N0. RJ-33) of the study area showing the annual

fluctuation of water level for a period of 10 years (1991 to 2000) as shown in the fig.-3.14 and 3.15. From the hydrograph it is evident that the water level is fluctuating between 1.95 to 16.90 m from the ground surface. It is also found that the maximum (16.90 m) decline of groundwater level occurs during the year 1991.

The relationship between the groundwater and surface water was studied by constructing long term (1991-2000) groundwater and river stage hydrographs along with rainfall data of the following stations.

Station 1:

Hydrograph of groundwater observation well at Porsha and river Punarbhaba along with corresponding rainfall data.

Station 2:

Hydrograph of groundwater observation well at Sapahar and river Punarbhaba along with corresponding rainfall data.

The rainfall charts and hydrographs of the above mentioned stations are shown in the fig. 3.14 and 3.15. The hydrographs show that the groundwater levels and river levels are apparently related to rainfall and groundwater level tends to rise with the intensity of rainfall. It is also observed that the groundwater levels correlate with the river stage suggesting lateral inflow from the river during the monsoon.

Studies have proved conclusively that there is a hydraulic connection between the groundwater reservoir and the streams. At high discharge stages there is a direct lateral recharge from the streams to the shallow groundwater induced by head differentials. During periods when the stream level is below the groundwater level the flow reverses and groundwater discharges into the streams as base flow.
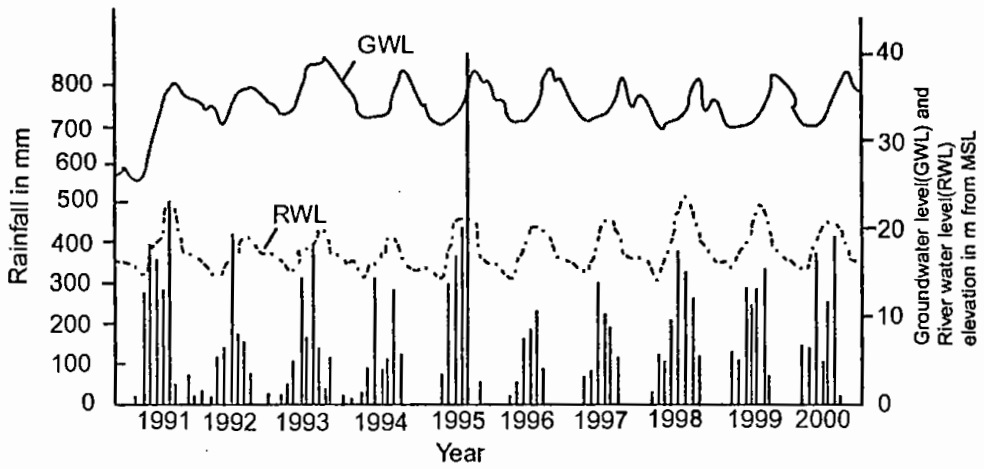
Fig.-3.14: Hydrograph of groundwater observation well with
corresponding river stage and rainfall at Sapahar
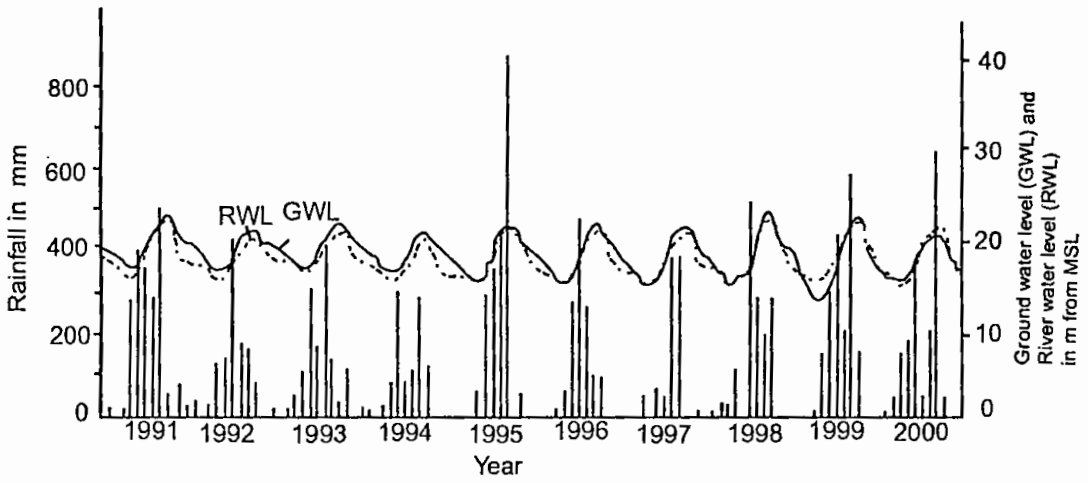
Fig.-3.15: Hydrograph of groundwater observation well with
corresponding river stage and rainfall at Porsha

3.10.2 Hydrographs Analysis

The Punarbhaba and Atrai rivers are effluent rivers from November to April. With the advent of the monsoon the rivers receive a huge amount of water and the water level reaches its peak from August to October and the river levels exceed the groundwater level. Groundwater levels start rising from the month of May and reach their peaks in the months of August and September. River water levels start receding and coincide with the groundwater levels in the months of October and November.

Groundwater table analysis shows that in most of the areas the dry season decline is getting higher and higher every year and it is not fully recovered during the wet season. As a result a gradual and permanent decline in the water table is observed.

It is needless to mention that the declination of water level is mainly due to excessive withdrawal of groundwater. Since 1984, Barind Multipurpose Development Authority (BMDA) has undertaken a program of installation of few thousands of deep tube wells for irrigation in the area. Soon after beginning of the functioning of the scheme, several adverse effects was found during the dry period, such as, abrupt fall of groundwater level, discharge of hand tube wells ceases to minimum and in some cases it is totally failed to yield any water and almost all the dug wells become dry. This declination of water level has been bringing some major ecological changes also in the region, particularly in the high Barind area.

3.11 Surface Water Potentiality

The study area is represented by a good surface water potentiality. The rivers Punarbhaba and Atrai provide a major source of surface water for study area. A number of beels are found in the study area. The beels serve to provide the permanent source of surface water. In the study area, a number of canals, small

rivers and ponds are also found. They serve as the sources of surface water. The surface water potentiality of the study area is shown in fig. 3.16.

3.12 Delineation of Water Bodies from Landsat Imagery

It is inferred from the landsat imagery (Fig. 3.17) that near about 12 to 15% of the total area is occupied by surface water bodies. These water bodies include large ponds, canals, depressions and small rivers and their tributaries and distributaries.
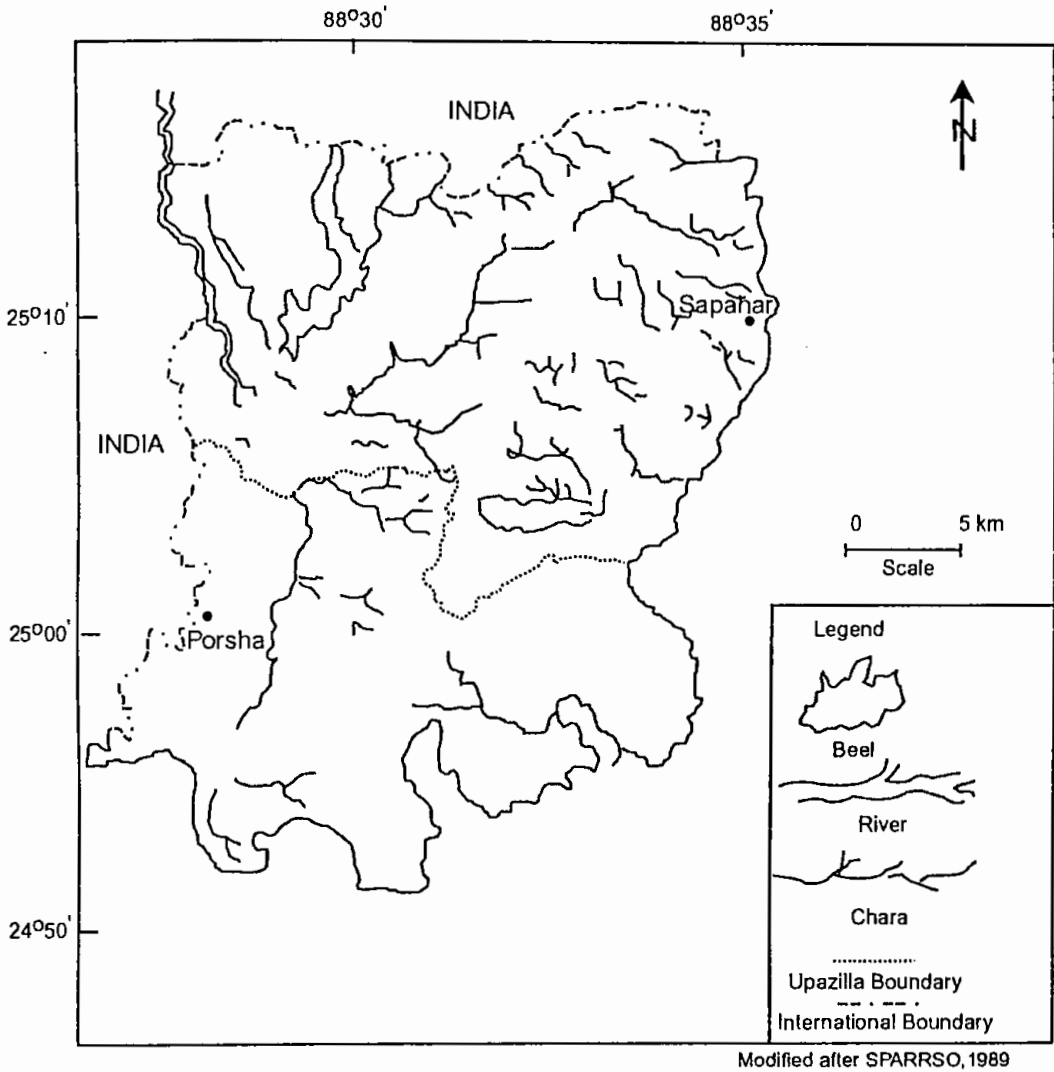
Fig.-3.16: Drainage map of the study area
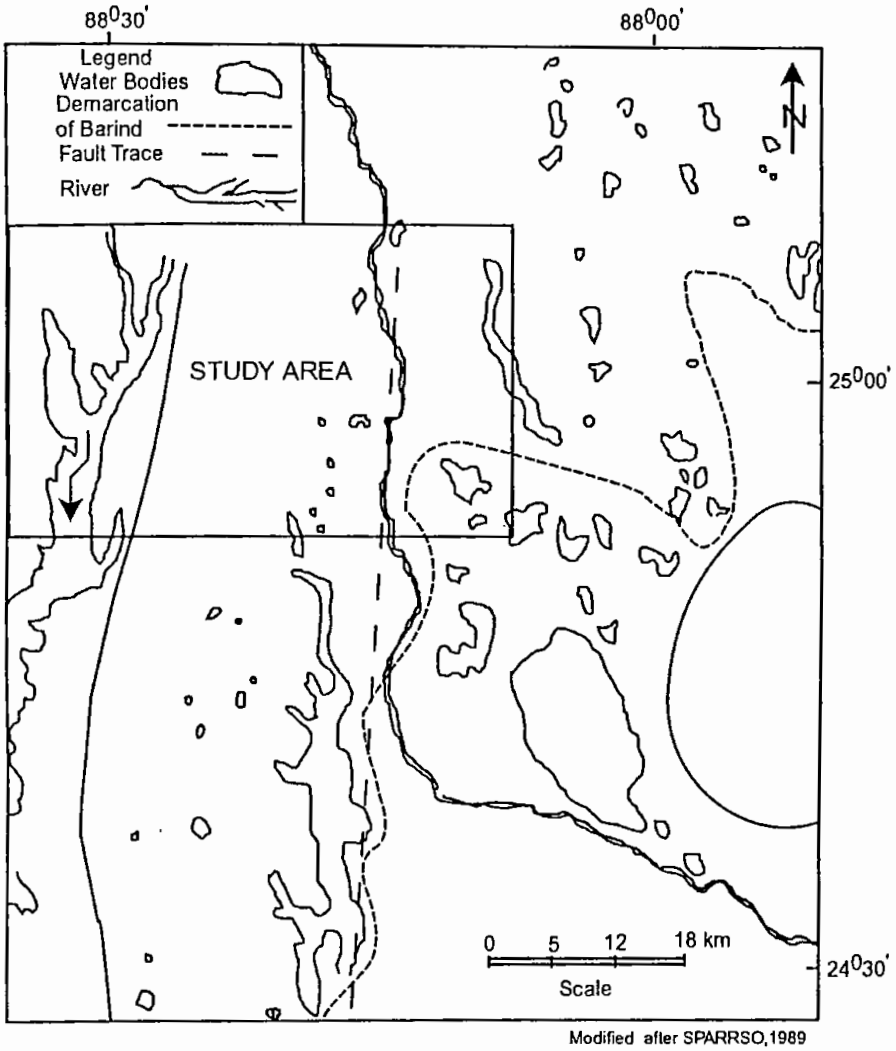
Fig.-3.17: Distribution of water bodies in Barind Tract from Landsat imagery

Chapter-4
Geo-electrical
Resistivity Survey

CHAPTER-4
GEO-ELECTRICAL RESISTIVITY SURVEY

Whatever the geophysical method being used to solve a particular problem the aim will be to acquire information quickly and cheaply consistent with obtaining enough data of sufficient accuracy for an adequate interpretation to be made. The choice of the method will depend to a considerable extent on the geology and nature of the problem involved.

In hydrogeology a very wide range of problem is met demanding for their solution anything from a few depth sounding to a long and detailed survey. Major investigations are likely to involve also drilling, borehole logging and the use of other geophysical methods. In some instances the resistivity survey may only be used to determine the geometry of unknown aquifer, that is, its depth and thickness, lateral extent and the degree, and nature of any faulting.

4.1 Basic Principles of Resistivity Method

Geo-electric exploration consists of exceedingly diverse principles and techniques and utilizes both stationary and variable currents produced either artificially or by natural process. One of the most widely used methods of geo-electric exploration is known as the resistivity method. In this method a current (direct or very low frequency) is introduced into the ground by two or more electrodes and the potential difference is measured between two points (probes) suitably chosen with respect to the current electrodes. The potential difference for unit current sent through the ground is a measure of the electrical resistance of the ground between the probes. The resistance is a function of the geometrical configuration of the electrodes and the electrical parameters of the ground. From knowledge of the potential drop, current and electrode spacing, the ground resistivity can be easily calculated.

For a quantitative treatment, let us consider a homogeneous isotropic earth layer of resistivity ρ, length L, resistance R and cross sectional area A, through which a current I is passing.

Ohm's law gives the potential difference across the ends:

$$\Delta V = RI \qquad\text{...(4.1)}$$

By definition, $R = \rho l/A$, the above equation can be rewritten as:

$$\Delta V = \rho I \; l/A$$

$$\text{or,} \quad \Delta V/I = \rho l/A$$

$$\text{or,} \quad \text{grad}V = \rho i \qquad\text{................................(4.2)}$$

Where, gradV stands for the potential gradient, and i is the current density.

The next step in the development of the theory is to derive the potential in a homogeneous medium due to a point source of the current. Now consider a semi-infinite conducting layer of uniform resistivity bounded by the ground surface and let a current of strength + I enter at point A on the ground surface (Fig.-4.1). This current will flow away radially form the point of entry and at any instant its distribution will be uniform over a hemispherical surface of the underground of resistivity ρ. At a distance r, away form the current source, the current density i, would be:

$$i = I/2\pi\, r^2 \qquad\text{...(4.3)}$$

The potential gradient $-\delta v/\delta r$ associated with the current is given by equation can be written as

$$-\delta v/\delta r = \rho i = \rho I/2\,\pi\, r^2 \qquad\qquad\text{............(4.4)}$$

The negative sign indicates here to express the fact those potential increases in the opposite direction to the current flow. The potential at a distance r (for example, at point P in fig.-4.1) is obtained by integrating equation (4.4) and is:
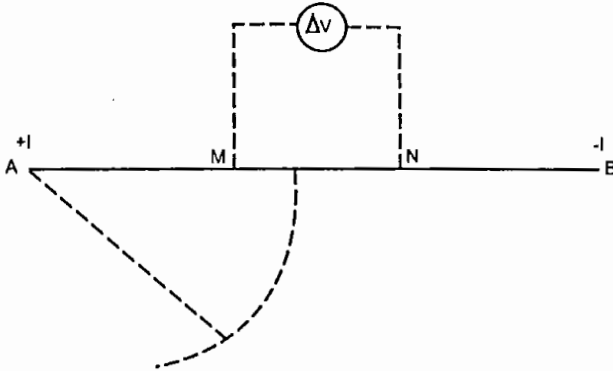
Fig.-4.1a: Method of calculating potential distribution due to current source in a homogeneous medium
Modified after Todd, 1980
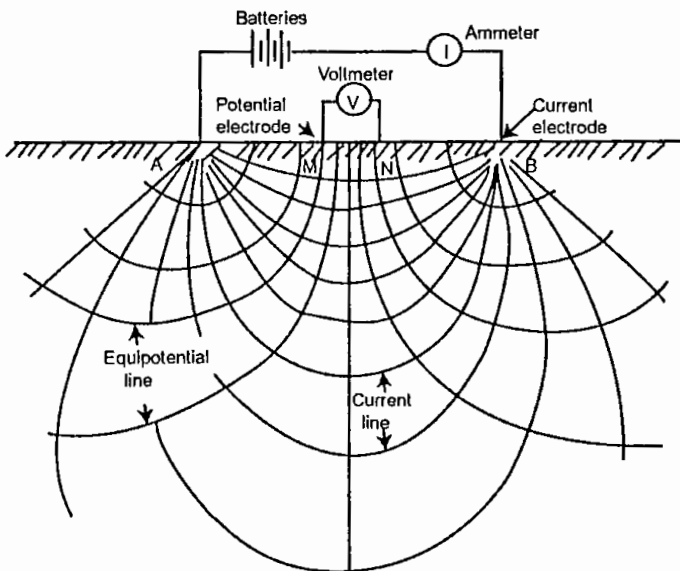
Fig.-4.1b: Electrical circuit for resistivity determination and electrical field for a homogeneous subsurface stratum
Modified after Todd, 1980

$$V = I\rho/2\,\pi\,r \quad \ldots\ldots\ldots\ldots\ldots\ldots\ldots\ldots\ldots\ldots(4.5)$$

This is the basic equation, which enables the calculation of the potential distribution in a homogeneous conducting semi-infinite medium. Fig.-4.1a,b shows the distribution of the potential and the lines of current flow in the vertical section of a homogeneous conducting underground medium due to a pair of current electrodes (Sharma, 1978).

4.2 Resistivity Measurement

From equation (4.5) it is easy to see that the potential difference between points M and N (Fig.-4.1b) caused by current +I at the source (entry point A) is:

$$V_A = (I\rho/2\,\pi).\,(1/AM-1/AN) \quad \ldots\ldots\ldots(4.6)$$

In the same manner, the potential difference between M and N caused by –I current at the sink is:

$$V_B = (-I\rho/2\,\pi).\,(1/AM-1/BM-1/AN + 1/BN) \ldots\ldots.(4.7)$$

The total potential difference V between M and N is, therefore given by the sum of the right hand side of equations 4.6 and 4.7:

$$V = (I\rho/2\pi).(1/AM-1/BM-1/AN+1/BN)$$

$$\text{or} \quad \rho = (2\,\pi V/I).\{1/(1/AM-1/BM-1/AN+1/BN)\}$$

$$\text{or} \quad \rho = (2\,\pi V/I).K \quad \ldots\ldots\ldots\ldots\ldots\ldots\ldots\ldots\ldots(4.8)$$

here K denotes the geometric factor of an electrode configuration. For field practice a number of different electrode configurations have been proposed. Several commonly used linear array type arrangements are: i) Wenner array, ii) Lee-partition array, iii) Schlumberger array, and iv) Dipole-Dipole array. Regardless of the specific electrode spread employed, there are really only two basic procedures in resistivity work. The particular procedure to be used depends

on whether one is interested in resistivity variations with depth or with lateral extent. The first is called electric sounding and the second electric profiling.

4.3 Data Acquisition

In the present study electrical resistivity survey is carried out in Sapahar and Porsha Upazillas and its surrounding area, which is a part of the High Barind Tract of Greater Rajshahi. Vertical Electrical Sounding (VES) employing Schlumberger configuration were conducted in different locations. A total of 12 (twelve) locations are selected (Fig.-4.2). Each location is assigned an individual VES number, such as, VES-1, VES-2, VES-3, VES-4, VES-5, VES-6, VES-7, VES-8, VES-9, VES-10, VES-11 and VES-12.

Fieldwork was carried out at least once in a year during the period of the field program the fieldwork was started in March. In the fieldwork twelve sounding points are covered. All this above fieldwork was made with the maximum current electrode separation of 170 m.

After allocating the VES stations data was acquired at each resistivity station by using the resistivity meter and employing Schlumberger configuration as discussed earlier. The instrument is positioned between the two current and potential electrodes.

Initially potential electrodes were at 1m on both sides and current electrode was placed at 5 m on both sides. The range selector and current selector were changed in need. Further readings were taken by changing he position of current and potential electrodes thus expanding the geometry. This positioning of electrodes is given in table 4.1.
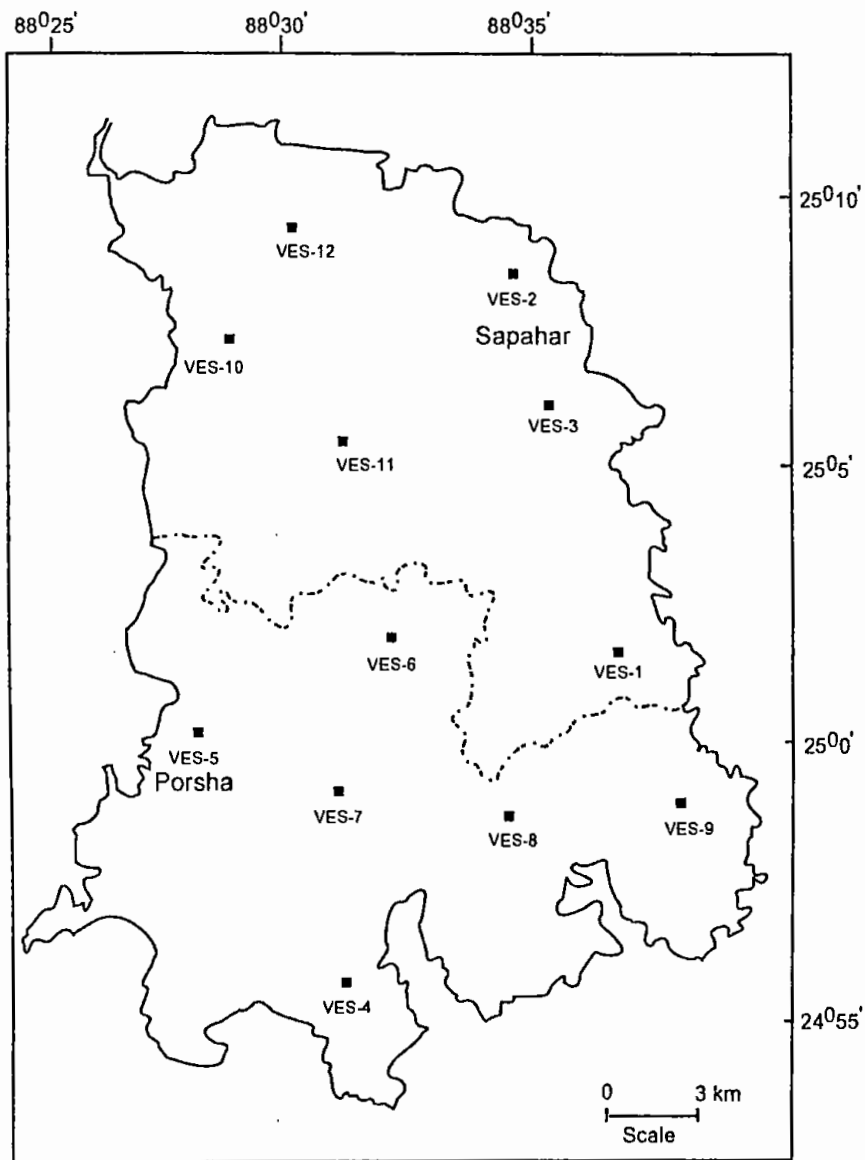
Fig.-4.2: Location map of VES stations of the study area

Table 4.1: Arrangement of electrodes spacing

SI No.	MN/2 (m)	AB/2 (m)
1	0.5	1
2		2
3		3
4		4
5	1.0	4
6		6
7		8
8		10
9	2.0	10
10		15
11		20
12	5.0	20
13		25
14		30
15		40
16		50
17	10.0	50
18		60
19		80
20		100
21	20.0	100
22		120
23		150
24	25.0	170

In this way data was acquired at each resistivity station along a line.

4.4 Interpretation

After acquisition of field data and primary indulge in the final process of interpretation. Interpretation simply means conversion of the processed field data into true geological information by using some standardized methods. Interpretation is basically of two types, that is, qualitative and quantitative, which are discussed below. The resistivity sounding curves were primarily interpreted using the semi-empirical Auxiliary Point Method. The interpretation of field observation in terms of layer parameters (for example, resistivity and thickness) is the basic task of a geo-electrical survey. The field data obtained in the form of an apparent resistivity curve (ρ_a) is interpreted in terms of basic theory and the

results are then correlated with available geo-hydrological information to arrive at a realistic picture of the subsurface structure. The first step is thus termed as physical interpretation and the subsequent procedure as geological interpretation.

Interpretation is broadly classified into qualitative and quantitative. The qualitative interpretation involves the study of the field data and types of the VES curves.

VES Curves:

The field values (VES data and curves) give a rough idea about the conductivity variation with depth. The VES curve is constructed and labeled and from this we know the number of layers and their relative resistivity. In the present study (Fig.-4.3 to 4.14) 12 VES curves were labeled and represented 3 and 4-layer cases. Among these eleven are 4-layer cases and one is 3-layer case.

Quantitative interpretation includes the computation of lithology as well as dimensions including the depth, thickness and lateral extension of the lithology. The thickness of a lithology is determined by partial curve matching technique as discussed above, whereas for the interpretation of lithology standardized tables, showing a range of resistivity values for a lithology, are used to express the true resistivity values in terms of some lithology. These standardized tables are available in literature, but these may not be applicable to the present study area because a lot of factors such as porosity, permeability and compactness due to overburden pressure greatly affect the resistivity values for a given lithology at any particular place. Thus such tables are prepared by studying samples of exposed rock, *nala* cutting and lithological logs for some predrilled wells.

Quantitative interpretation is made as indirect and direct depending upon the manner in which the parameters of the subsurface are deduced form the field observations.

Indirect Method:

In this method the field curve is compared with a set of precalculated master curves (Compagnie General de Geophysique, 1963; Orellana and Mooney, 1966; Rijkswaterstaat, the Netherlands, 1975) for known geological condition of the earth. A match of the curves is interpreted as a match of the parameters. There are four approaches, which may be used in interpreting multiple layer resistivity sounding data (Keller and Frischknecht, 1982): 1) Complete curve matching; 2) Partial curve matching; 3) Equivalent curve matching and 4) Observation of the position of the maxima and minima on the field data.

Out of these methods, the partial curve matching technique is widely used for preliminary interpretation. This semi-empirical method is also termed as "Auxiliary Point Method".

Direct Method:

Direct method is such method in which attempts have been made to determine the layer distribution directly form field measurements, by taking the help of certain mathematical process. Langer (1933) laid the foundation of the direct method and subsequently it has been widely investigated by different authors (Slichter, 1933; Pekeris, 1940; Vozoff, 1958; Koefoed, 1968; Moinardus, 1970; Kunetz and Rocroi, 1970) by means of different numerical or graphical procedures.

Twelve sounding points are selected for the study of the depth and thickness of aquifer. The field data of the twelve sounding (VES-1, VES-2, VES-3, VES-4, VES-5, VES-6, VES-7, VES-8, VES-9, VES-10, VES-11 and VES-12) have been interpreted.

4.5 Direct Interpretation of Field Data

The field data were interpreted by the direct method (Zohdy, 1989). The method of computerized interpretation of VES curves over horizontally stratified media

may be divided into two groups: the first group performs the transformation of VES curves into the corresponding resistivity transform curve using forward filters (Ghosh, 1971 and Koefoed, 1979). This resistivity transform curve is then interpreted using methods based on Pekeris (1940). But this technique has many drawbacks. The second group of interpretation method relies on inverting the sounding curve itself without first transforming it to its resistivity transform curve (Zohdy, 1975). In this iterative procedure a layering model is obtained directly from a digitized sounding curve. This method does not require a preliminary guess for the number of layers, their resistivity and thickness and it does not require extrapolation of first and last branches of the sounding curve to their respective asymptotes. The number of layers is equal to the number of digitized points and the layer boundaries are spaced uniformly on a logarithmic scale. This method provides a theoretical curve that fits the observed field curve as closely as possible and gives a corresponding well behaved layering model eliminating unusually high or low resistivity of extremely thin layers. In the present study this method has been adopted for interpretation of VES curves.

Initial Data Processing:

In general, a sounding curve is the composition of several overlapping segments. Then the segmented field curve is processed and reduced to a continuous curve prior to its interpretation in terms of horizontal stratified model. The purpose of digitizing the sounding curve is to speed up the computations of the succession theoretical sounding curves used in the iterative process. A sampling interval of six points per logarithmic cycles is considered optimal for defining the form of a sounding curve. The iterative process depends on the following initial assumptions:

1) The number of layers in the model equals the number of digitized points on the observed curve. The assumption remains unchanged throughout the iterative process.

2) The depths of the model layers are equal to the digitized electrode spacing, which are equal on a logarithmic scale.

3) The true resistivity of the model equals the apparent resistivity.

In practice, the true resistivity depth curve is unknown. Having calculated a theoretical curve using shifted depth and apparent resistivities, a better fit between the observed and calculated sounding curves is obtained by adjusting the amplitude of layer parameter. The iterative process is terminated when one of the following conditions are met:

1) 2 rms percent of deviation of field data.

2) Less than 5 percent fit.

3) Maximum of 30 iterations is reached. However, an average of 10 iterations is considered.

A fast iterative method for the automatic interpretation of Schlumberger sounding curves based on Zohdy (1989) has been used to determine the layer parameters of horizontally stratified subsurface media to propose a multi-layer model in the sounding locations.

VES-1: The sounding station is located in the eastern portion of study area. The surface elevation of the station is 38 m AMSL. The orientation of the profile was in E-W direction. 10 layers have been identified within the depth of 170 m. These results have been used in reducing this multi layer model to a 3-layer model. The thin layers of extremely low and high resistivities have been compressed and a model is prepared to best fitting with the digitized curve. The results show the fitting tolerance of 1.1 percent with the field curve. The field curve, the automatic interpreted results and reduced multi-layer model of VES-1 are shown in fig.-4.3a, 4.3b and 4.3c respectively. The layer parameters are presented in table 4.2.

a)

o--o--o
FIELD CURVE   VES-1

R
E
S
I
S
T
I
V
I
T
Y

O
H
M
-
M

ELECTRODE SPACING (AB/2) IN METERS

b)

o   o   o   ----------
DIGITIZED   CALCULATED   VES-1

R
E
S
I
S
T
I
V
I
T
Y

O
H
M
-
M

ELECTRODE SPACING (AB/2), OR DEPTH, IN METERS

c)

FIT=   1.815543E-02   VES-1

R
E
S
I
S
T
I
V
I
T
Y

O
H
M
-
M

ELECTRODE SPACING (AB/2), OR DEPTH, IN METERS

Fig. 4.3: a)Field Curve b) Automatic Interpreted Results
c) Reduced Multilayer Model of VES-1

Table 4.2: The interpreted results of VES-1

Layer number	Depth to the layer in meter	Thickness of the layer in meter	Resistivity of the layer in ohm-m
1	1.8	1.80	85.0
2	21.0	19.2	22.0
3	**	**	75.0

**Undetermined

VES-2: The sounding station is located in the northeastern portion of study area. The surface elevation of the station is 37 m from MSL .The orientation of the profile was in N10°E direction. 10 layers have been identified within the depth of 130 m. These results have been used in reducing this multi layer model to a 4-layer model. The thin layers of extremely low and high resistivities have been compressed and a model is prepared to best fitting with the digitized curve. The results show the fitting tolerance of 1.1 percent with the field curve. The field curve, the automatic interpreted results and reduced multi layer model of VES-2 are shown in fig.-4.4a, 4.4b and 4.4c respectively. The layer parameters are presented in table 4.3.

Table 4.3: The interpreted results of VES-2

Layer number	Depth to the layer in meter	Thickness of the layer in meter	Resistivity of the layer in ohm-m
1	1.32	1.32	85
2	13	11.68	23
3	41	28	19
4	**	**	85

**Undetermined

VES-3: The sounding station is located in the eastern portion of study area. The surface elevation of the station is 38 m from MSL. The orientation of the profile was in N25°E direction. 10 layers have been identified within the depth of 115 m.

a)

b)

c)

Fig. 4.4: a) Field Curve b) Automatic Interpreted Results
c) Reduced Multilayer Model of VES-2

These results have been used in reducing this multi layer model to a 4-layer model. The thin layers of extremely low and high resistivities have been compressed and a model is prepared to best fitting with the digitized curve. The results show the fitting tolerance of 1.1 percent with the field curve. The field curve, the automatic interpreted results and reduced multi layer model of VES-3 are shown in fig.-4.5a, 4.5b and 4.5c respectively. The layer parameters are presented in table 4.4.

Table 4.4: The interpreted results of VES-3

Layer number	Depth to the layer in meter	Thickness of the layer in meter	Resistivity of the layer in ohm-m
1	1.52	1.52	56.0
2	10.0	8.48	25.0
3	37.0	27.0	70.0
4	**	**	12.0

**Undetermined

VES-4: The sounding station is located in the southern portion of study area. The surface elevation of the station is 30 m from MSL. The orientation of the profile was in N35°E direction. 10 layers have been identified within the depth of 100 m. These results have been used in reducing this multi layer model to a 4-layer model. The thin layers of extremely low and high resistivities have been compressed and a model is prepared to best fitting with the digitized curve. The results show the fitting tolerance of 1.1 percent with the field curve. The field curve, the automatic interpreted results and reduced multi layer model of VES-4 are shown in fig.-4.6a, 4.6b and 4.6c respectively. The layer parameters are presented in table 4.5.

VES-5: The sounding station is located in the south - eastern portion of study area. The surface elevation of the station is 26 m from MSL. The orientation of the profile was in N5°E direction. 10 layers have been identified within the depth

a)

b)

c)

Fig. 4.5: a) Field Curve b) Automatic Interpreted Results
c) Reduced Multilayer Model of VES-3

a)

b)

c)
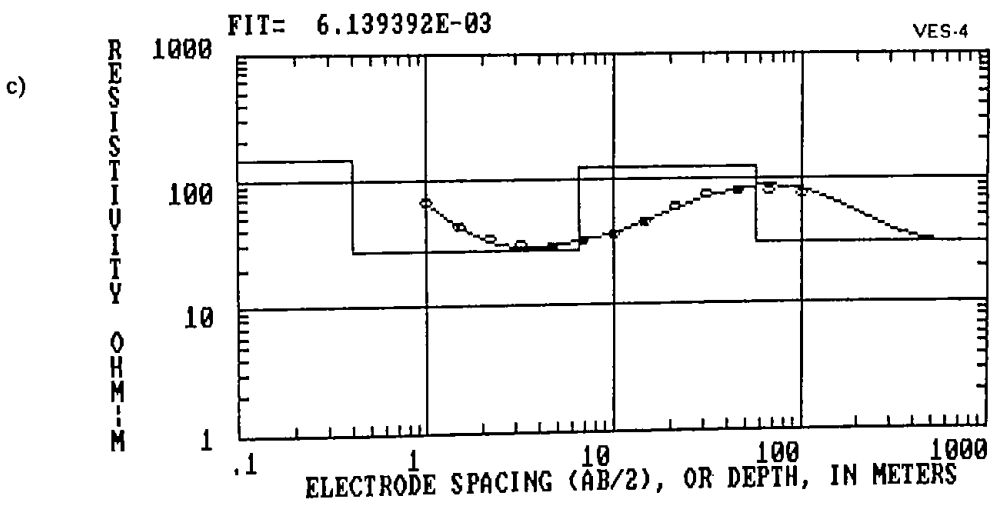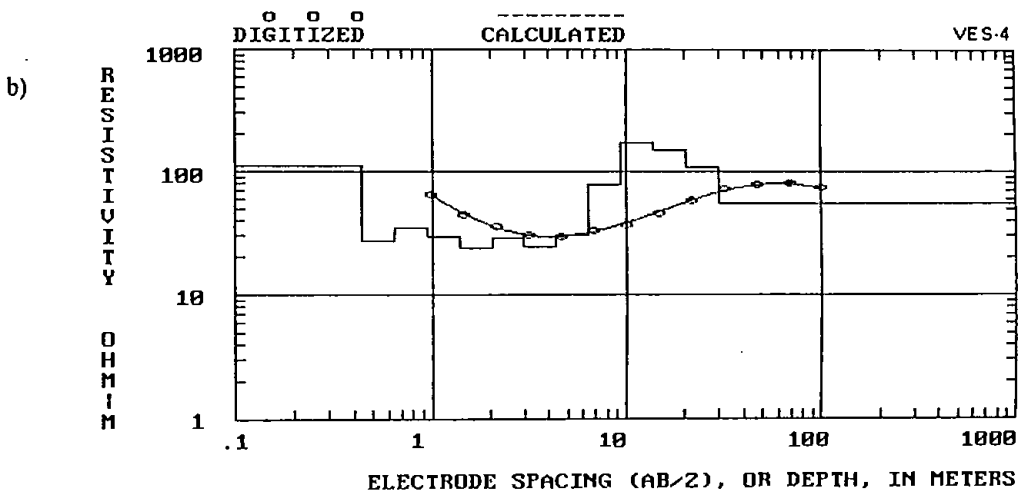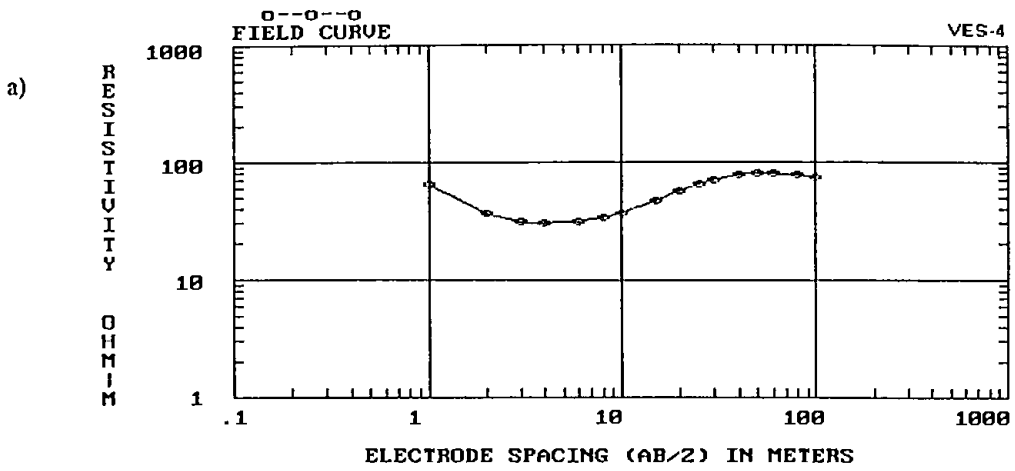
Fig. 4.6: a) Field Curve b) Automatic Interpreted Results
c) Reduced Multilayer Model of VES-4

of 165 m. These results have been used in reducing this multi layer model to a 4-layer model. The thin layers of extremely low and high resistivities have been compressed and a model is prepared to best fitting with the digitized curve. The results show the fitting tolerance of 1.1 percent with the field curve. The field curve, the automatic interpreted results and reduced multi layer model of VES 5 are shown in fig.-4.7a, 4.7b and 4.7c respectively. The layer parameters are presented in table 4.6.

Table 4.5: The interpreted results of VES-4

Layer number	Depth to the layer in meter	Thickness of the layer in meter	Resistivity of the layer in ohm-m
1	0.4	0.4	143.0
2	6.5	6.1	27.0
3	58.0	51.5	120.0
4	**	**	30.0

**Undetermined

Table 4.6: The interpreted results of VES-5

Layer number	Depth to the layer in meter	Thickness of the layer in meter	Resistivity of the layer in ohm-m
1	1.32	1.32	70.0
2	21.0	19.2	15.0
3	16.8	13.3	10.0
4	**	**	50.0

**Undetermined

VES-6: The sounding station is located in the central portion of study area. The surface elevation of the station is 32 m AMSL. The orientation of the profile was in N45°W direction. 10 layers have been identified within the depth of 100 m. These results have been used in reducing the multi layer model to a 4-layer model. The thin layers of extremely low and high resistivities have been compressed and a model is prepared to best fitting with the digitized curve. The results show the

Fig. 4.7: a) Field Curve b) Automatic Interpreted Results

c) Reduced Multilayer Model of VES-5

fitting tolerance of 1.1 percent with the field curve. The field curve, the automatic interpreted results and reduced multi-layer model of VES-6 are shown in fig.-4.8a, 4.8b and 4.8c respectively .The layer parameters are presented in table 4.7.
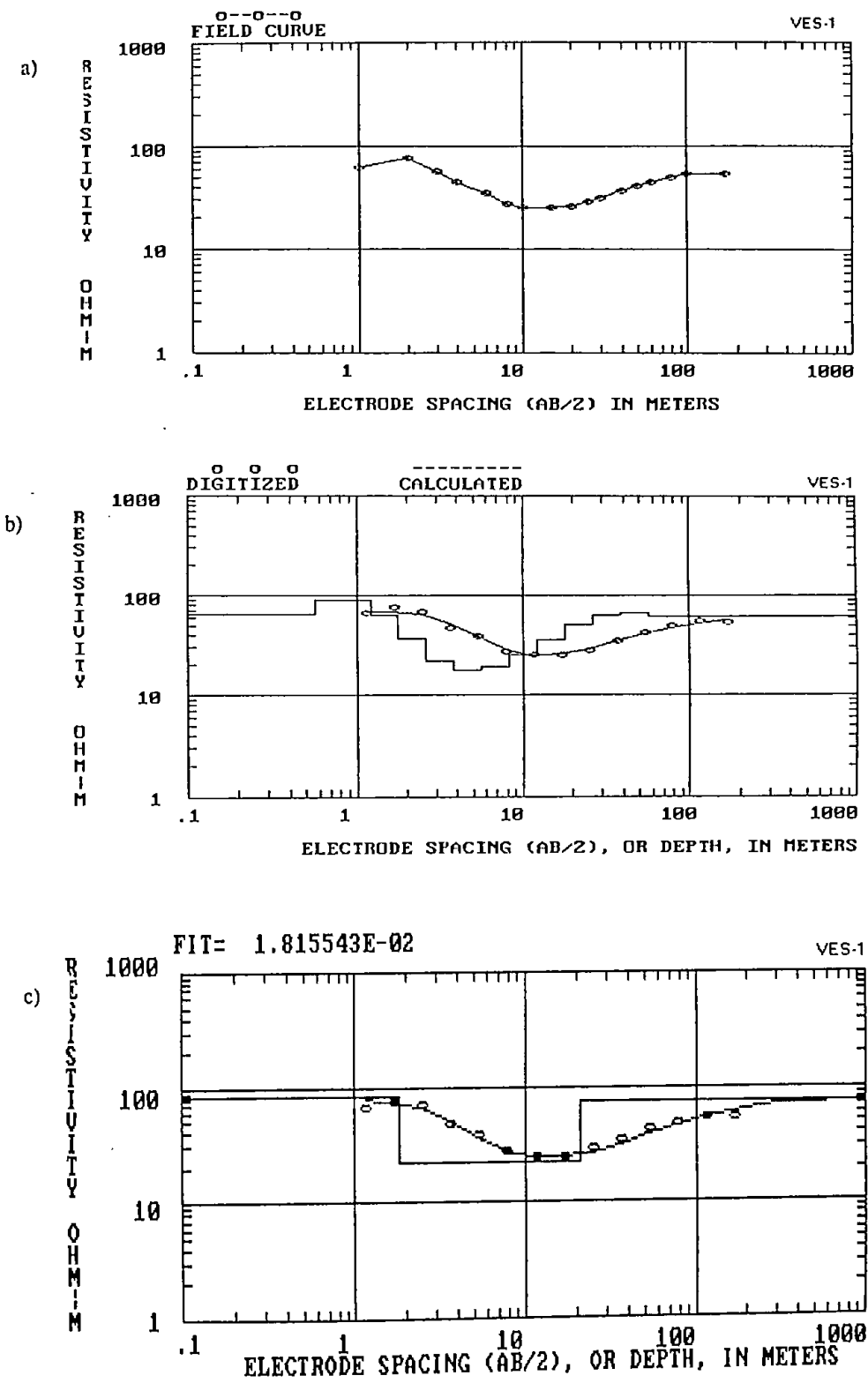
Table 4.7: The interpreted results of VES-6

Layer number	Depth to the layer in meter	Thickness of the layer in meter	Resistivity of the layer in ohm-m
1	1.02	1.02	69.0
2	4.8	3.78	30.0
3	44.0	39.2	270.0
4	**	**	18

**Undetermined

VES-7: The sounding station is located in the southern portion of study area. The surface elevation of the station is 32 m MSL. The orientation of the profile was in N-S directio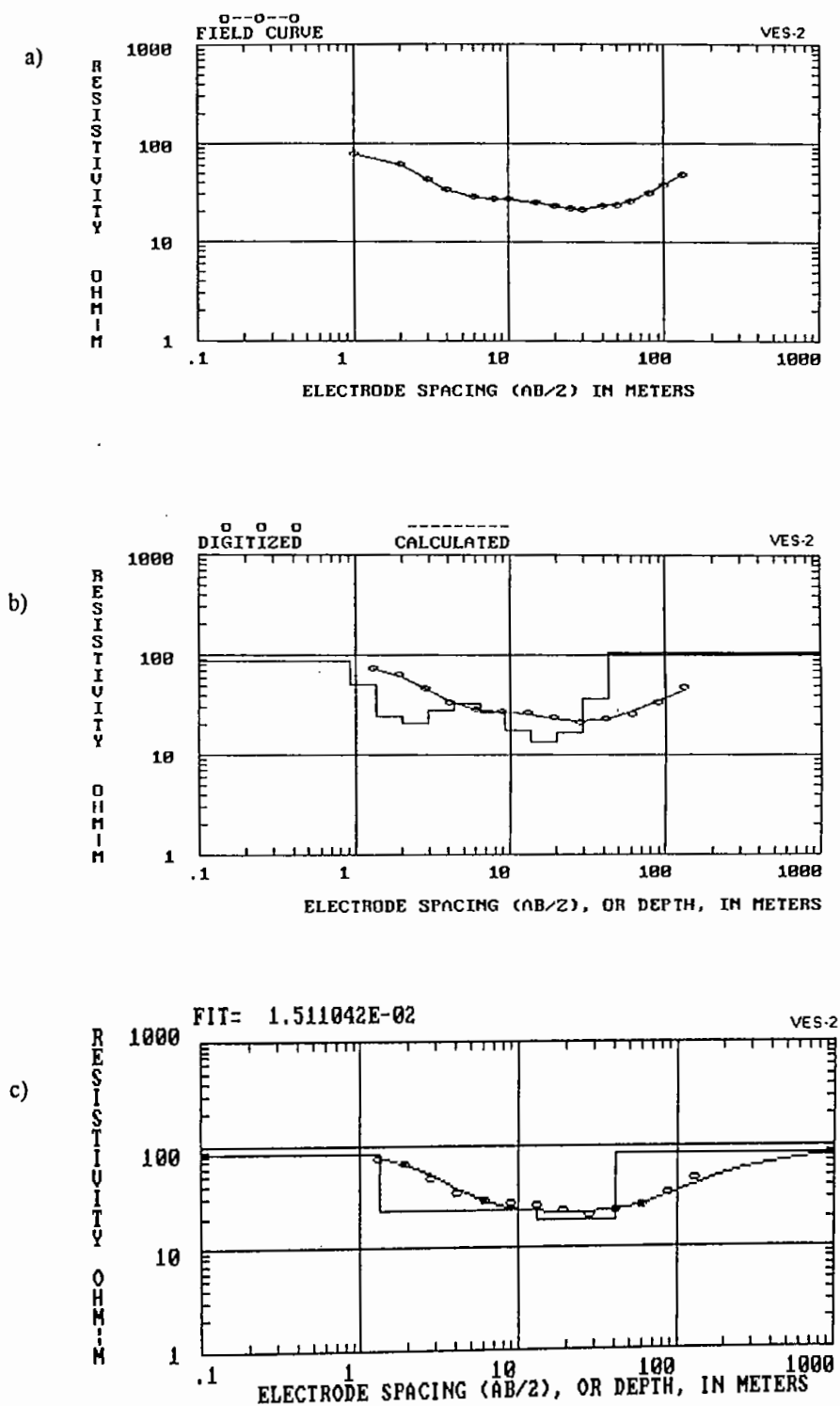n. 10 layers have been identified within the depth of 100 m. These results have been used in reducing this multi layer model to a 4-layer model. The thin layers of extremely low and high resistivities have been compressed and a model is prepared to best fitting with the digitized curve. The results show the fitting tolerance of 1.1 percent with the field curve. The field curve, the automatic interpreted results and reduced multi-layer model of VES-7 are shown in Fig.4.9a, 4.9b and 4.9c respectively. The layer parameters are presented in table 4.8.

Table 4.8: The interpreted results of VES-7

Layer number	Depth to the layer in meter	Thickness of the layer in meter	Resistivity of the layer in ohm-m
1	0.6	0.6	100.0
2	4.0	3.4	20.0
3	45.0	41.0	106.0
4	**	**	10.0

**Undetermined

a)

```
          o--o--o                                              VES-6
      FIELD CURVE
      1000
  R
  E
  S
  I
  S
  T   100
  I
  U
  I
  T
  Y    10
  O
  H
  M
  I
  M    1
        .1         1         10        100       1000
        ELECTRODE SPACING (AB/2) IN METERS
```

b)

```
      DIGITIZED          CALCULATED                 VES-6
      1000
  R
  E
  S
  I
  S
  T   100
  I
  U
  I
  T
  Y    10
  O
  H
  M
  I
  M    1
        .1         1         10        100       1000
        ELECTRODE SPACING (AB/2), OR DEPTH, IN METERS
```

c)

```
      FIT=  2.976716E-02                             VES-6
  R   1000
  E
  S
  I
  S   100
  T
  I
  U
  I    10
  T
  Y
  O
  H
  M    1
  I    .1         1         10        100       1000
  M    ELECTRODE SPACING (AB/2), OR DEPTH, IN METERS
```
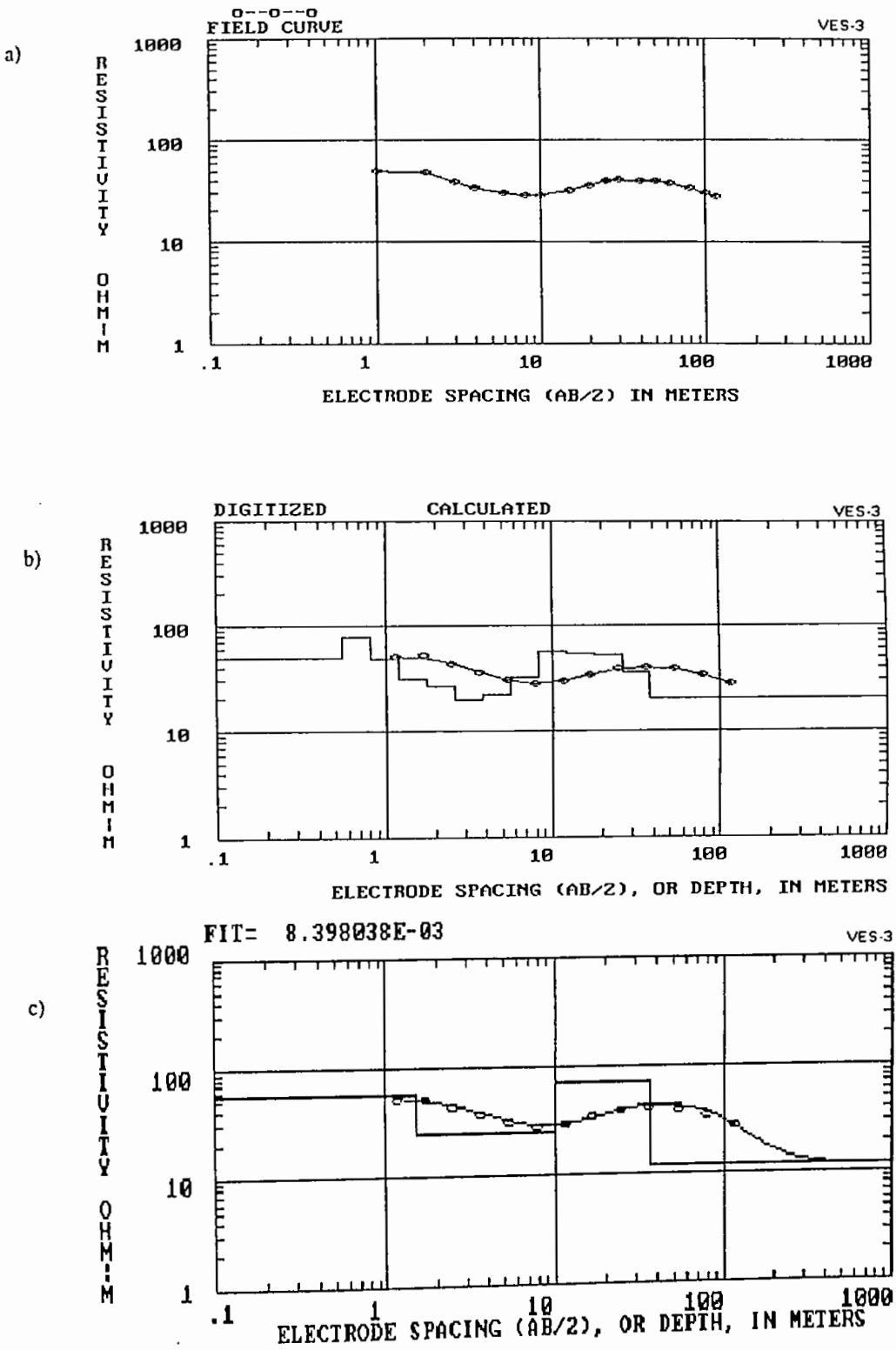
Fig. 4.8: a) Field Curve b) Automatic Interpreted Results
          c) Reduced Multilayer Model of VES-6

a)

b)

c)
c)

Fig.4.9 a) Field Curve b) Automatic Interpreted Results

c) Reduced Multilayer Model of VES-7

VES-8: The sounding station is located in the southern portion of study area. The surface elevation of the station is 33 m from MSL .The orientation of the profile was in N15°E direction. 10 layers have been identified within the depth of 100 m. These results have been used in reducing this multi layer model to a 4-layer model. The thin layers of extremely low and high resistivities have been compressed and a model is prepared to best fitting with the digitized curve. The results show the fitting tolerance of 1.1 percent with the field curve. The field curve, the automatic interpreted results and reduced multi layer model of VES-8 are shown in Fig.4.10a, 4.10b and 4.10c respectively. The layer parameters are presented in table 4.9.

Table 4.9: The interpreted results of VES-8

Layer number	Depth to the layer in meter	Thickness of the layer in meter	Resistivity of the layer in ohm-m
1	1.0	1.0	85.0
2	4.0	3.0	13.0
3	40.0	36.0	80.0
4	**	**	30.0

**Undetermined

VES-9: The sounding station is located in the southeastern portion of study area. The surface elevation of the station is 32 m from MSL. The orientation of the profile was in N10°E direction. 10 layers have been identified within the depth of 100 m. These results have been used in reducing this multi-layer model to a 4-layer model. The thin layers of extremely low and high resistivities have been compressed and a model is prepared to best fitting with the digitized curve. The results show the fitting tolerance of 1.1 percent with the field curve. The field curve, the automatic interpreted results and reduced multi layer model of VES-9 are shown in Fig.4.11a, 4.11b and 4.11c respectively. The layer parameters are presented in table 4.10.

Fig.4.10: a) Field Curve b) Automatic Interpreted Results
c) Reduced Multilayer Model of VES-8

Fig. 4.11: a) Field Curve b) Automatic Interpreted Results
c) Reduced Multilayer Model of VES-9

Table 4.10: The interpreted results of VES-9

Layer number	Depth to the layer in meter	Thickness of the layer in meter	Resistivity of the layer in ohm-m
1	1.0	1.0	78.0
2	5.0	4.0	34.0
3	54.0	49.0	205.0
4	**	**	25.0

**Undetermined

VES-10: The sounding station is located in the northwestern part of study area. The surface elevation of the station is 24 m from MSL. The orientation of the profile was in N25°E direction. 10 layers have been identified within the depth of 100 m. These results have been used in reducing this multi-layer model to a 4-layer model. The thin layers of extremely low and high resistivities have been compressed and a model is prepared to best fitting with the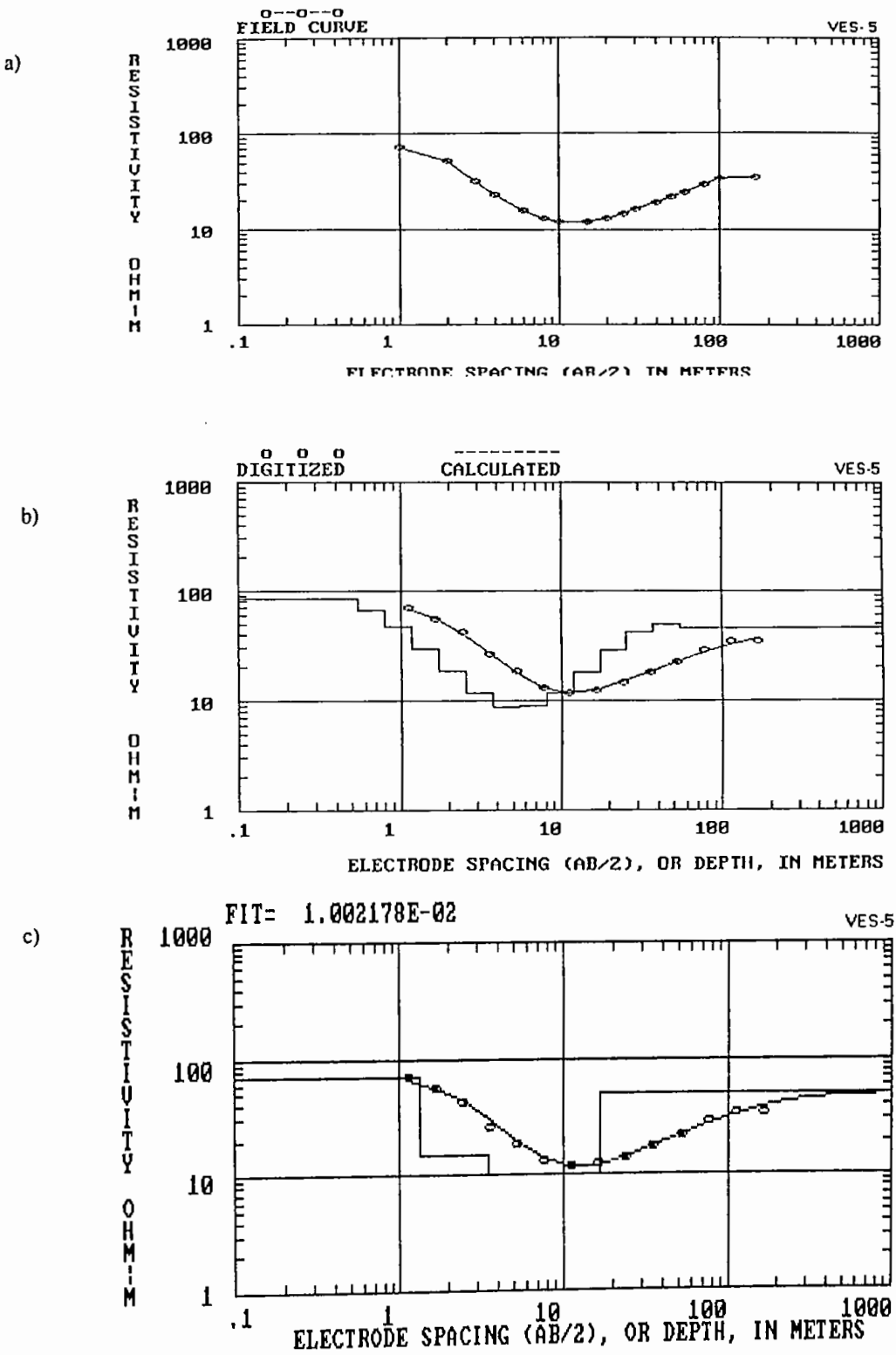 digitized curve. The results show the fitting tolerance of 1.1 percent with the field curve. The field curve, the automatic interpreted results and reduced multi-layer model of VES-10 are shown in Fig.4.12a, 4.12b and 4.12c respectively. The layer parameters are presented in table 4.11.

Table 4.11: The interpreted results of VES-10

Layer number	Depth to the layer in meter	Thickness of the layer in meter	Resistivity of the layer in ohm-m
1	1.5	1.5	90.0
2	12.0	10.5	22.0
3	37.0	25.0	46.0
4	**	**	16.0

**Undetermined
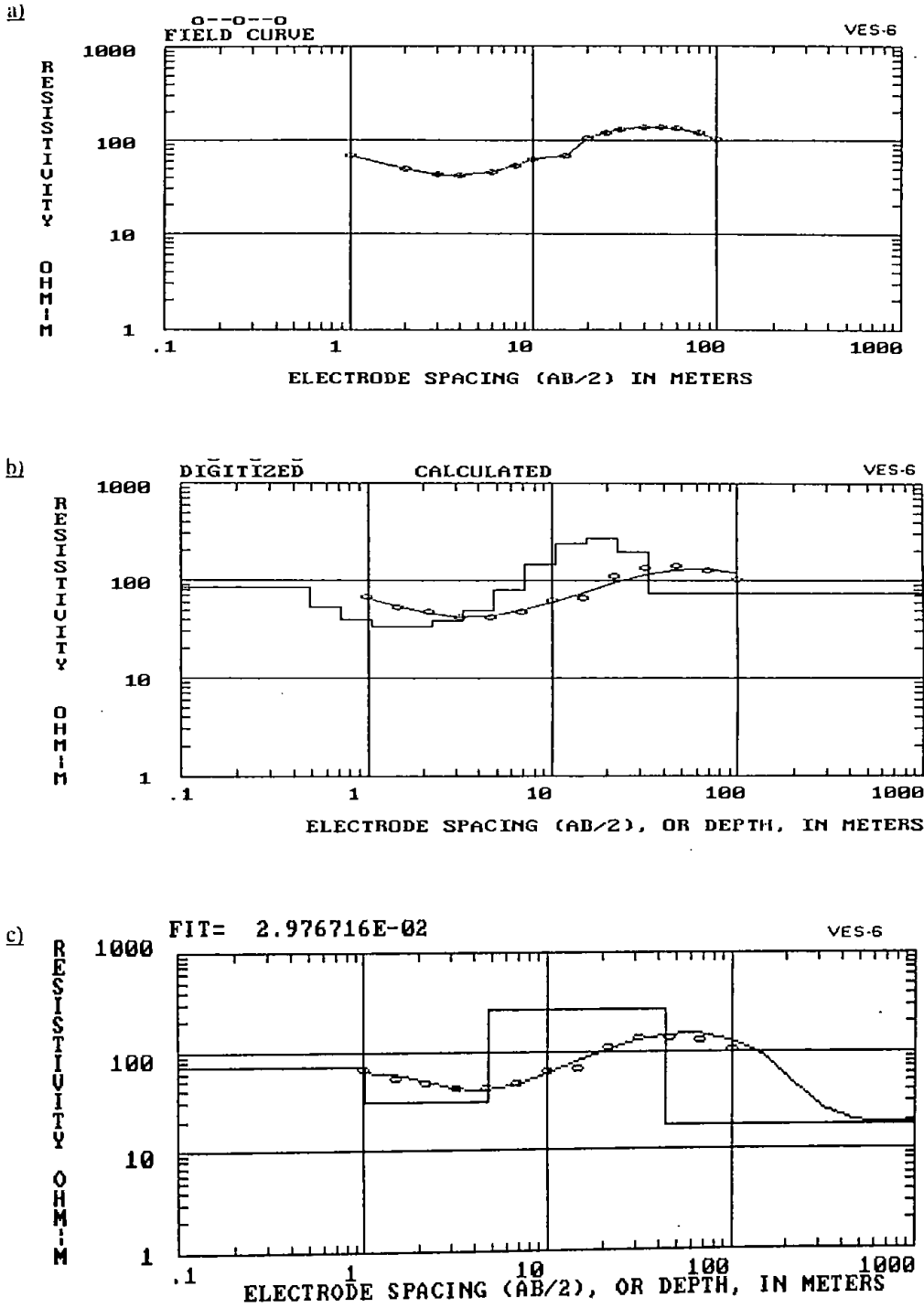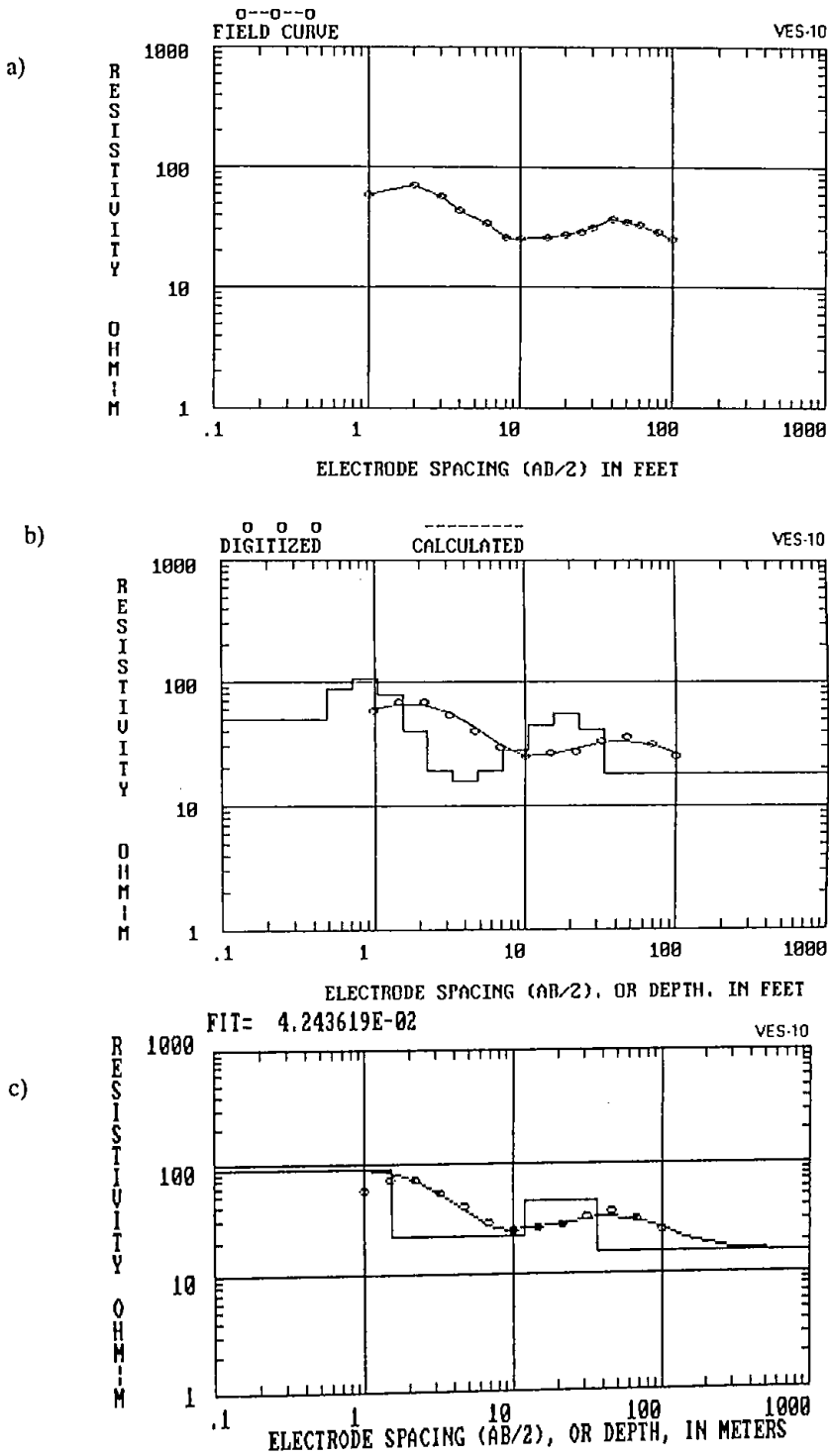
Fig.4.12: a) Field Curve b) Automatic Interpreted Results
c)Reduced Multilayer model of VES-10

VES-11: The sounding station is located in the central north portion of study area. The surface elevation of the station is 30 m from MSL. The orientation of the profile was in N10°E direction. 10 layer have been identified within the depth of 100 m. These results have been used in reducing this multi-layer model to a 4-layer model. The thin layers of extremely low and high resistivities have been compressed and a model is prepared to best fitting with the digitized curve. The results show the fitting tolerance of 1.1 percent with the field curve. The field curve, the automatic interpreted results and reduced multi layer model of VES 11 are shown in Fig.4.13a, 4.13b and 4.13c respectively. The layer parameters are presented in table 4.12.

Table 4.12: The interpreted results of VES-11

Layer number	Depth to the layer in meter	Thickness of the layer in meter	Resistivity of the layer in ohm-m
1	1.0	1.0	75.0
2	12.0	11.0	35.0
3	38.0	26.0	70.0
4	**	**	25.0

**Undetermined

VES-12: The sounding station is located in the northwestern part of study area. The surface elevation of the station is 29 m AMSL. The orientation of the profile was in N 30°W direction. 10 layers have been identified within the depth of 100 m. These results have been used in reducing the multi-layer model to a 4-layer model. The thin layers of extremely low and high resistivities have been compressed and a model is prepared to best fitting with the digitized curve. The results show the fitting tolerance of 1.1 percent with the field curve. The field curve, the automatic interpreted results and reduced multi-layer model of VES-12 are shown in Fig.4.14a, 4.14b and 4.14c respectively. The layer parameters are presented in table 4.13.
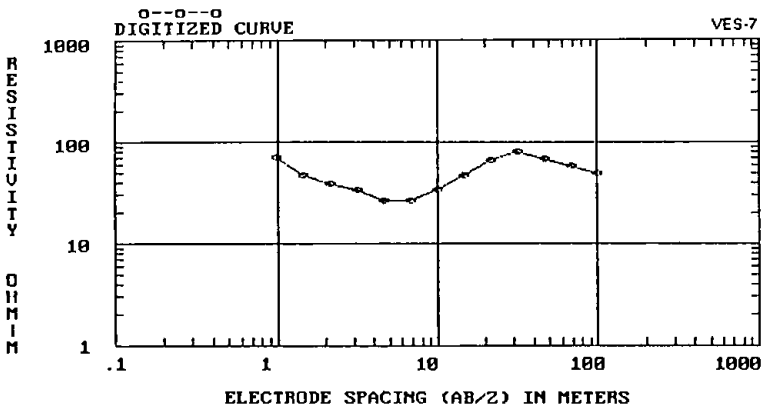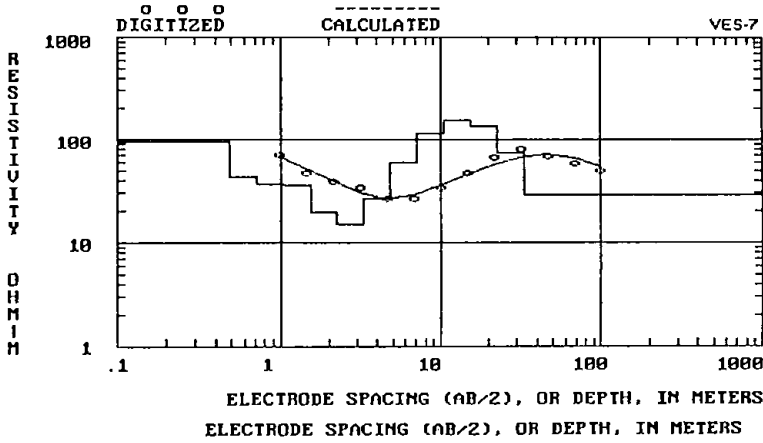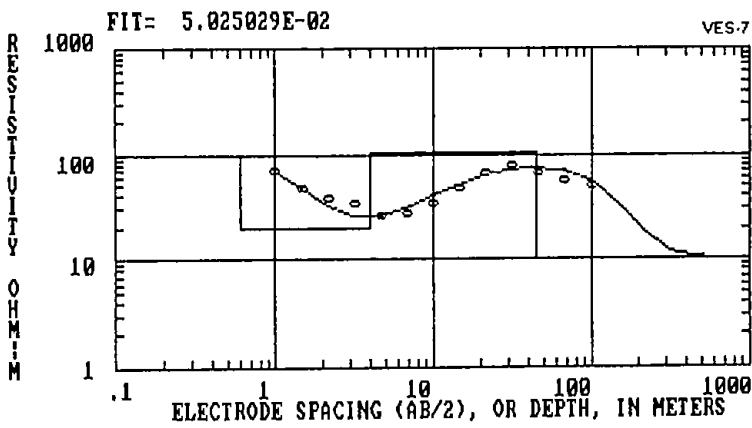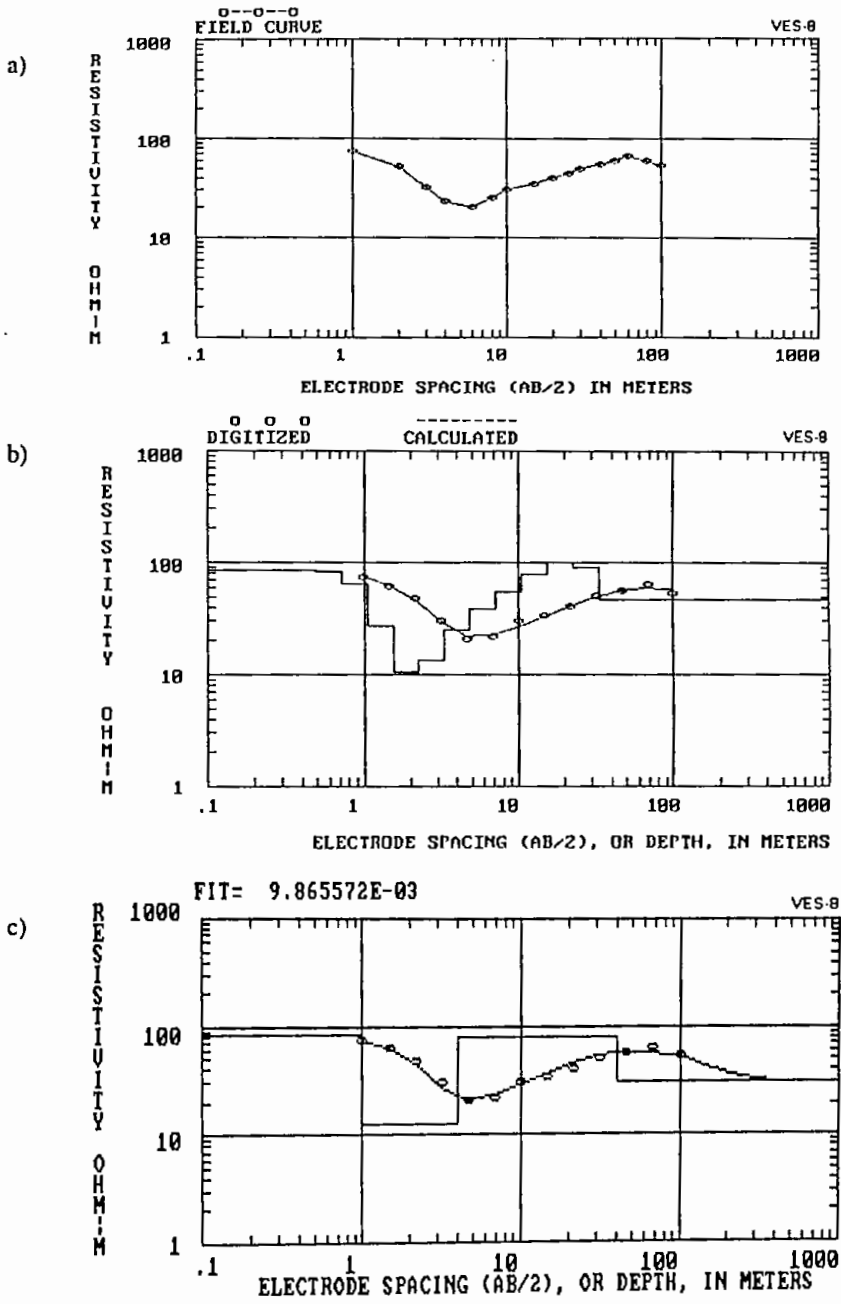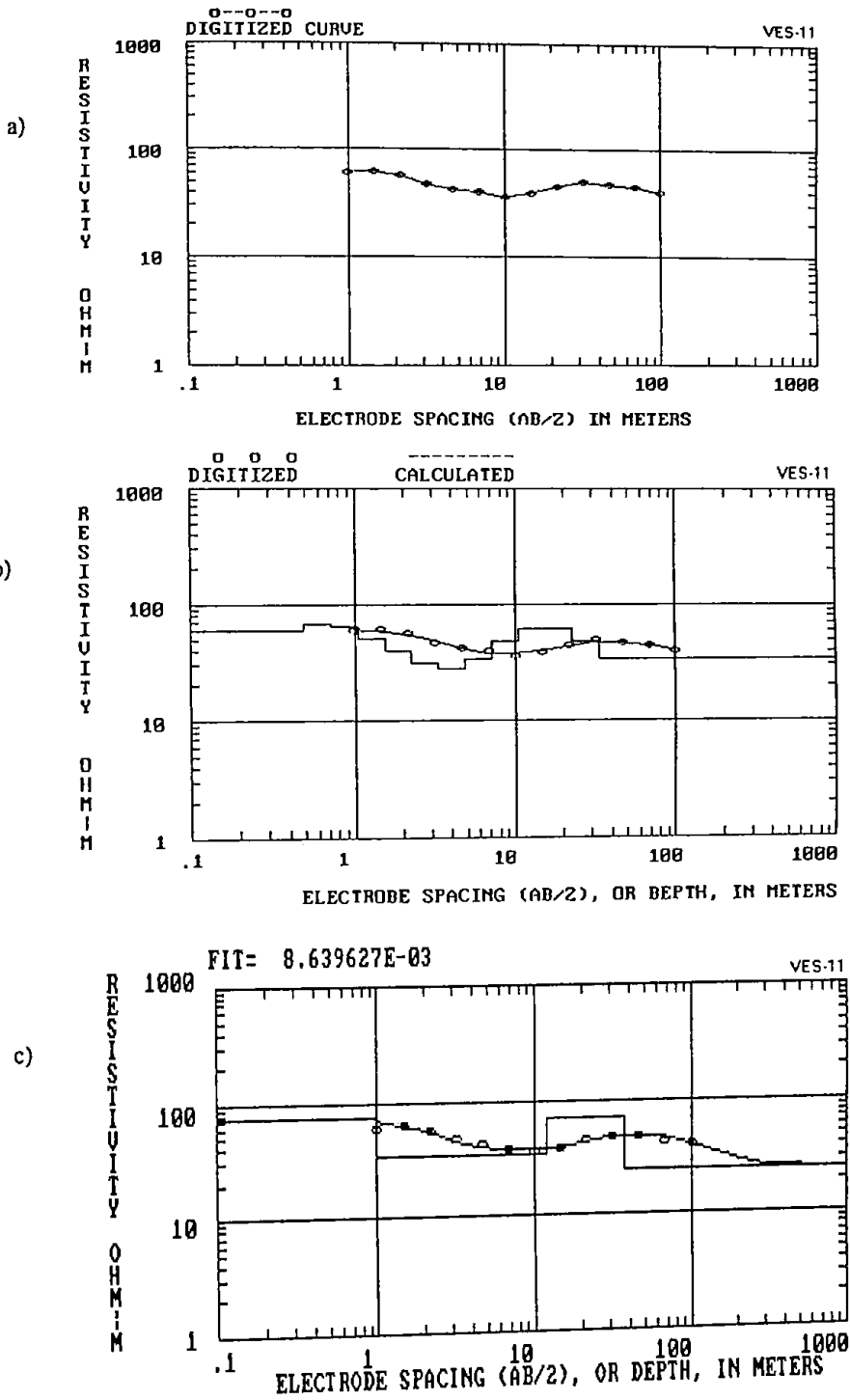
Fig. 4.13: a) Field Curve b) Automatic Interpreted Results
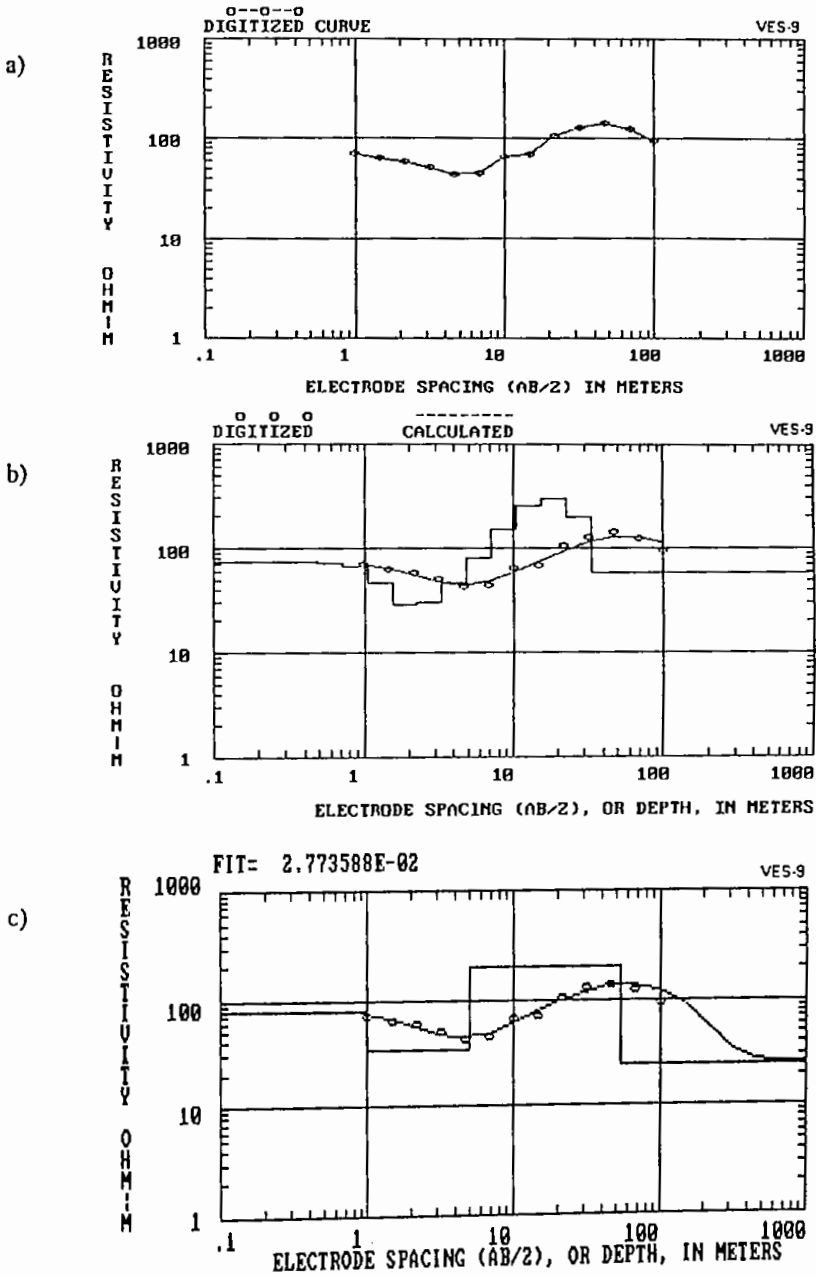c) Reduced Multilayer Model of VES-11
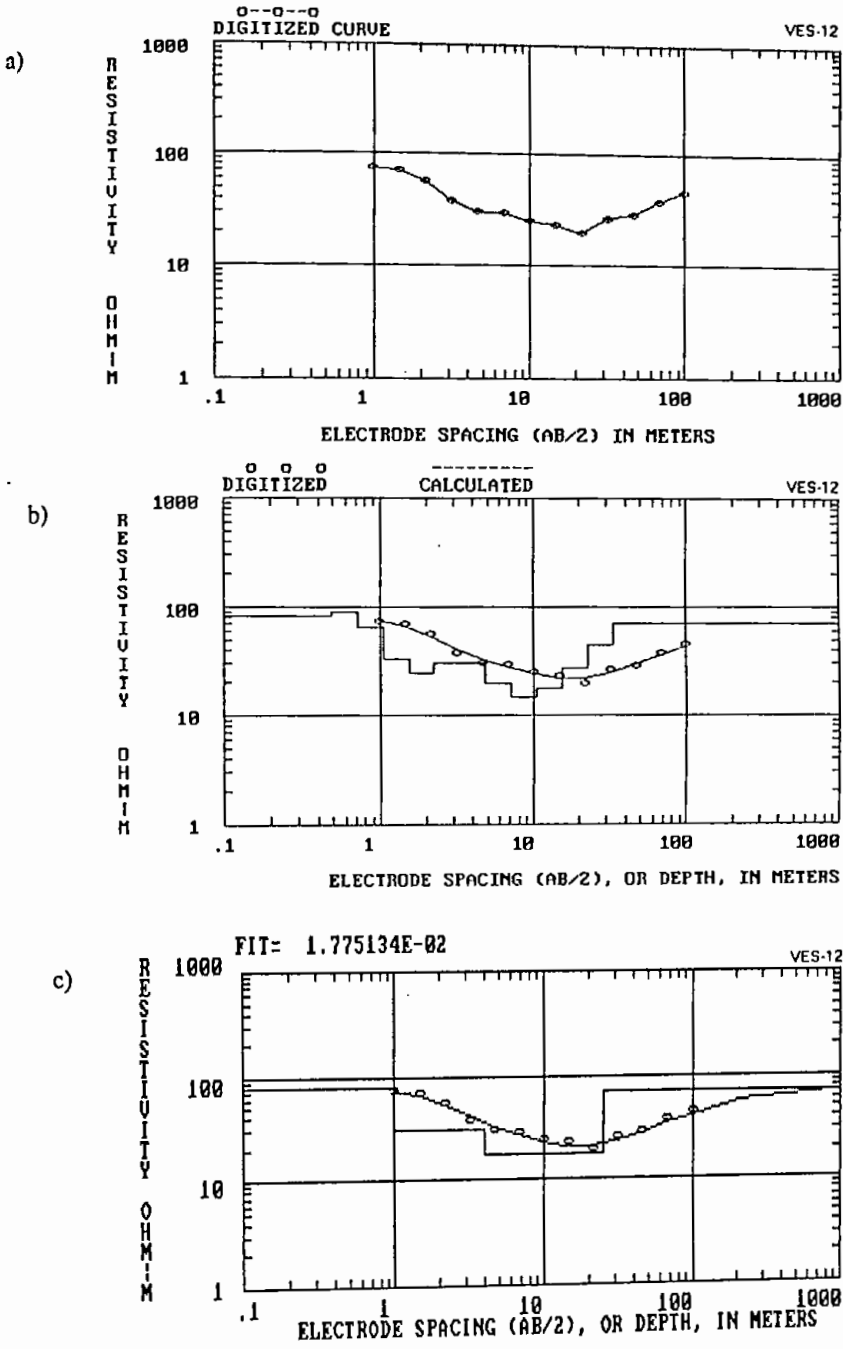
Fig. 4.14 a) Field Curve b) Automatic Interpreted Results
c) Reduced Multilayer Model of VES-12

Table 4.13: The interpreted results of VES-12

Layer number	Depth to the layer in meter	Thickness of the layer in meter	Resistivity of the layer in ohm-m
1	1.01	1.01	80.0
2	4.0	2.99	30.0
3	25.0	21.0	18.0
4	**	**	70.0

**Undetermined

4.6 Geo-Electric Layer Isopach Map

After the determination of the thickness and resistivities of the geo-electric layers comprising the total geo-electric column from VES curve the thickness are used to construct isopach maps of the respective geo-electric layers. These maps provide information about the lateral variation of thickness of specific geo-electric layers, which resemble to specific geological formations. Lateral variation of the thickness is used to correlate the geo-electric layer to specific hydrostratigraphic units and ultimately establish the hydrogeology of a particular area. For the present study two isopach maps have been prepared for the first and second geo-electric layers, which are represented in fig.-4.15 and 4.16.

4.6.1 Isopach Map of Top Sandy and Silty Clay

This map is constructed at a contour interval of 2 m (Fig.-4.15). The thickness of the top sandy and silty clay layer varies from 4 to 41 m. The highest thickness is observed at Shiranti of Sapahar Upazilla and the lowest thickness is observed in the southern portion of the area. Overall the thickness of the top sandy and silty clay layer is higher in northeastern part of Sapahar Upazilla and lower in other parts of the study area.
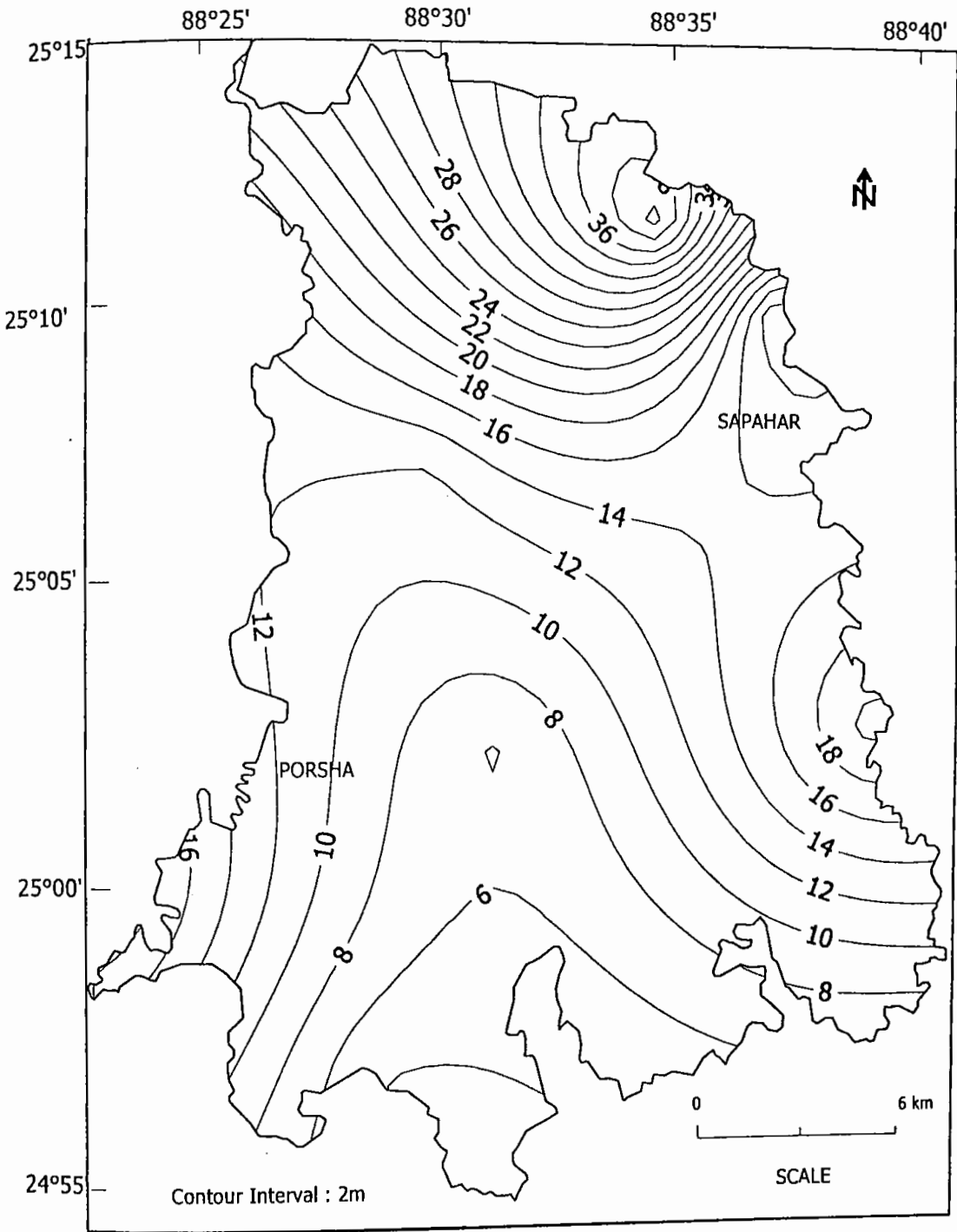
Fig.-4.15: Isopach Map of Sandy and Silty Aquitard
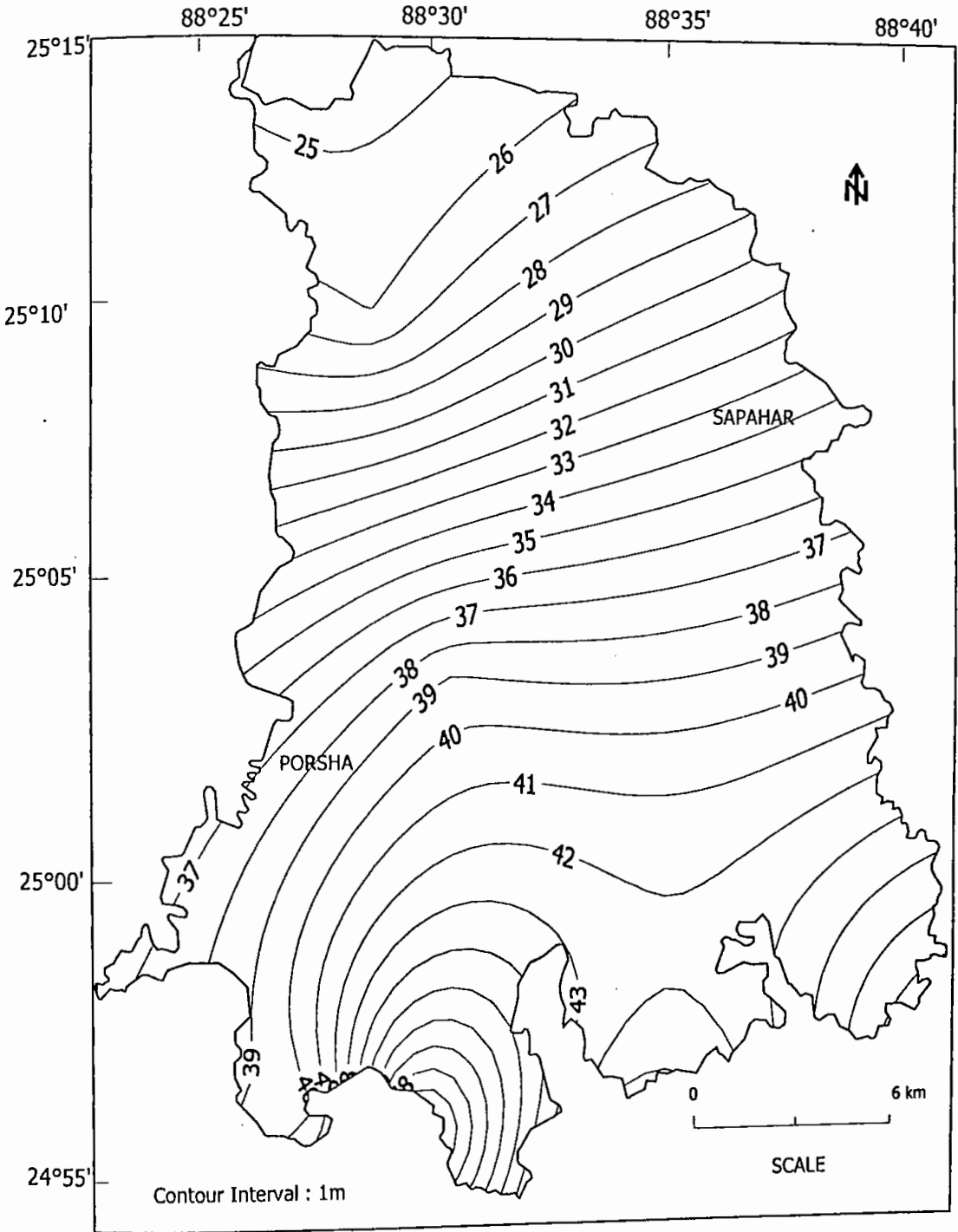
FIg.-4.16: Isopach Map of Aquifer

Geologically this layer resembles the upper clay, silty clay layer where the presence of huge amount of impervious clay materials reduces the amount of groundwater available form infiltration. This clayey nature reduces the groundwater potentiality of this layer. This layer is suitable for installation of hand pumps and dug-wells provided it contains sufficient amount of sand lenses within it.

4.6.2 Isopach Map of the Aquifer

This map constructed with a contour interval of 1 m (Fig.-4.16). The thickness of the aquifer varies from 25 to 51.5 m. The highest thickness (51.5 m) is encountered at Khatirpur station of Porsha Upazilla and the lowest values (25 m) is observed at Karmudanga station of Sapahar Upazilla. The overall thickness of the aquifer is high in Porsha Upazilla.

Lithologically fine sand, medium sand and medium to coarse sand with gravel represent this layer and hydrogeologically it represents the aquifer zone of the study area.

4.7 Comparison of Geo-electrical Sections and Lithologs

For the present study area making a close analogy between the lithological logs of some wells in the study area and VES curves of some nearby resistivity station did a proper standardization of the resistivity values. Thus in quantitative interpretation, the true resistivity and thickness of different layers are expressed in the form of vertical columns. The VES columns for the resistivity stations are represented in fig.-4.17 to 4.28 and have been compared with the geological section wherever available. The descriptions of the VES columns are given below.

VES-1: In this station the top sandy and silty clay comprising of the first two geo-electric layers of resistivity ranging from 22 to 85 ohm-m lies within the depth of 21 m from the ground surface. The third layer is composed of fine sand and
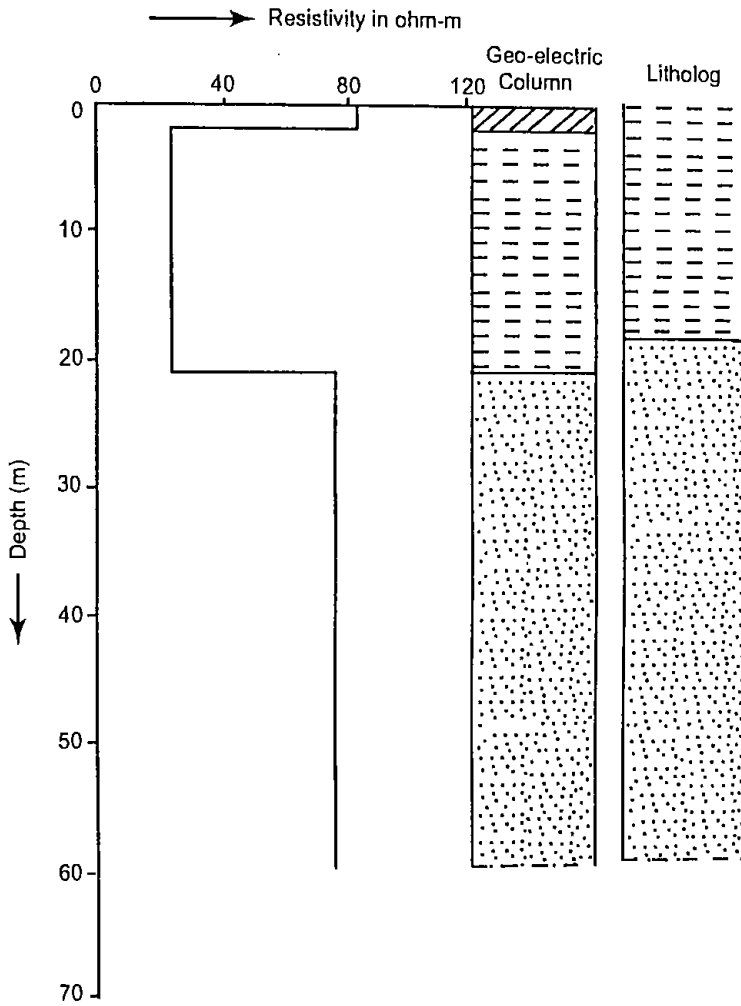
Fig.-4.17: Comparison of geo-electric column of VES-1 and litholog
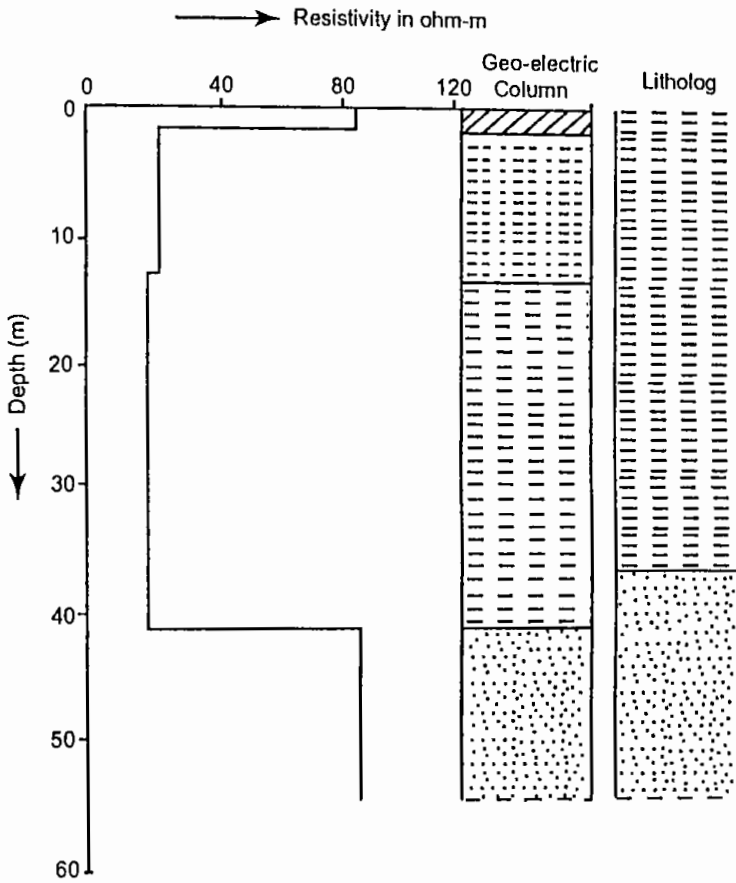
Fig.-4.18: Comparison of geo-electric Column of VES-2 and Litholog
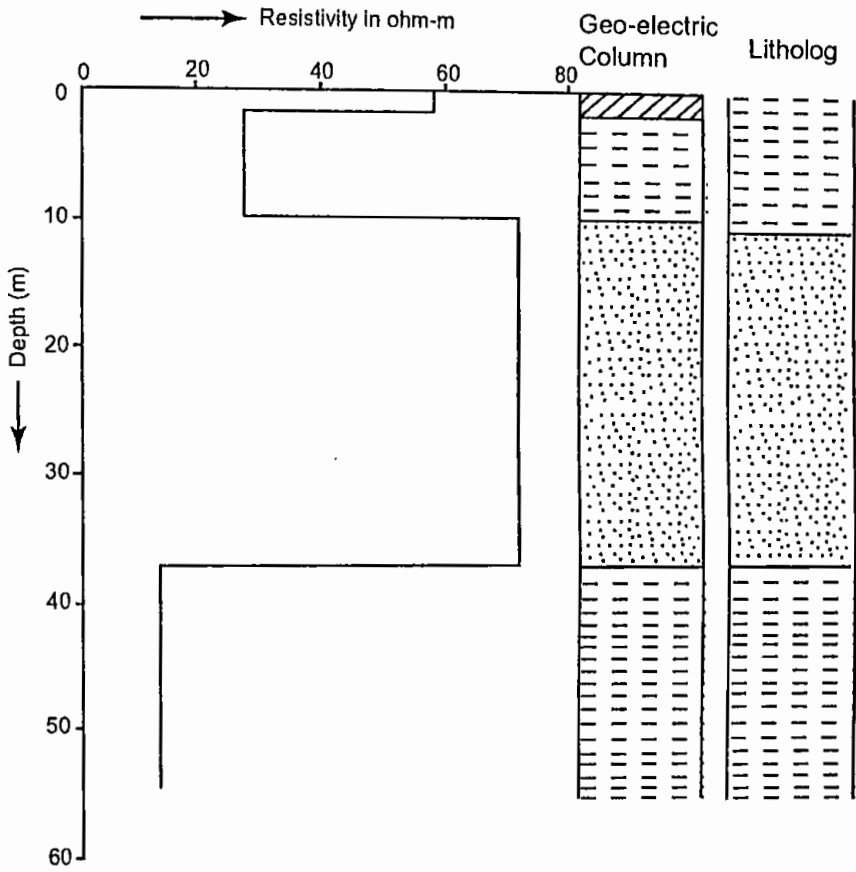
Fig.-4.19: Comparison of geo-electric Column of VES- 3 and litholog
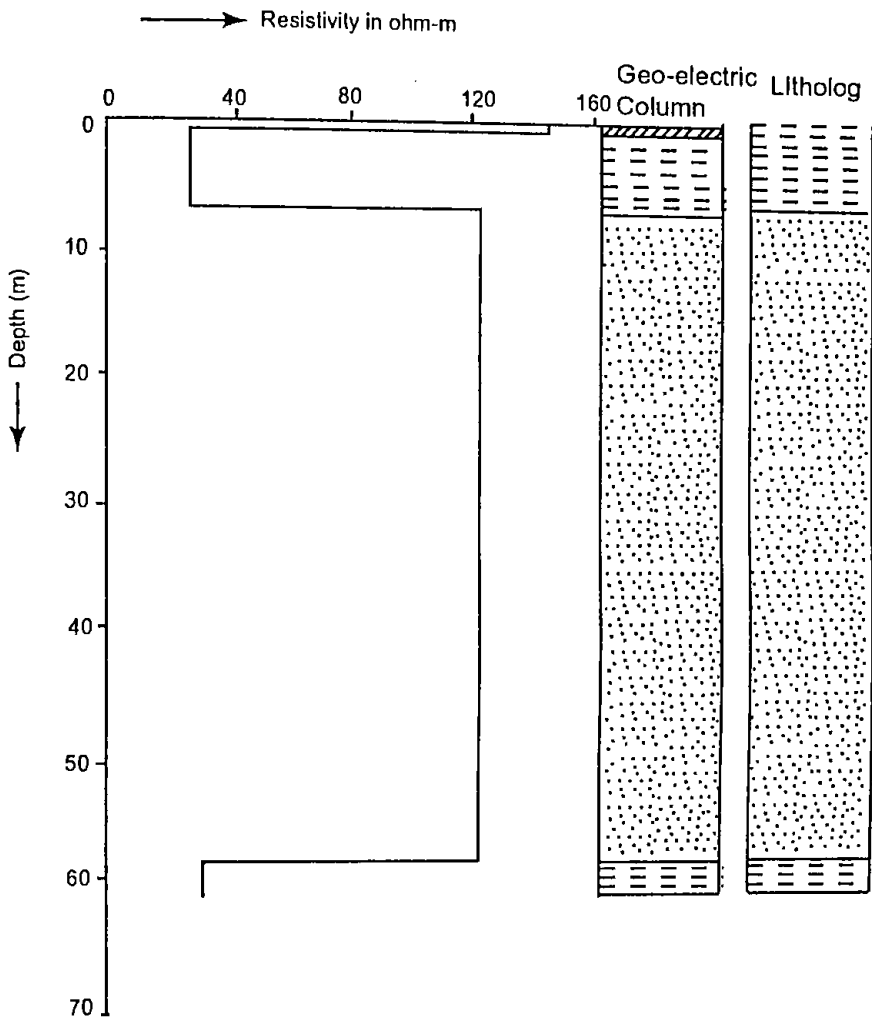
Fig.-4.20: Comparison of geo-electric column of VES-4 and litholog
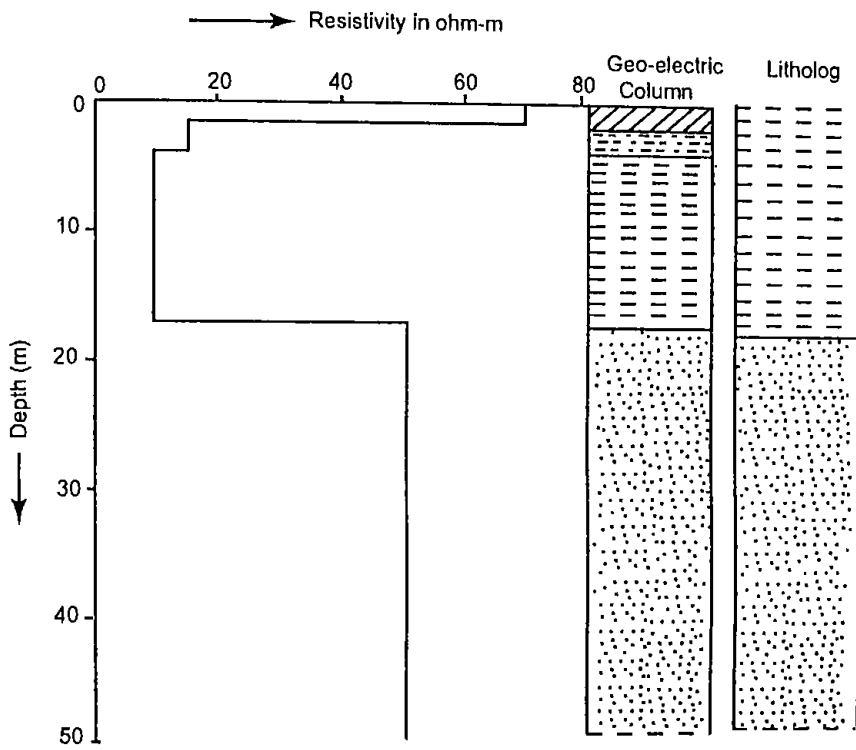
Fig.-4.21: Comparison of geo-electric column of VES-5 and litholog
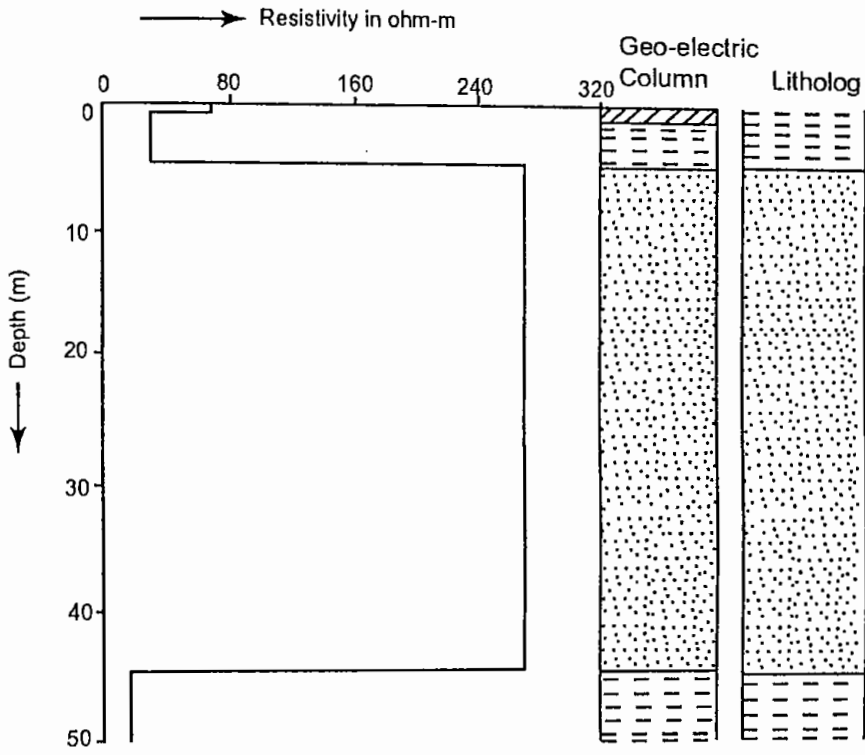
Fig.-4.22: Comparison of geo-electric column of VES-6 and litholog
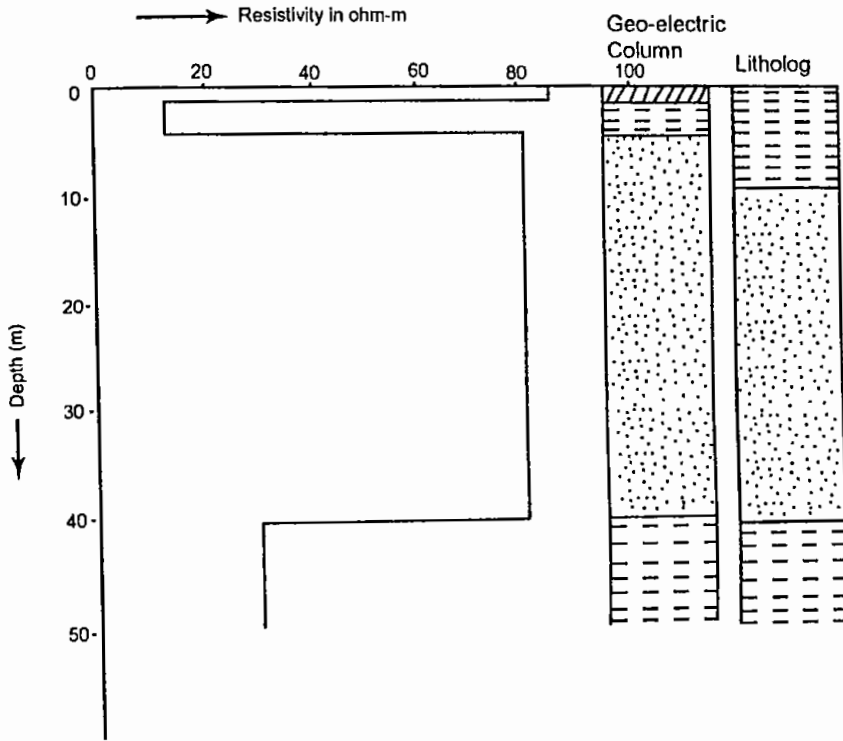
Fig.-4.23: Comparison of geo-electric column of VES- 7 and litholog
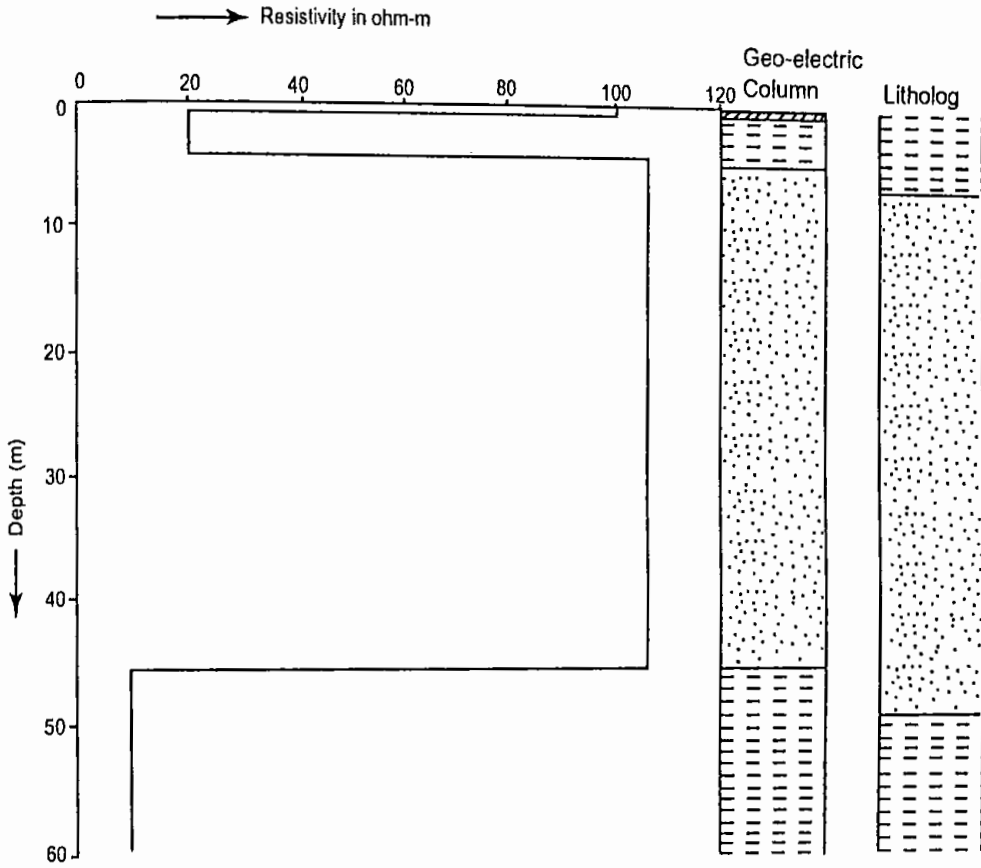
Fig.-4.24: Comparison of geo-electric column of VES- 8 and litholog
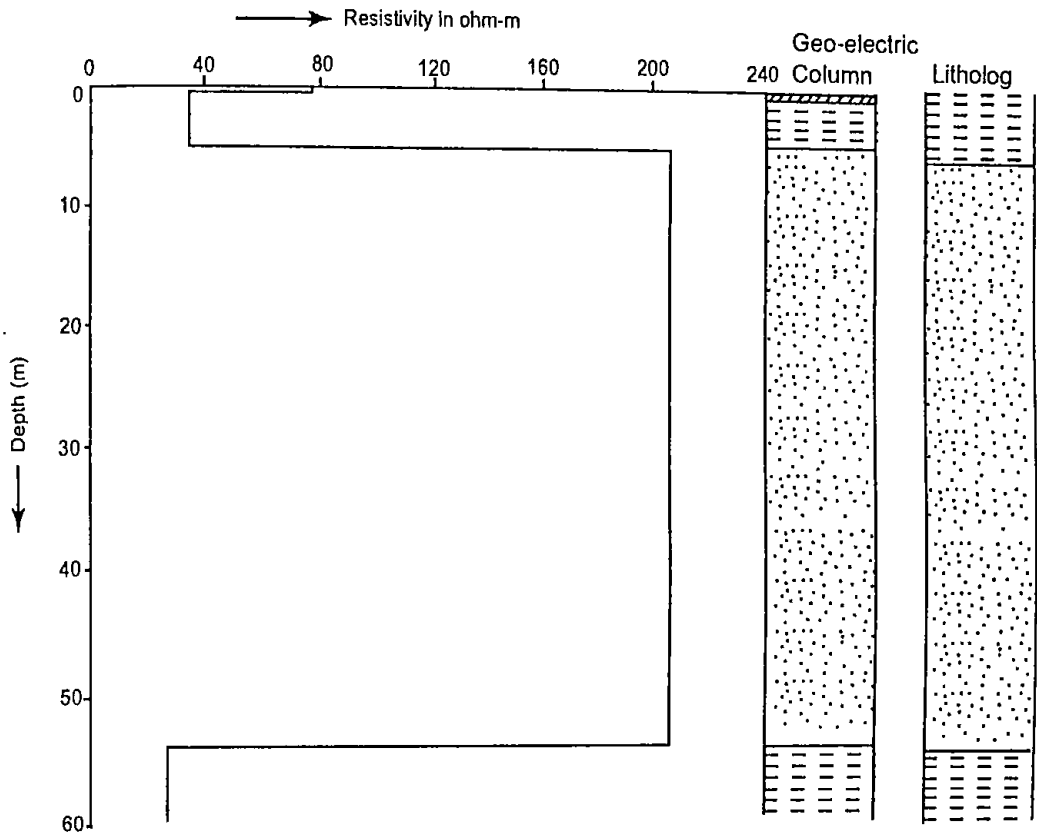
Fig.-4.25: Comparison of geo-electric column of VES- 9 and litholog
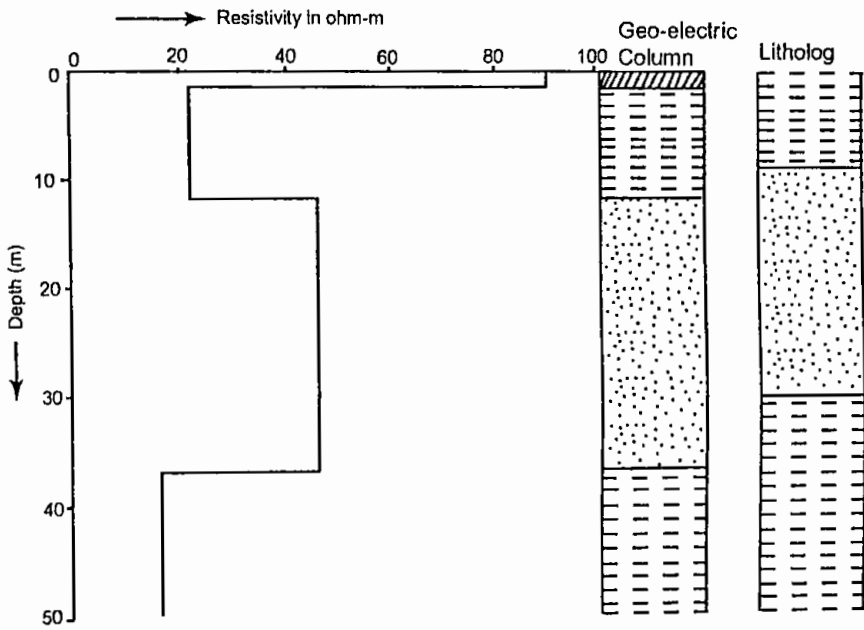
Fig.-4.26: Comparison of geo-electric column of VES- 10 and litholog
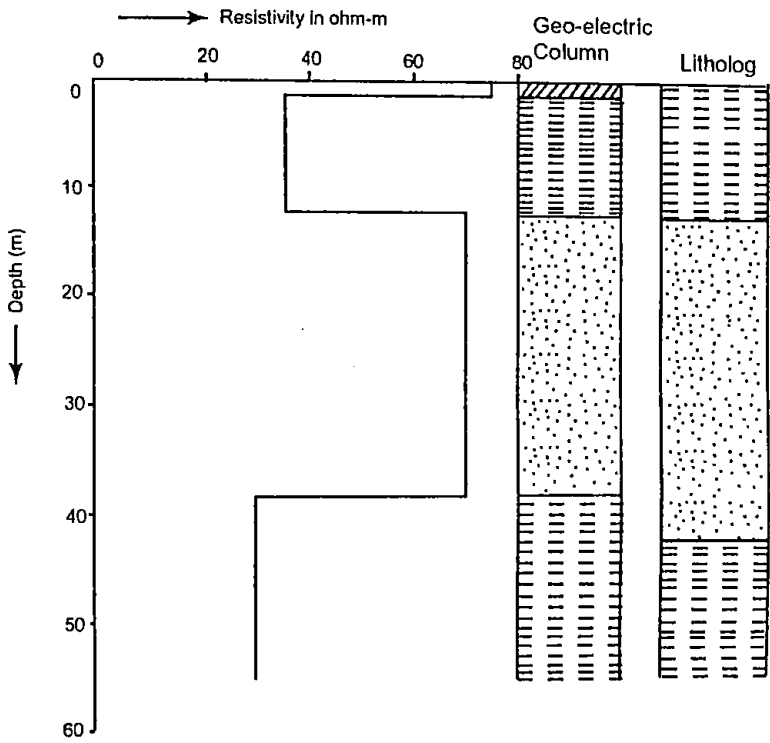
Fig.-4.27: Comparison of geo-electric column of VES- 11 and litholog
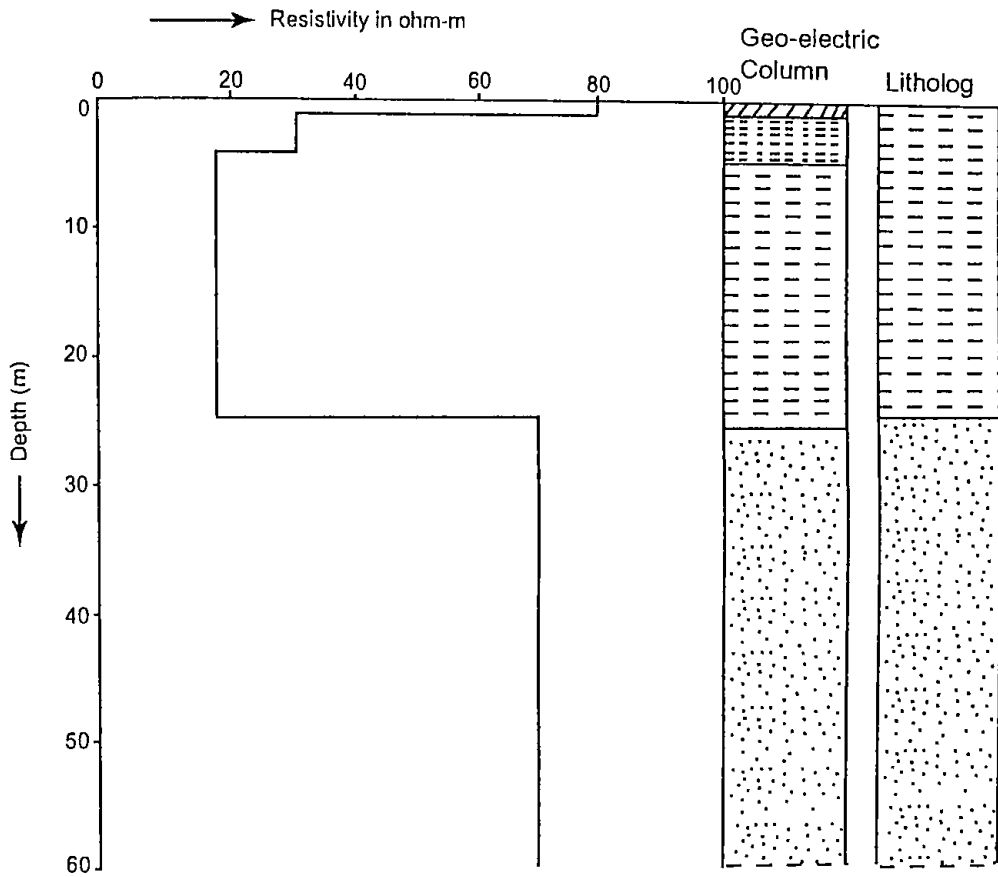
Fig.-4.21: Comparison of geo-electric column of VES- 12 and litholog

medium sand and this layer is the potential water-bearing zone having a resistivity of 75 ohm-m.

VES-2: In this station the top sandy and silty clay comprising of the first three geo-electric layers of resistivity ranging from 19 to 85 ohm-m lies within the depth of 41 m from the ground surface. The forth layer is composed of very fine to medium sand which is the potential water bearing zone having a resistivity of 85 ohm-m.

VES-3: In this station the top sandy and silty clay comprising of the first two geo-electric layers of resistivity ranging from 25 to 56 ohm-m lies within the depth of 10 m from the ground surface. The third layer is composed of fine sand, medium sand and coarse sand having a thickness of 27 m with a resistivity of 70 ohm-m. Below these sand layer a layer of clay is encountered having a resistivity of 12 ohm-m. The layer composed of medium sand is the most potential water-bearing zone of this column.

VES-4: In this station the top sandy and silty clay comprising of the first two geo-electric layers of resistivity ranging from 27 to 143 ohm-m lies within the depth of 6.5 m from the ground surface. The third layer is composed of medium sand with clay lenses having a thickness of 51.5 m and this is the most potential water-bearing zone having a resistivity of 120 ohm-m. Below this layer of very fine sand, clay and silt is encountered having a resistivity of 30 ohm-m.

VES-5: In this station the top sandy and silty clay comprising of the first three geo-electric layers of resistivity ranging from 10 to 70 ohm-m lies within the depth of 16.8 m from the ground surface. The forth layer is composed of medium sand with fine sand having a resistivity of 50 ohm-m.

VES-6: In this station the top sandy and silty clay comprising of the first two geo-electric layers of resistivity ranging from 30 to 69 ohm-m lies within the depth of 4.8 m from the ground surface. The third layer is composed of coarse sand

admixture with medium sand having a thickness of 39.2 m. This is the most potential aquifer material having a resistivity of 270 ohm-m. The downward extending layer is clay layer having a resistivity of 18 ohm-m.

VES-7: In this station the top sandy and silty clay comprising of the first two geo-electric layers of resistivity ranging from 20 to 100 ohm-m lies within the depth of 4 m from the ground surface. The third layer is composed of fine sand and medium sand and this layer is the potential water-bearing zone having a thickness of 41 m with a resistivity of 106 ohm-m. Below this sandy layer, a layer of clay is encountered having a resistivity value of 10 ohm-m.

VES-8: In this station the top sandy and silty clay comprising of the first two geo-electric layers of resistivity ranging from 13 to 85 ohm-m lies within the depth of 4 m from the ground surface. The third layer is composed of very fine to medium sand which is the potential water bearing zone having thickness of 36 m with a resistivity of 80 ohm-m. The downward extending layer is clay layer having a resistivity of 30 ohm-m.

VES-9: In this station the top sandy and silty clay comprising of the first two geo-electric layers of resistivity ranging from 34 to 78 ohm-m lies within the depth of 5 m from the ground surface. The third layer is composed of fine sand, medium sand and coarse sand having a thickness of 49m with a resistivity of 205 ohm-m. Below these sand layer a layer of clay is encountered having a resistivity of 25 ohm-m. The layer composed of medium sand is the most potential water-bearing zone of this column.

VES-10: In this station the top sandy and silty clay comprising of the first two geo-electric layers of resistivity ranging from 22 to 90 ohm-m lies within the depth of 12 m from the ground surface. The third layer is composed of medium sand with clay lenses having a thickness of 25 m and this is the most potential water-bearing zone having a resistivity of 46 ohm-m. Below this layer of very fine sand, clay and silt is encountered having a resistivity of 16 ohm-m.

VES-11: In this station the top sandy and silty clay comprising of the first two geo-electric layers of resistivity ranging from 35 to 75 ohm-m lies within the depth of 12 m from the ground surface. The third layer is composed of medium sand with fine sand having a thickness of 26 m with a resistivity of 70 ohm-m.

VES-12: In this station the top sandy and silty clay comprising of the first three geo-electric layers of resistivity ranging from 18 to 80 ohm-m lies within the depth of 25 m from the ground surface The downward extending layer is sandy layer having a resistivity of 70 ohm-m.

4.8 Study of Geo-Electric Anisotropy

All steps taken in the process of interpretation of geo-electric resistivity data are based upon the assumption that geo-electric layers are electrically isotropic. However, in reality all geological formations are appeared to be anisotropic. This phenomenon is quite common in clay or shale rich formations. In such conditions the electrical resistivity is the same in all directions along a layer and has different (more specifically a higher) value in the direction perpendicular to the stratification. The ratio between the resistivity in the perpendicular direction and that in the direction of the stratification is termed as co-efficient of anisotropy. Anisotropy of thick individual beds of anisotropic rocks are referred to as macro-anisotropy and the anisotropy characteristic for thin layers of anisotropic rocks or being inherently anisotropic because of some preferential orientation of texture.

Another phenomenon has also evidenced by electrical measurements is that for geological formations of an alternation of two different facies made up of wide thin beds, the current flows more readily in the direction along the strata than in the perpendicular direction. This condition is referred to as pseudo-anisotropy. The electrical current field in this condition of pseudo-anisotropy is described by exactly the same laws and conditions of true resistivity (Schlumberger, 1930).

The average electrical properties of each unit in a layered geo-electric section may be described by five parameters: the average resistivity along the bedding panes ρ_l, Generally termed as longitudinal resistivity, S the total conductance in the direction of the bedding planes through a column of 1 m²; the average resistivity across the bedding plane ρ_t, frequently called transverse resistivity; the total resistance through a 1 m² column cut perpendicular to the bedding planes, T and co-efficient of anisotropy λ .

4.8.1 Transverse and Longitudinal Resistivity

The transverse and longitudinal resistivities are the true resistivities of the earth. It is possible to measure them in samples in the case of micro-anisotropy or to compute them from a succession of field resistivity measurements in the case of macro-anisotropy. The apparent resistivity obtained in the field is related to these true resistivities through rather strange relationship.

In the present work macro-anisotropic study of earth's subsurface formation to the depth of about 170 m has been studied. The layer parameters of best-fit model of 12 locations have been used to determine the transverse and longitudinal resistivities at different depths. The total resistance to the current flowing vertically through a geo-electric unit of multiple layers is found simply by adding in series the resistance contributed by each individual layer. The resistance of a single layer, the i-th layer (Fig.-4.29) is found from definition of resistivity to be:

$$R_i = \rho_i \frac{1}{A}$$

Where I is the distance current flows in the i-th layer or the thickness h_i, and A is the cross-sectional area presented for current flow. Since the column is 1 m², the above equation reduces to:

$$R_i = \rho_i h_i$$
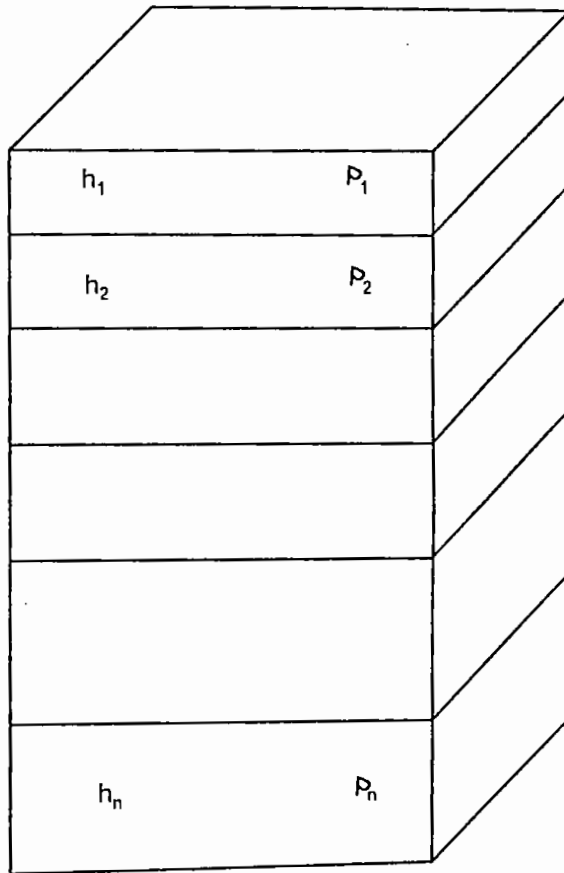
Fig.-4.29: A layered prism of unit cross-section

The sum resistance contributed by all the beds in the section is the transverse resistance, T:

$$T = \sum_{i=1}^{n} \rho_i h_i$$

$$\rho_t = \frac{T}{H} = \frac{\sum_{i=1}^{n} \rho_i h_i}{\sum_{i=1}^{n} h_i}$$

The average resistivity to current flowing across the bedding planes, that is, the transverse resistivity, ρ_t is found by dividing the transverse resistance, T, by the total thickness of the unit, H

The conductance for current flowing through the column is found by summing the conductance through each individual layer for the i-th layer, the conductance is:

$$\frac{1}{R_i} = \frac{1}{\rho_i} \cdot \frac{A}{l}$$

$$\frac{1}{R_i} = \frac{h_i}{\rho_i}$$

Designating the total conductance as S, it is found to be:

$$S = \sum_{i=1}^{n} \frac{h_i}{\rho_i}$$

The average conductivity for the horizontal current flow is determined by dividing the total conductance by the height of the column.

$$\sigma_i = \frac{S}{H}$$

The reciprocal of this average conductivity is the average longitudinal resistivity ρ_l, that is,

$$\rho_l = \frac{H}{S} = \frac{\sum_{i=1}^{n} h_i}{\sum_{i=1}^{n} \frac{h_i}{\rho_i}}$$

The longitudinal resistivity (ρ_l) is always smaller than the transverse resistivity (ρ_t). This dependence of resistivity upon the direction of current flow is the anisotropy.

For the present study transverse resistivity and longitudinal resistivity for different depths for all 12 of the studied VES sections were calculated and the results are presented in table 4.14.

It is obvious from the finding that, in all the cases at different depths the transverse resistivity is greater than the longitudinal resistivity.

4.8.2 Determination of Anisotropy

The assumptions, upon which the traditional methods of resistivity sounding interpretation stand, are those that the resistivity in each layer is constant and there is no dependence of resistivity on the direction of current flow. These assumptions represent a reasonable approximation to the situation occurring most frequently in the subsurface. However there are also are situations in which the resistivity changes with depth in a continuous and more or less regular manner over an appreciable depth range. This situation has received considerable attention because of its interpretation interest in geo-electric survey for groundwater resource evaluation. Most of the recent work on this problem is based upon the assumption of a specific law of change of resistivity with depth in a transitional layer in the subsurface. Niwas and Upadhyay (1974) considered an anisotropic transitional layer in which the conductivity in the vertical direction changes according to a power law expression, while the resistivity in the horizontal direction remains constant. Thus, the co-efficient of anisotropy may be defined by taking the square root of the ratio of resistivities measured in the two principal directions. The transverse (ρ_t) and longitudinal (ρ_l) resistivities are the resistivity of the formation across the bedding plane and along the bedding plane respectively.

So, the co-efficient of anisotropy is calculated as:

$$\lambda = \sqrt{\frac{\rho_t}{\rho_l}}$$

In an anisotropic medium the Laplace's equation does not apply, although the divergence of current density must be zero. The potential distribution in planes perpendicular to the axis of rotation remains the same and the equipotential curves will be similar ellipses elongated parallel to the stratification and the ratio of the two axes will be λ.

4.8.3 Co-efficient of Anisotropy

In the present study the co-efficient of anisotropy have been calculated for different formations and thickness for 12 VES locations. The layer parameters for the best-fit model (section 4.2) were taken into consideration in calculating the co-efficient of anisotropy of different layer combinations. The variation of the co-efficient of anisotropy up to the depth ranging from 16 to 58 m has been estimated (Table 4.14).

It is observed from the values reported in the (Table 4.14) that in each of the locations at an intermediate depth attains comparatively higher values, gradually falling both towards higher and lower depths excepts in VES-1, 3, 4, 6, 9 and 11 etc in which the increase in the values of co-efficient of anisotropy bears gradual character.

It indicates from the increasing values of coefficient of anisotropy that in the central and southeastern parts of the study area the main aquifer zone is located at relatively lower depths than in other parts. This observation is well correlated with the findings of the study of the subsurface hydrogeological, data that is, water table data, lithological information etc.

Table 4.14: Layer parameters of the study area as calculated from VES data

VES Station	Layer Number	Depth to the layer (meter)	Resistivity of the layer (ohm-m)	Transverse Resistivity (ohm-m)	Longitudinal Resistivity (ohm-m)	Coefficient of Anisotropy (λ)
VES-1	1	1.8	85.0	85.0	85.0	1.0
	2	21.0	22.0	27.4	23.49	1.08
VES-2	1	1.32	85.0	85.0	85.0	1.0
	2	13.0	23.0	29.29	24.83	1.08
	3	41.0	19.0	22.26	20.53	1.04
VES-3	1	1.52	56.0	56.0	56.0	1.0
	2	10.0	25.0	29.71	27.29	1.04
	3	37.0	70.0	59.11	49.19	1.096
VES-4	1	0.4	143.0	143.0	143.0	1.0
	2	6.5	27.0	34.13	28.41	1.096
	3	58.0	120.0	110.37	88.16	1.11
VES-5	1	1.32	70.0	70.0	70.0	1.0
	2	3.5	15.0	35.74	21.31	1.29
	3	16.8	10.0	15.36	11.24	1.16
VES-6	1	1.02	69.0	69.0	69.0	1.0
	2	4.8	30.0	38.28	34.09	1.059
	3	44.0	270.0	244.72	153.86	1.26
VES-7	1	0.6	100.0	100.0	100.0	1.0
	2	4.0	20.0	32.0	22.72	1.18
	3	45.0	106.0	99.42	79.97	1.11
VES-8	1	1.0	85.0	85.0	85.0	1.0
	2	4.0	13.0	31.0	16.5	1.37
	3	40.0	80.0	75.10	57.77	1.14
VES-9	1	1.0	78.0	78.0	78.0	1.0
	2	5.0	34.0	42.8	38.56	1.05
	3	54.0	205.0	189.98	146.48	1.13
VES-10	1	1.5	90.0	90.0	90.0	1.0
	2	12.0	22.0	30.5	24.29	1.12
	3	37.0	46.0	40.97	35.66	1.07
VES-11	1	1.0	75.0	75.0	75.0	1.0
	2	12.0	35.0	38.33	36.64	1.04
	3	38.0	70.0	60.0	54.37	1.05
VES-12	1	1.01	80.0	80.0	80.0	1.0
	2	4.0	30.0	42.62	36.0	1.08
	3	25.0	18.0	21.94	19.57	1.05

Chapter-5
Aquifer
Characteristics

CHAPTER-5
AQUIFER CHARACTERISTICS

The water, which occurs below ground surface in the zone of saturation, is termed as groundwater. Groundwater occurs in the voids of rock formation. It is essential to evaluate groundwater movement of the water bearing formation. Pumping test is one of the most commonly used methods to determine the hydraulic properties of the water-bearing unit. The method involves pumping a well and observing the response either in the same well and/or at a distant well, tapping the water bearing formations. There are various methods developed to analyze the observed response.

The occurrence and movement of groundwater in the aquifer is characteristically defined by two parameters, namely transmissivity and storage coefficient. The ease with which groundwater flows in the aquifer is defined by permeability.

The transmissivity is the product of average hydraulic conductivity (permeability) and the thickness of the aquifer. Consequently it is the rate of flow under unit hydraulic gradient equals to unity through a cross section of unit width over the whole thickness of the aquifer. It is designated by the symbol T and expressed in m^3/day.

Storage coefficient is defined as the volume of water released or stored per unit surface area of aquifer, per unit change in the component of head normal to the surface. It is designated by the symbol (S) and is dimensionless. The storage coefficient refers only to the confined parts of an aquifer and depends on the elasticity of aquifer materials and fluid.

Flows in the aquifer are defined by permeability. It is often expressed as the quantity of water, which flows across the unit cross-section of aquifer under unit hydraulic gradient per unit time. It is designated by the symbol (K) and expressed in m/day.

5.1 Pumping Test

Pumping test is a very simple technique. A well screened in aquifer is pumped and the fall of water level (drawdown) is measured in the nearby observation wells at regular interval. As the pumping stops, the water level in the well rises and this rise is also measured at suitable intervals. These measured water levels are used to determine the aquifer characteristics. The pumping test data provides information about the yield and drawdown of the well. Aquifer behavior is ascertained from the pumping test.

After a certain period of pumping, the rate of fall of water level decreases. The discharge is kept constant throughout the pump test.

During the pump test the time, drawdown and discharge data are collected and processed before analyzing. The time data is converted into single unit (days). These data are then plotted on logarithmic paper, which gives the time-drawdown curve.

5.1.1 Analysis of Pump Test Data

Several methods have been developed to analyze the pumping test depending on different types of aquifer. The following method is used in the present study.

Jacob's modified non-equilibrium method:

Coefficient of transmissivity is calculated by the following relationship.

$$T = 2.3Q/4\pi\Delta s \quad \text{----------- (5.1)}$$

Where, T = coefficient of transmissivity;

Q = pumping rate in gpd;

Δs = slope of the time drawdown graph expressed as the change in drawdown between any two vales of time on the log scale whose ratio is 10.

The storage coefficient is also readily calculated from the time-drawdown graph by using zero drawdown of the straight line as one of the terms in the equation. The following relationship is used to calculate the storage coefficient of aquifer.

$$S = 2.25 \, Tt_0/r^2 \text{ --------- (5.2)}$$

Where, S = storage coefficient, T = coefficient of transmissivity in gpd/m, t_0 = intercept of the straight line at zero drawdown (in days), r = distance (in meter) from pumped well to observation well where drawdown measurements were made.

- The procedure for calculating T and S are based on the following assumptions.

- The aquifer is homogeneous, isotropic and of infinite horizontal extent.

- The flow in the aquifer is in a horizontal direction only (Dupuit-Forchheimer flow).

- Water is released from storage in the aquifer in immediate response to drop in piezometric surface. The case of delayed yield is treated separately.

- There is no flow in the aquifer other than the flow caused by pumping the well.

- The well is pumped at a constant rate.

- The well completely penetrates the aquifer and is screened perforated or otherwise opened for the entire height of the aquifer.

In the study area, the hydraulic properties of the aquifer at two stations have been calculated on the basis of pumping test record held by Bangladesh Water Development Board (BWDB). The time-drawdown graphs are shown in fig.-5.1 and 5.2.
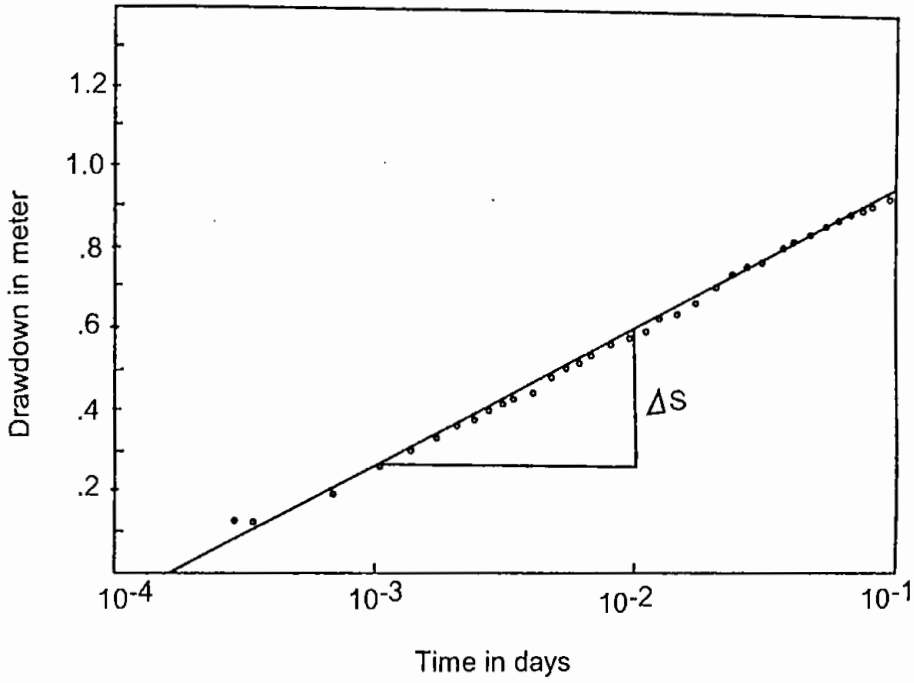
Fig.-5.1: Time - Drawdown analysis of Karmudanga (Sapahar Upazilla)
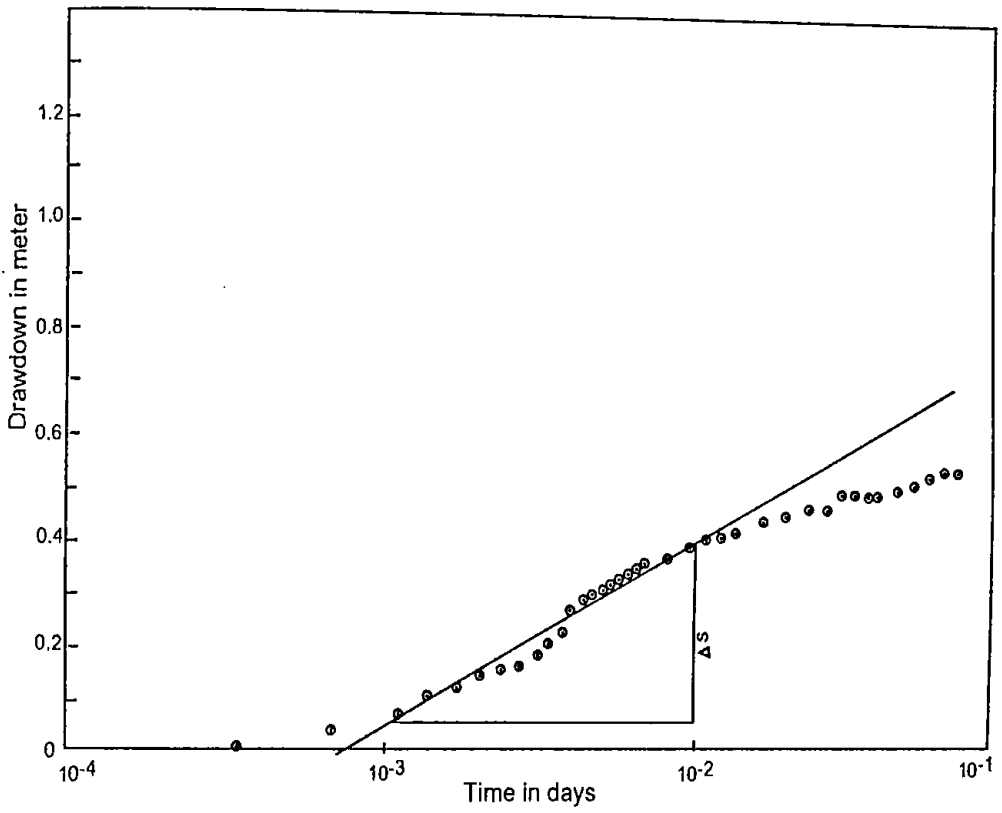
Fig.-5.2:Time-drawdown analysis of Ghatnagar (Porsha Upazilla)

Table 5.1: Results of pumping test analysis of the study area

Well Location	Porsha Mouza: Ghatnagar	Sapahar Mouza: Karmudanga
Discharge (Q) (gpd)	7.23×10^5	9.6×10^5
Transmissivity (T) (m^2/day)	1411.66	1566
Storage coefficient (S)	9.27×10^{-4}	8.05×10^{-2}
Hydraulic Conductivity (m/day)	22	74

5.1.2 Results and Discussions

The transmissivity (T) values calculated from the pump tests in the study area ranges from 1411.66 to 1566 m^2/day. Higher transmissivity (1566 m^2/day) is observed in Sapahar Upazilla and lower transmissivity value (1411.66 m^2/day) is observed in Porsha Upazilla. The storage coefficient value ranges from 9.27×10^{-4} to 8.05×10^{-2}. Higher storage coefficient value is observed in Sapahar Upazilla and lower values are observed in Porsha Upazilla. The hydraulic conductivity value of the aquifer zone ranges from 22 to 74 m/day. Higher hydraulic conductivity is observed in Sapahar Upazilla lower hydraulic conductivity is observed in Porsha Upazilla. The study reveals that the aquifer of Sapahar and Porsha are probably more potential for groundwater abstraction and further development.

5.2 Specific Yield Evaluation of the Study Area

Specific yield is defined as the volume of water released by the downward movement of a unit area of the water table over a unit distance. Childs (1969) demonstrated that the specific yield couldn't be regarded as a constant especially, when the water table as in Bangladesh, is near the surface. This is quite contrary to the normal parametric hydrogeological interpretation. Boulton (1963) developed a semi-empirical mathematical model that regarded the water released from storage as sum of two component S, the volume of water instantaneously released by elastic compression of the aquifer and an exponentially time varying

component Sy, that becomes quasiconstant after a finite time. The most consistent and successful attempts to model specific yield evaluations from rising or falling water table data in Bangladesh must be conducted with some caution if realistic results are to be obtained.

Information on storage capacity is essential for quantitative evaluation of a hydrologic balance in any groundwater basin where a change in groundwater level is occurring.

Information on the storage capacity of an entire groundwater basin or reservoir may be needed in connection with planned management or operation of the basin. For proper planning of the exploitation policy of the groundwater potential of the study area, which is a part of high Barind Tract in the northwestern part of Bangladesh, the knowledge about the specific yield of the aquifer of that area is very essential.

The specific yield of unconsolidated sediments is related to texture classes and within classes, depending upon the composition: the more sand in the sediments the higher the specific yield; the higher the clay content, the lower the specific yield. The water bearing sandy deposits of the study area have been encountered just below the upper clay layer in most of the area.

Because aquifer storage is an important parameter and several field based methods have been used to estimate specific yields. There are:

    a) Lithological analysis;

    b) Catchment water balance; and

    c) Long term pumping test data.

It is expected that analysis based on the lithology will give good estimates of seasonal specific yield expectation over the depth range of interest, but they depend very largely upon the accuracy of lithological descriptions.

Catchment water balance analyses have the disadvantages as it only gives information about the dewatered zone. In Bangladesh, this commonly occurs in the top 6m of the aquifer. Long-term pumping test data, although produced under carefully controlled conditions, have the same disadvantage (Pitman, 1982); Jahan, et al., (1994).

A classic study on specific yield was done by Eckis (1934). The hydrologic laboratory of the U.S. Geological Survey in Denver, Colorado has undertaken more recent research on the specific yield of unconsolidated materials (Johnson, 1976). Preliminary results of this work are shown in table 5.2. The storage capacity of any volume of geological material can be obtained by summing up the specific yield vales of all the unit volumes it contain. Since nearly all such zones include various type of materials with different specific yield values, it is necessary to weight each material according to its proportion of the entire volume. This method is used in the present study to calculate specific yield values. The results of lithological analyses done from bore logs of BADC were used as base. The computations were performed for some 21 selective boreholes of the study area. The specific yield values (maximum and minimum) of the exploitable aquifer of each Upazilla are given in table 5.3.

5.2.1 Results and Discussions

A contour map based on the calculated specific yield values of the study area at 1% interval has been prepared and is shown in fig.-5.3. The estimated specific yield value varies from 10 to 28 % for the study area. The thickness of the top sandy and silty clay aquitard has inverse relationship with the specific yield value and thickness of top aquitard is greater in the northeastern part than in other parts of the study area. The depth of the top of the exploitable aquifer has direct relationship with specific yield value and specific yield is lower in the northeastern part of the study area than in other parts where depth to the top of the exploitable aquifer is higher.
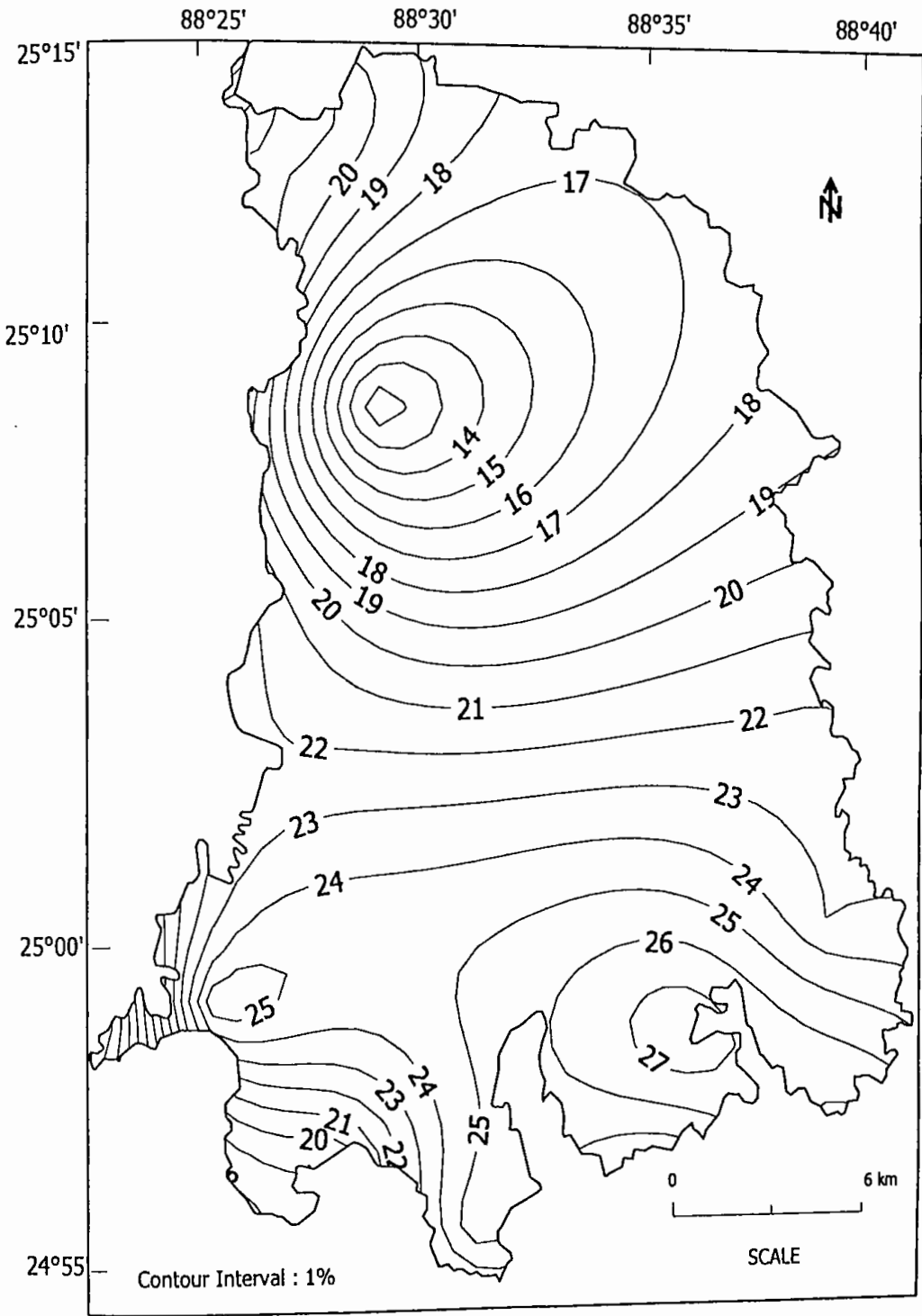
Fig.- 5.3: Specific Yield Map of the Study Area

Table 5.2: Provisional values of specific yield of USGS Hydrologic Lab

Materials	Specific yield (%)
Clay	1
Silty clay	2
Sandy clay	3
Clay-silt	5
Silt	7
Clay-sand	7
Sandy-silt	14
Silty sand	20
Fine sand	26
Medium sand	35
Coarse sand	33
Sand (undifferentiated)	32
Values from Eckis (1934)	
Fine gravel	25
Medium gravel	20
Coarse gravel	14

Table 5.3: Specific yield value of the exploitable aquifer of the study area

Name of Upazilla	Specific Yield %	
	Minimum	Maximum
Sapahar	10	28
Porsha	11	28

Chapter-6
Estimation of
Recharge and Discharge

CHAPTER-6
ESTIMATION OF RECHARGE AND DISCHARGE

6.1 Estimation of Recharge

Groundwater recharge is the mean annual volume of water, which enters the saturated zone. The main source of recharge is the precipitation, which may penetrate the soil directly to the groundwater or may enter the surface streams. Lakes, reservoirs etc, and percolate from these channels to the groundwater.

The aquifer recharge is often defined, as the mean annual volume of water, which may in the long term, be available for abstraction. In certain circumstances the current rate of aquifer recharge can prove a practical as well as theoretical limit to the aquifer yield. Therefore, recharge rates for aquifers must be estimated before groundwater resources are evaluated.

There are several potential sources of recharge to groundwater reservoir, which vary in their relative importance across the area. These include:

i) Rainfall;

ii) Flood water which overflow river and stream banks that infiltrate and percolate;

iii) Lateral seepage and/or vertical percolation from rivers and canals;

iv) Percolation from permanent sources of water (water bodies lying above water table);

v) Vertical percolation of irrigation water from irrigated lands that is not evaporated or transpired by crops;

vi) Lateral flow of groundwater from adjacent areas with higher water levels;

vii) A fraction of used and lost domestic and industrial withdrawals.

Infiltration of rain water for recharge to groundwater reservoir depends on several factors, important of which are: availability of rainfall in excess of evapotranspiration, depth and duration of standing water in the fields, soil type,

porosity, vertical conductivity of the top soil, storing space in the underground reservoir, vegetal cover and land use.

In this area, it is mentioned that there are large numbers of beels, canals, ponds that cannot keep them connected with big river after the flooding season. Hence, water from these bodies are evaporated and partly percolated to recharge the under ground reservoir. Top sandy and silty clay aquitard of the investigated area comprises mostly loose clay, silt and very fine sand, which are favorable for percolation of rainwater. Flooding in the study area usually occurs due to heavy sudden rainfall in monsoon. This excessive rainwater remains stagnant for a considerable period.

Moreover every year during rainy season, the water level of the river rises high enough to exert lateral pressure of groundwater towards land surface and, in turn, helps to recharge the groundwater sources.

The groundwater system in Bangladesh is considered to be in dynamic equilibrium that is the annual recharge is approximately equal to the discharge. Recharge exceeds discharge during the rainy season and groundwater level rise but during the dry season discharge exceeds recharge and groundwater level decline.

Recharge to groundwater reservoir of an area can be estimated by:

a) Water balance method.
b) Budgeting soil moisture at root zone of the plants;
c) Water balance based on hydrodynamic data only;
d) Well hydrograph (safe yield); and
e) Vertical infiltration rate i.e. hydraulic conductivity of topsoil strata.

The accuracy of the estimation of recharge to groundwater reservoir in case of water balance method depends on accurate accounting of all incoming and outgoing water in the area and actual evaporation. It depends on extensive gauging and definite physiographic unit.

Budgeting plot-wise soil moisture of the root zone of the plants throughout the year is practically impossible for variation of the types of soils, crops, and plants from place to place in the study area. Through the water balance method, the potential recharge is estimated which is mainly based on hydrodynamic data, rainfall data, potential evapotranspiration and the run-off coefficient of different watersheds. Except for rainfall, accurate data of the other parameters are hardly available. So the water balance method is not suitable in evaluating the actual recharge of groundwater.

The well hydrograph method has been used to determine the groundwater recharge of aquifer in the investigated area. In this method specific yield and area of the aquifer multiply the fluctuation in groundwater levels. A quantitative assessment of groundwater recharge has been made for the study area. A variety of techniques can be used for estimating groundwater recharge. Generally recharge due to rainfall, surface water bodies and irrigation return are estimated individually using different formulas to have the total amount of annual recharge. The well hydrograph method is based on the facts that all water that enter into the groundwater which is being reflected in the rise of water table but some parts of it is continuously lost to the atmosphere when the water table lies very close to land surface and some part of it is lost by discharging to the nearby rivers and discharging to the lower areas. A fair indication of the maximum days of recharge to groundwater is achieved from the method.

But in the present process annual recharge has been estimated only considering the fluctuation of groundwater table. In the case of recharge the rising of groundwater table from dry to rainy season is considered and volume between them is calculated. Then the calculated volume is multiplied by the specific yield of that formation filled with groundwater to have the recharge/volume of water. But the calculated volume may be within the formations of variable specific yields. For this calculation the whole study area has been divided in to 10 polygons (Fig.-6.1) following Thiessen polygons method in such a way that each polygon is under the

influence of a single observation well (Todd, 1980). Specific yield has been calculated for different polygons from the bore logs within the same polygon.

Different parts of the studied area form different polygons as shown in fig.6.1. Sapahar Upazilla comprises P-1, P-2, P-3, P-4, P-5a, P-6b, P-6c, and P-9a and Porsha Upazilla comprises P-6a, P-7a, P-7b, P-7c, P-5b, P-5c, P-5d, P-8a, P-8b, P-9b and P-10. This can be formulated as follows:

$$Q = V \times S_y$$

V = volume between dry and rainy season;

S_y = Specific yield within the fluctuation zone.

For the estimation of total volume of water recharged during the 1991-1992, the first amount of water recharged consider in the water level fluctuation between dry and after rainy season of 1991. The estimated annual recharge of the year 1991 to 2000 has been tabulated in the table 6.1.

Table 6.1: Calculated annual recharge of aquifer of the study area (1991-2000)

Year	Sapahar (Mm^3)	Porsha (Mm^3)
1991	171.64	236.76
1992	106.41	164.63
1993	140.37	228.36
1994	110.67	187.62
1995	193.01	224.14
1996	118.26	191.77
1997	127.25	171.21
1998	167.82	244.26
1999	173.97	243.1
2000	206.06	216.03
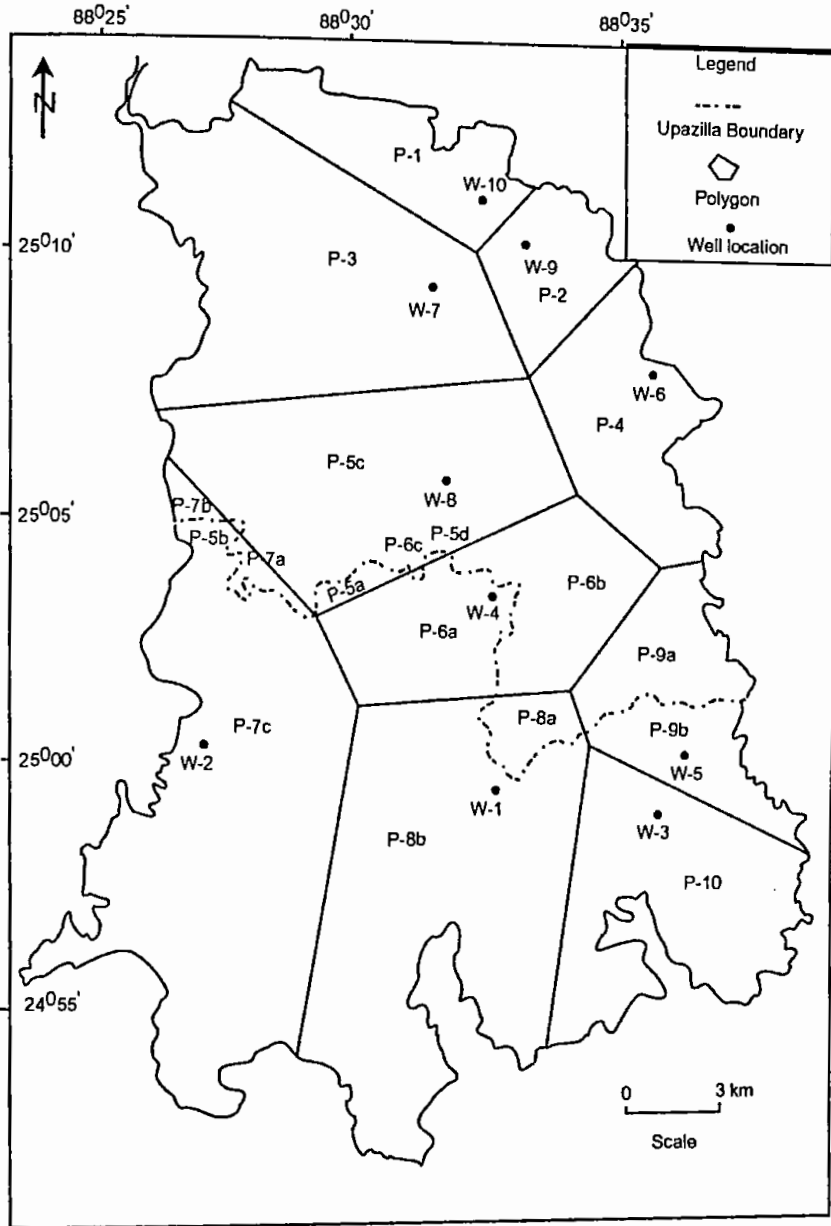
Fig.-6.1: Polygon of the study area

6.2 Estimation of Discharge

A quantitative assessment of groundwater discharges has been made for the study areas. A variety of techniques can be used for estimating groundwater discharge. Discharge is measured taking evaporation loss, evaporation transpiration loss, natural discharge and leakage into account. In the present process annual discharge have been estimated only considering the fluctuation of groundwater table. For discharge estimation, volume covered by shifting water table from rainy to dry season is considered. For the estimation of total volume of water discharged during the 1991-1992 and the volume of water discharge is calculated with the fluctuation between the pre-monsoon of 1991 and dry season 1992. The estimated annual discharge of the year 1991 to 2000 is given in the table 6.2.

Table 6.2: Estimated annual discharge of the study area (1991-2000)

Year	Sapahar (Mm³)	Porsha (Mm³)
1991	105.05	224.41
1992	93.77	170.07
1993	133.53	219.17
1994	193.46	228.76
1995	182.4	227.72
1996	136.46	175.11
1997	139.17	166.06
1998	176.15	275.05
1999	220.13	200.04
2000	276.94	291.7

The estimated annual recharge and discharge of the year 1990 to 2000 have been presented in fig.-6.2 and 6.3.
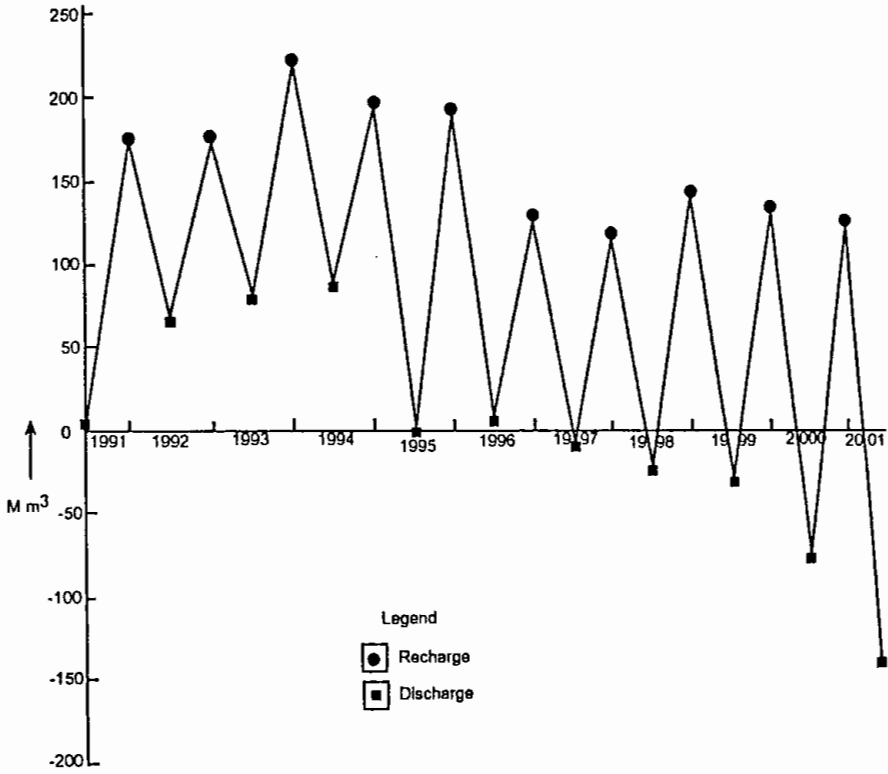
Fig .-6.2: Annual recharge and discharge of groundwater of Sapahar Upazilla (1991-2000)
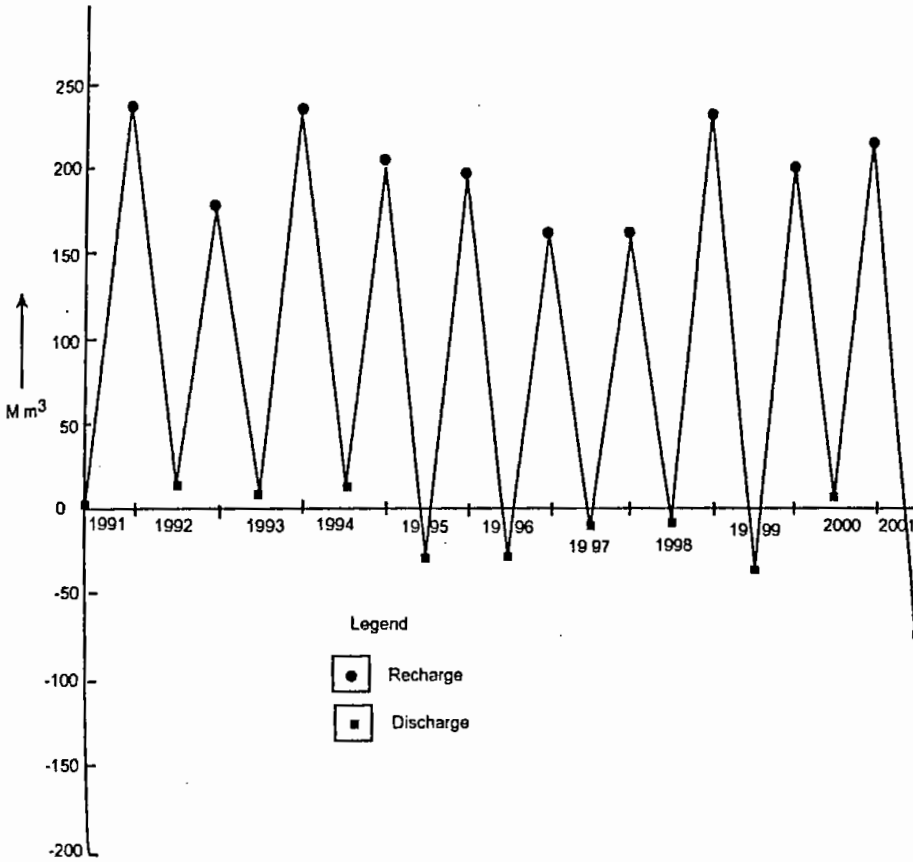
Fig.-6.3: Annual recharge and discharge of groundwater of Porsha Upazilla (1991-2000)

6.2.1 Discharge of Groundwater by Artificial Abstraction

In general the main component of groundwater discharge are:

a) Evaporation, particularly in low-lying areas where the water table is close to the ground surface;

b) Natural discharge by means of spring flow and effluent seepage into surface water bodies;

c) Groundwater leakage and out flow through aquitards into adjacent aquifer;

d) Artificial abstraction.

In the present study significant amount of discharge occurs chiefly due to artificial abstraction.

During earlier part of 1980's Barind Multipurpose Development Authority (BMDA) has initiated an irrigation program in Barind area. Under this program, a large number of deep tube wells have been installed since 1984 and still the installation program is continued. Besides this a large number of shallow tube wells have been functioning in the study area. There is also a number of low-lift pump used in irrigation from surface water bodies.

Available information regarding the number of tube wells installed in each year is collected from the respective organizations. For convenience, all types of discharging equipment with their respective discharge rate and discharging hour during the period of 1991 to 2000 are given in table 6.3. With a view to groundwater management the discharge of groundwater accomplished by the different discharging equipment is computed for the period of 1991 to 2000. The discharge is calculated individually according the discharge rate and discharging hour of the respective. Discharged water is used in the study area for both the domestic and irrigation purposes. The obtained results are provided in table 6.4.

6.3 Groundwater Balance Study

Water typically carries a special constraint; it is regarded as renewable natural resource. Thus when water well is drilled, people presume that production of well water will continue indefinitely with time. In effect, this can occur if there exist a balance between water recharge to the basin from the surface sources and water pumped from within the basin by wells. But if groundwater is withdrawn at a rate exceeding the recharge mining yield exist and if mining continues different types of hazards may occurred such as declination of water levels, deterioration of water quality, destruction of hydraulic properties. The present study area suffers from some of the above problems, for a large-scale abstraction of groundwater due to irrigation purposes. The annual discharge for each of the discharge equipment is computed individually and presented in a tabular form. Groundwater balance for the study area is workout using the following assuming the natural groundwater inflow to be equal to the groundwater outflow.

$$\Delta S = I - O$$

ΔS = Change in storage

I = Annual input to groundwater system

O = Annual output from ground system

Adopting the above methodology, the water balance of the study area is worked out with the observation data for the period 1991-2000. Calculated water balance for the study area is given in table 6.5.

Table 6.3: Total number of discharging wells running during 1991-2000

Discharge equipment with discharge rate and hours	Number of discharging equipments during 1991-2000									
	91	92	93	94	95	96	97	98	99	2000
	Sapahar Upazilla									
DTWs DR =1.6 cft/sec DH =1200 h/yr Efficiency = 80%	94	94	97	107	109	114	119	122	122	122
STWs DR = 0.5 cft/sec DH = 1200 h/yr Efficiency = 80%	198	198	198	198	467	467	467	484	484	484
LLPs DR = 1.5 cft/sec DH = 1200 h/yr Efficiency = 85%	215	225	225	215	215	225	225	225	410	410
	Porsha Upazilla									
DTWs DR = 1.6 cft/sec DH = 1200 h/yr Efficiency = 80%	107	108	138	162	182	181	187	192	194	194
STWs DR = 0.5 cft/sec DH = 1200 h/yr Efficiency = 80%	200	218	218	216	216	216	216	216	216	216
LLPs DR = 1.5 cft/sec DH = 1200 h/yr Efficiency = 85%	428	428	428	428	438	428	428	428	428	428

Table 6.4: Amount of annual discharge by different discharging equipments for domestic and irrigation purposes (1991-2000)

Period	Discharge for Domestic and Irrigation Purposes by Surface Water and Groundwater (Mm³)			Total Groundwater Discharge (Mm³)
	DTWs	STWs	LLPs	
Sapahar Upazilla				
1991	14.47	9.52	32.97	56.96
1992	14.47	9.52	34.51	58.5
1993	14.88	9.52	34.51	58.91
1994	16.49	9.52	32.97	58.98
1995	16.79	22.47	32.97	72.23
1996	17.5	22.47	34.51	74.48
1997	18.26	22.47	34.51	75.24
1998	18.72	23.29	34.51	76.52
1999	18.79	23.29	62.88	104.96
2000	18.79	23.29	62.88	104.96
Porsha Upazilla				
1991	16.47	9.62	65.64	91.74
1992	16.63	10.49	65.64	92.76
1993	21.25	10.49	65.64	97.38
1994	24.85	10.39	65.64	100.98
1995	28.03	10.39	67.18	105.60
1996	27.78	10.39	65.64	103.91
1997	28.7	10.39	65.64	104.83
1998	29.47	10.39	65.64	105.6
1999	29.78	10.39	65.64	105.91
2000	29.78	10.39	65.64	105.91

Table 6.5: Groundwater balance of the study area for 1991-2000

Period	Rainfall	Input (Mm^3)	Output (Mm^3)	Change in storage (Mm^3)	Position of Storage in 2000 (Mm^3)
Sapahar Upazilla					
1991	1965	171.64	105.05	+66.59	
1992	1296	106.41	93.77	+12.64	
1993	1320	140.37	133.53	+6.84	
1994	1053	110.67	193.46	-82.79	
1995	1977	193.01	182.4	+10.61	
1996	783	118.26	136.46	-18.2	-141.6
1997	1031	127.25	139.17	-11.92	
1998	1603	167.82	176.15	-8.33	
1999	1525	173.97	220.13	-46.16	
2000	1485.9	206.06	276.94	-70.88	
Porsha Upazilla					
1991	1998.8	236.76	224.41	+12.35	
1992	1200.6	164.63	170.07	-5.44	
1993	1420.1	228.36	219.17	+9.19	
1994	1120.1	187.62	228.76	-41.14	
1995	2144.7	224.14	227.72	-3.58	-70.21
1996	1387.9	191.77	175.11	+16.66	
1997	1055.2	171.21	166.06	+5.15	
1998	1750.4	244.26	275.05	-30.79	
1999	1990.4	243.1	200.04	+43.06	
2000	1387.9	216.06	291.7	-75.67	

6.4 Results and Discussion

The annual groundwater recharge of aquifer of the study area estimated by hydrograph method following Thiessen Polygon method varies from 106.41 to 244 Mm^3. The Annual groundwater discharge of aquifer of the study area estimated by hydrograph method following Thiessen Polygon method varies from 93.77 to 291.7 Mm^3. The annual recharge and discharge of last 10 years has been presented in fig.-6.2 and 6.3. The calculated groundwater recharge of aquifer of the study area shows

that the rate of groundwater recharge of aquifer in Porsha Upazilla is higher than that of Sapahar Upazilla and is characterized by very suitable groundwater storage potential. Thus the overall study in the study area indicates that there used to exist a balance between annual recharge and withdrawal up to 1993 but after period of 1993 discharge exceeds the recharge continuing till date. A cumulative annual deficit is found to exist because of progressive annual discharge in Sapahar Upazilla. It is observed that during the period 1994 and 2000, the deficit of groundwater is maximum. It appears from the results that the amount of water withdrawn varies from 56.96 to 105.91 Mm^3 in the study areas of different Upazillas. 56.96 to 105.91 Mm^3 of groundwater is discharged by discharging mechanisms. The rest of the reserve is presumed to have lost as underground flow to other aquifers of the region. This phenomenon may have resulted from the tectonic control of the groundwater movement especially in the High Barind Tract (Jahan and Ahmed, 1997). As an example of the above phenomenon, during the year 2000 in Sapahar Upazilla, whereas the amount of total recharge was 206 Mm^3, the discharge constituted only 276 Mm^3 and hence causing a deficit of 70 Mm^3. Of the total discharge of 276 Mm^3, only 105 Mm^3 was abstracted by tubewells and the rest of the total loss contributed is attributed as underground flow to the neighboring aquifers.

Chapter-7
Conclusions
and
Recommendations

CHAPTER-7
CONCLUSIONS AND RECOMMENDATIONS

7.1 Conclusions

The hydrogeological and geo-electrical study of the area under present study has enabled to arrive at the following conclusions:

The ground elevation contour map of the study area represents undulatory geomorphic features and central parts of Sapahar and Porsha Upazillas are highly elevated. Based on lithological constituents, the subsurface layers of study area are divided into three zones: Zone-I: composed mainly of sandy and silty clay varies in thickness from 4 to 36 m, characterized by low permeability. Zone-II is composed of fine, medium and coarse sand and the thickness of this zone varies from 15 to 51 m. Zone-III is the lower most boundary of the composite aquifer composed of silty shale layer.

Stratigraphic panel diagram also shows a top sandy and silty clay layer of 4 to 36 m thickness, which decreases towards the southern part of the study area. The thickness of the composite layer varies from 15 to 51 m. Lower silty shale layer represents the lower boundary of the aquifer.

Clay-sand interface map also indicates a diverging zone in the study area. While the thickness map of top sandy and silty clay layer indicates an east-west elongated thick zone located in the northeastern portion of Sapahar Upazilla.

It is observed from the maximum and minimum elevation of groundwater table contour map that the central part of the study area was a prominent north south elongated water divide. Groundwater flows radially towards east, west, north and south from the central part of the study area.

The maximum and minimum elevation of groundwater table of the study area varies from 20 to 34 m and 15 to 32 m respectively. Higher value of maximum

elevation of groundwater table is observed in the central part of Porsha and lower value of maximum elevation of groundwater table is observed in the northwestern part of Sapahar and southeastern portion of Porsha Upazilla. Higher value of minimum elevation of groundwater table is observed in the central part of Porsha and lower value of minimum elevation of groundwater table is observed in the northwestern part of Sapahar and southeastern portion of Porsha Upazilla. The groundwater table fluctuation of the study area varies between 2 and 8 m. The maximum and minimum fluctuations are observed in northwestern part of Sapahar and in the central part of Porsha respectively. From the hydrograph, it is observed that the water level is gradually declining. A large number of deep tube wells have been installed under an irrigation program. It is evident that this abrupt fall of groundwater level is mainly due to the large abstraction of groundwater by the deep tube wells. It is inferred from landsat imagery that about 12 to 15% of the total area is occupied by surface water bodies.

Geo-electric survey employing vertical electric sounding (VES) technique was carried out in 12 locations. The data have been interpreted as a multi-layer step function resistivity model by means of an iterative process of interpretation .A equivalent model with minimum number of layers has been constructed for each of the VES locations. The transverse and longitudinal resistivities at different depth levels along with the coefficient of anisotropy have been calculated.

Results of the resistivity survey reveal the subsurface configuration consists of three to four layers. On the basis of hydrogeological behaviors, interpreted geo-electrical layers are grouped into two forms: aquitard and aquifer. The first layer of top sandy and silty clay and in some cases, second and third layers, if critically analyzed from hydrogeological point of view, may be considered as aquitard and the rest of the layers, which are mainly composed of sandy formations, can be considered as the only aquifer present in the study area. The top sandy and silty clay aquitard shows a general increasing trend in depth towards the northeastern

part of the study area and the composite aquifer shows higher thickness in the southeastern and southwestern parts of the study area. In this work, an attempt has been made to evaluate the availability of groundwater resources, its occurrences and characteristics of groundwater aquifers, particularly its depth and thickness. Results of geo-electrical investigation indicate that there exist composite aquifer at a depth between 37-58 m and this is the only aquifer, which have been exploited for both the domestic and irrigation purposes. The aquifer level and its thickness as derived from the interpreted result are correlated with the available information of observation wells and borehole lithology of the area.

Increasing trends of coefficient of anisotropy towards the central and southwestern parts of the study area indicate that the main aquifer zone is located at relatively lower depths than other parts.

Transmissivity values are as derived from pumping test data analysis, varies from 1411 to 1566 m^2/day which is indicative of a higher degree of transmissivity and suitability for the groundwater resource for utilization in irrigation and drinking water supply. Storage coefficient value varies from 9.27×10^{-4} to 8.05×10^{-2}. Hydraulic conductivity value of aquifer zone in the study area ranges from 22 to 74 m/day. The estimated transmissivity, storage coefficient and hydraulic conductivity indicate that the area is suitable for groundwater exploitation for irrigation and domestic purposes (Pitman, 1982).

The study area has the estimated specific yield values varying from 10 to 28%, which increase as the thickness of top sandy and silty clay layer decreases and vice versa. The estimated specific yield values also conform to the calculated values of hydraulic properties of aquifer and indicate that the area is suitable for groundwater extraction for irrigation and drinking water supply purposes.

The annual groundwater recharge and discharge of aquifer of the study area are estimated using Thiessen polygon method varies from 106.41 to 244 Mm^3 and 93.77 to 291 Mm^3 respectively.

For groundwater management study an attempt has been made for groundwater balance study of 10 years with the input/output stresses of the present aquifer system of the area. The result of this balance study shows that there is an annual deficit of groundwater storage.

From the overall observation it is found that overexploitation of groundwater for the irrigation purposes is the main reason for the on going permanent declination of water level.

The average annual rainfall is which is the chief source of groundwater recharge of the study area is almost same and from the well hydrograph it is observed that the recharge of groundwater is almost same and during the last few years it is somewhat increased.

According to groundwater balance study it is found that an annual deficit is observed. It is mentionable that the number of discharging equipment is gradually increasing and hence the discharge exceeds the recharge.

Thereafter, with the increase of discharging equipment an appreciable change of annual deficit of groundwater storage is observed. Thus the aquifer is being depleted to the extent and no longer yields enough water to meet demand.

The declination of groundwater level is bringing some major hydrogeological and ecological changes in the area. For the progressive depletion of groundwater reservoir water level go down below the economic level of pumping and so that the domestic demand of water supply is severely handicapped. The river Punarbhaba flows across the western portion of the area. Now-a-days the river becomes dry during dry season causing the river stages go down below the groundwater level, which results in the loss of water from groundwater storage as base flow at higher rate.

The regional climate and vegetation also aggravate the situation. The area posses very thin vegetation and normally the temperature recorded is very high in comparison to other parts of the country. Under these circumstances, the area is characterized as a high evaporation zone. All the above adversities affect the ecological balance of the area and some parts of the area shows evidences of desertification.

7.2 Recommendations

With a view to gather more specific knowledge about the groundwater potentiality of the study area and to plan the groundwater use, the following recommendations could be followed:

1. More detailed database, that is, satellite information and other remote sensing techniques should be used to study the groundwater resource.

2. To avoid overexploitation of the groundwater resource, the installation of deep tube wells for the purposes of irrigation and drinking water supply should be done in a planned way. Proper well spacing should be followed. The existing tube wells should be maintained properly to get sufficient discharge.

3. Use of surface water in a planned way could reduce the pressure on groundwater resources of the area; if necessary the numerous tanks and canals situated in the study area have to be utilized as reservoir for surface water.

References

REFERENCES

Avery, T.E. 1977. *Interpretation of aerial photographs*, Burgess Publishing Minneapolis, 392p.

Bakhtine, M.I. 1966. Major Tectonic Features of Pakistan, Part-ii, Eastern Province: *Science,* v.4. n.2. PCSIR, Karachi. p.80-100.

Boulton, N.S. 1963. Analysis of data from non-equilibrium pumping tests allowing the delayed yield from storage. *Proc. Inst. Of Civil Engineers.* v.26. p.469-482.

Bowden, L.W., and Pruit, E.L. (eds) 1975. Manual of remote sensing, vol. (ii), Interpretation and applications, *Amer. Soc. Photogrammetry*, Falls Church. Virginia, p.869- 2144.

Childs, E.C. 1969 .The physical basis of soil moisture phenomenon,John wiley.

Compagnie General de Geophysique, 1955. Abaques de sondages electriques: *Geophys. Prosp.*, v.3, supplement no. 3.

Compagnie General de Geophysique, 1963. *Master curves for electrical sounding,* 2nd revised edition, E.A.E.G., The Hague.

Deparment of Soil Survey, 1984. Reconnaissance Soil Survey, Rajshahi District, v.1 and 2. 212p and 150p.

Deppermann, K. and Thiele, J. 1969. *Geoelectric resistivity survey in East Pakistan 1968*, Unpublished report of Bundesanstalt fur Bodenforschung, 70p., 7app., 10 fig., 2 photo. (Hanover)

Eckis, Rollen 1934. South coastal basin investigation Geology and groundwater storage capacity of valley fill. *Bull.45, California Division of Water Resources.*

Ghosh, D.P. 1970. The application of linear filter theory to the direct interpretation of geoelectrical resistivity measurement, Doctoral thesis, Technical University, Delft.

Ghosh, D.P. 1971. The application of linear filter theory to the direct interpretation of geo-electrical resistivity sounding measurements: *Geophys. Prosp.*, v.19, p.192-217.

Griffiths, D.H. and King, R.E. 1981. *Applied Geophysics for Geologists and Engineers*, Pergamon Press, Oxford, 230p.

Guha, D.K. 1978. Tectonic Framework and Oil and Gas Prospects of Bangladesh. *Proc., of 4th Annual Conference, Bangladesh Geological Society*, Dhaka. p.65-78.

Jahan, C.S. and Ahmed, M. 1997: Flow of Groundwater in Barind Area, Bangladesh: Implication of Structural Framework, *Jour. Geological Society of India*, v.50, p.743-752.

Jahan, C.S. *et al.*, 1994. Specific Yield Evaluation: Barind area, Bangladesh, *Journal of the Geological Society of India*. v-39.

Johnson, A.I. 1967. Specific yield - compilation of specific yields for various materials, *U.S. Geological survey Water Supply Paper 1662-D*, 74p.

Keller, G.V. and Frischknecht, F.C. 1982. *Electrical Methods in Geophysical Prospecting,* Pergamon Press, New York.

Khan, A.A. and Ahmed, S.T. and Ahmed, S.S. 1986. Ground water potentiality of Rajshahi city and its surroundings. The Rajshahi University Studies (part-B), XIV, pp.91-102.

Khan, A.A. and Rahman, T. 1992. An analysis of gravity field and tectonic evaluation of the north-western part of Bangladesh. Tectonophysics, v.206. p.351-364.

Khandaker, R.A., 1989. Development of major tectonic elements of the Bengal Basin: a plate tectonic appraisal. *The Bangladesh Journal of Scientific Research,* v.7, n.2. p.221-232.

Khandoker, R.A. 1987. Origin of Elevated Barind-Modhupur Area, Bengal Basin: Result of Neotectonic Activities. *Bangladesh Journal of Geology*, vol.6, p.1-9.

Koefoed, O. 1968. The application of the Kernel function in interpreting geoelectrical measursments: Berlin-Stuttgart, Gebruder-Borntraeger, *Geoexplor. Monograph*, series 1, no. 2.

Koefoed, O. 1970. A fast method for determining the layer distribution from the raised kernel function in geoelectrical soundings, *Geophysical Prospecting*, v.18, p.564-570.

Kunetz, G. 1966. *Principles of direct current resistivity prospecting*: Berlin, Gebruder Borntraeger, 103 p.

Kunetz, G. and Rocroi, J.P. 1970. Traitment automatique des sondages electriques, *Geophysical Prospecting*, v.18. p.157-198.

Langer, R.E. 1933. An inverse problem in differential equations: *Am. Soc. Math. J.*, v.39, p.14-28.

Meinardus, H.A. 1970. Numerical interpretation of resistivity soundings over horizontal beds, *Geophysical Prospecting*, v.18, p.415-433.

Mooney, H.M. and Wetzel, W.W. 1956. *The potential about a point electrode and apparent resistivity curves for a two-three, and four-layer earth.* Minneapolis, Univ. Minnesota Press, 146p.

Morgan, J.P. and McIntyre, W.G. 1959. Quaternary geology of the Bengal Basin, East Pakistan and India, *Bull, Geol. Soc. Am.*, v.70, p.319-342.

Orellena, E. and Mooney, H.M. 1966. *Master tables and curves for vertical electrical sounding over layered structures,* Interciencia, Madrid.

Patella. D. 1975. A numerical computation procedure for the direct interpretation of geoelectrical soundings, *Geophysical Prospecting*, v.23. p.335-362.

Pekeris, C.L. 1940. Direct method of interpretation in resistivity prospecting, *Geophysical Exploration*, v.5, p.31-42.

Pitman, G.T.K. 1982. *Aquifer Evaluation and Recharge in Bangladesh*, UNCTCD/BWDB (GWC) Technical Note.8.188p.

Raghunath, H.M. 1985. *Hydrology*, Wiley Eastern Limited, 482p.

Ray, R.G. 1960. Aerial photographs in geologic interpretation and mapping, U.S. Geological Survey Prof. Paper 373, 227p.

Sharma, P.V. 1978. *Geophysical Methods in Geology*, Elsevier Scientific Publishing Company, New York, 428p.

SPARRSO (Space Research and Remote Sensing Organization), 1989. " *Fisheries Resources Survey System*" Report on FAO/UNDP project in Bangladesh. Contact No. DP/BGD/79/015-2/Fi, 1984.

Todd, D.K. 1980. Groundwater Hydrology. John Wiley & Sons, New York, 535 p.

Vozoff, K. 1958. Numerical resistivity analysis: horizontal layers, *Geophysics*, v.3, p.536-556.

Wenner, F. 1912. The four-terminal conductor and the Thomson bridge: *U.S. Bur. Standards Bull.*, v. 8, p. 559-610.

Zaher, M.A. and Rahman, A. 1980. Prospects and Investigations for Mineral in the Northern Part of Bangladesh. *Petroleum and Mineral Resources of Bangladesh, Seminar and Exhibition*, October 08-12, 1980. Dhaka. p.9-18.

Zohdy, A.A.R. 1975: Automatic interpretation Schlumberger sounding curves using modified Dar Zarrouk functions, *USGS Bull. No. 1913-e*, 39p.

Zohdy, A.A.R. 1989: A new method for the automatic interpretation of Schlumberger and Wenner sounding curves. *Geophysics*, v.54, n.2. p.245-253.

Zohdy, A.A.R., Eaton, G.P. and Mabey, D.R. (1974): Application of surface geophysics to groundwater investigations. *Tech. of Water Resources Investigations of the USGS*, Book 2, Chap. D1.